

BRIDGING THE GAP BETWEEN PUPPING AND MOLTING PHENOLOGY:
BEHAVIORAL AND ECOLOGICAL DRIVERS IN WEDDELL SEALS

By

Roxanne Santana Beltran, B.Sc., M.Sc.

A Dissertation Submitted in Partial Fulfillment of the Requirements

for the Degree of

Doctor of Philosophy

in

Biological Sciences

University of Alaska Fairbanks

August 2018

APPROVED:

Dr. Jennifer Burns, Committee Co-Chair

Dr. Greg Breed, Committee Co-Chair

Dr. J. Ward Testa, Committee Member

Dr. Diane O'Brien, Committee Member

Dr. Brian Barnes, Committee Member

Dr. Kris Hundertmark, Chair

Department of Biology and Wildlife

Dr. Leah Berman, Interim Dean

College of Natural Science and Mathematics

Dr. Michael Castellini, *Dean of the Graduate School*

Abstract

In Antarctica, the narrow window of favorable conditions constrains the life history phenology of female Weddell seals (*Leptonychotes weddellii*) such that pupping, breeding, foraging, and molting occur in quick succession during summer; however, the carry-over effects from one life history event to another are unclear. In this dissertation, I characterize the phenological links between molting and pupping, and evaluate feeding behavior and ice dynamics as mechanistic drivers. First, I review the contributions of natural and sexual selection to the evolution of molting strategies in the contexts of energetics, habitat, function, and physiology. Many polar birds and mammals adhere to an analogous biannual molting strategy wherein the thin, brown summer feathers/fur are replaced with thick, white winter feathers/fur. Polar pinnipeds are an exception to the biannual molting paradigm; most rely on blubber for insulation and exhibit a single molt per year. Second, I describe the duration and timing of the Weddell seal molt based on data from 4,000 unique individuals. In adult females, I found that successful reproduction delays the molt by approximately two weeks relative to non-reproductive individuals. Using time-depth recorder data from 59 Weddell seals at the crucial time between pupping and molting, I report a striking mid-summer shallowing of seal dive depths that appears to follow a vertical migration of fishes during the summer phytoplankton bloom. The seals experience higher foraging success during this vertical shift in the prey distribution, which allows them to re-gain mass quickly before the molt. Across four years of study, later ice break-out resulted in later seal dive shallowing and later molt. In combination, the data presented in this dissertation suggest that molting, foraging, and pupping phenology are linked in Weddell seals and are affected by ice break-out timing.

Table of Contents

	Page
Abstract	iii
List of Figures	xi
List of Tables	xv
Preface.....	xviii
Acknowledgments.....	xxi
Dedication	xxiii
Chapter 1. General Introduction	1
1.2 Literature Cited	6
Chapter 2. Convergence of biannual moulting strategies across birds and mammals.....	15
2.1 Abstract	15
2.2 Introduction	16
2.3 Functional roles and forms of pelage and plumage.....	17
2.4 Metabolic costs of moult	18
2.5 Selection pressures and moulting strategies.....	20
2.6 Special considerations for aquatic species	24
2.7 Physiological mechanics of pelage and plumage replacement	27
2.8 Feedbacks between moult and global change	29
2.9 Conclusion.....	30

2.10 Acknowledgments	31
2.11 Literature Cited	36
Chapter 3. Reproductive success influences molt phenology and subsequent colony attendance in Weddell seals	53
3.1 Abstract	53
3.2 Introduction	54
3.3 Methods	56
3.3.1 Fieldwork methods	56
3.3.2 Analytical methods	59
3.3.3 Estimating molt stage durations	59
3.3.4 Estimating molt initiation dates	60
3.3.5 Accounting for error propagation	61
3.3.6 Drivers of molt phenology	62
3.3.7 Interactions between pupping success/phenology and molt phenology	63
3.4 Results	64
3.4.1 Demography of molting animals	64
3.4.2 Molt duration	64
3.4.3 Links between pupping phenology and molting phenology in one season	65
3.4.4 Inter-annual variation in ice dynamics, molt phenology, and colony attendance	66

3.4.5 Links between pupping and molting phenology in one season and pupping in the next	67
3.5 Discussion	67
3.5.1 Reproductive history affects molt phenology	68
3.5.2 Inter-annual variation in ice dynamics, molt phenology, and colony attendance	70
3.5.3 Cross-year carryover effects between molting and pupping	70
3.5.4 Implications of links between pupping and molting phenology	72
3.6 Acknowledgements	73
3.7 Literature Cited	87
Chapter 4. Seal diving behavior suggests shallowing of fish distributions during sea-ice driven phytoplankton blooms	97
4.1 Abstract	97
4.2 Introduction	98
4.3 Methods	99
4.3.1 Field methods	99
4.3.2 Diving data analysis	100
4.3.3 Percent ice cover	102
4.3.4 Diet analysis	103
4.4 Results and discussion	105
4.4.1 Seal dives become shallower in summer	105

4.4.2 Shallow dives are unrelated to pupping or molting	105
4.4.3 No evidence that diet changes during shallow diving period	106
4.4.4 Ice-driven physical-biological coupling	107
4.4.5 Summer shallowing of ocean biomass	107
4.4.6 Effect of the shallow diving period on foraging efficiency	110
4.4.7 Conclusions	111
4.5 Acknowledgments	112
4.6 Literature Cited	125
Chapter 5. An evaluation of three-dimensional photogrammetric and morphometric techniques for estimating volume and mass in Weddell seals <i>Leptonychotes weddellii</i>	135
5.1 Abstract	135
5.2 Introduction	136
5.3 Materials and Methods	139
5.3.1 Ethics statement	139
5.3.2 Field methods	140
5.3.3 Cones method	140
5.3.4 Correction equation method	141
5.3.5 Silhouette slice method	142
5.3.6 Statistical methods	143
5.4 Results	144

5.4.1 Actual mass.....	144
5.4.2 Processing time.....	144
5.4.3 Volume	144
5.4.4 Apparent (estimated) density	145
5.4.5 Estimated mass	146
5.5 Discussion	146
5.5.1 Summary.....	146
5.5.2 Apparent density values.....	148
5.5.3 Volume estimates	149
5.5.4 Field applications of morphometric and photogrammetric methods.....	151
5.6 Acknowledgments	153
5.7 Literature Cited	160
Chapter 6. General Conclusions	167
6.1 Literature Cited	173
Appendix. IACUC Approvals and NMFS Marine Mammal Permit	179

List of Figures

	Page
Figure 2.1. Selective pressures (squares) on moulting strategies (circles), including the group of endotherms that typically exhibits each strategy. Note that catastrophic moult is an extreme case of the annual moult.	34
Figure 2.2. Rock ptarmigan <i>Lagopus muta</i> (top, photographs by Jared Hughey) and snowshoe hares <i>Lepus americanus</i> (bottom, research photographs by Mills lab) both undergo complete biannual moults, shedding into a thicker, white plumage/pelage before winter and a thinner, dark plumage/pelage before summer.	35
Figure 3.1. During surveys, each individual was assigned a molt code: 0 (unmolted), 1 (head or dorsal stripe molted), 2 (head and wide dorsal stripe molted), 3 (flank starting to molt), or 4 (completely molted).	81
Figure 3.2. Based on individual sightings, adult female Weddell seals were assigned a phenology category for three life history events: pupping in Year 1, molting in Year 1, and pupping in Year 2. During the pupping season, Early-Puppers gave birth before the first 25%ile of the pupping distribution; Mid-Puppers gave birth on or between the 25-75%ile of the pupping distribution; Late-Puppers gave birth after the last 75%ile of the pupping distribution; Skip-Puppers had previously pupped but were not parturient in a given year; and Missing-Parous had been seen during the Year 1 pupping and molting season but were missing during the Year 2 pupping season. During the molting season, Early-Molters began molting before the first 25%ile of the molt start date distribution; Mid-Molters began molting on or between the 25-75%ile of the molting distribution; and Late-Molters gave began molting after the last 75%ile of the molt start date distribution.....	82

Figure 3.3. Molt sighting data from a theoretical animal with molt code n shown as numbers along the date axis. Each sighting is represented as a grey circle with molt code n shown. Mean molt stage durations τ_n were used to back-calculate a start date for each individual when the animal was not observed in a molt code n . A glossary of parameters is shown in the top panel. 83

Figure 3.4. Molt initiation dates across reproductive categories and years (panels; AS13 is the 2013 Austral Year including the December 2013 – February 2014 molt). Within each year, different letters denote significantly different molt initiation dates across reproductive categories (Tukey’s HSD, $p < 0.05$). During all study years, sexually mature females that did not produce a pup (Skips) molted earlier than all other reproductive categories. On the contrary, sexually mature females that produced a pup (Puppers) tended to molt later than sexually immature females (Immatures, significant difference in AS13, AS15, AS16), and Males (significant difference in AS13, AS16). 84

Figure 3.5. Proportion of seals in each molt category in Year 1 comprised of different reproductive categories from Year 1. Molt phenology was not independent of pupping phenology: the Early-Molters category was predominated by Skip-Puppers, whereas the Late-Molters category was predominated by Puppers. 86

Figure 4.1. Jaw motion events (b, red circles) were identified using a 0.3g amplitude threshold for surge acceleration based on the raw acceleration data (a). The number of wiggles per dive were also characterized as vertical excursions during the bottom phase (b). 116

Figure 4.2. Conceptual figure of deep-shallow-deep diving pattern (a) and empirical diving data from Weddell seals that exhibited that pattern (b). Dashed reference lines represent the start and end of “shallow” period, denoted as mean dive depth ≤ 200 meters. The ice break-out is coupled to the annual phytoplankton bloom, and larval krill undergo a developmental ascent to surface

waters seeking food [15], adult krill come to the surface to spawn [15], and fish larvae inhabit near-surface waters to feed on zooplankton [17]. We hypothesize that this aggregates seal prey into shallower waters and thus causes seals to dive shallower during the phytoplankton bloom.

..... 117

Figure 4.3. Maximum depth of each dive (grey open circles) plotted against time for one seal (#13468, gained 1.48kg/day), with results from the Generalized Additive Mixed Model (blue polygon) on 95th quantile of maximum dive depth (black closed circles). 119

Figure 4.4. Mean and standard deviation stable isotope values of Weddell seal prey groups (colored shapes) adjusted for trophic enrichment factors, along with Weddell seal whisker samples (white circles). 120

Figure 4.5. Seven-day running mean of percent ice cover for the four study years in McMurdo Sound, Ross Sea, Antarctica (satellite-derived sea ice concentration courtesy of the US National Snow and Ice Data Center; NASA Bootstrap SMMR-SSM/I combined dataset). The ice break-out (defined as <50% ice cover, red line) occurred earliest in AS15 and latest in AS16. 121

Figure 4.6. Model fits for 95th quantile of dive depth across summer, separated by year (top panel) and the tight relationship between Julian date of shallowest seal diving and Julian date of ice break-out (bottom panel). For each year, the day of shallowest diving occurred within 8-19 days of ice break-out (bottom panel). 122

Figure 4.7. Mean \pm standard deviation metrics for non-benthic dives of all seals: 95th quantile of seal dive depth (A), number of bottom wiggles per minute bottom time (proxy for feeding effort, B) and difference between ascent and descent rate (C) across the summer. For reference, semitransparent boxes encompass the “shallow period” days where the 95th quantile of dive

depth does not exceed 231 meters (within 25% of minimum daily dive depth 95th quantile, 23-day duration). 123

Figure 5.1. The photogrammetry procedure requires the photographer to slowly circle the seal, taking 8-12 photographs from all possible perspectives (i.e. kneeling, standing, portrait photographs, and landscape photographs). Photos are imported into PhotoModeler and a 3D shape is created by referencing scaled photographs to one another. 155

Figure 5.2. For the “silhouette slice” method, the portion of the seal below the ground plane is identified in PhotoModeler (top panel) and is removed to reduce error (bottom panel). 156

Figure 5.3. Estimated body density for adult, female Weddell seals calculated from actual body mass and estimated volume. The elliptical “cones” method estimated a higher density than both “correction equation” and “silhouette slice” methods. For reference, vertical lines show the density of seawater (black dotted line, 1.027 g cm⁻³ [37]), blubber (black dashed line, 0.920 g cm⁻³, this paper), and lean tissue (black dashed-dotted line, 1.1 g cm⁻³ [35]). 157

Figure 5.4. Regressions between actual and estimated mass for the three methods discussed: the equations calculated from de Bruyn et al. [32] (“correction equation”, left panel, $p < 0.0001$), the above-ground estimation (“silhouette slice”, middle panel, $p < 0.0001$), and the truncated cones method (“elliptical cones”, right panel, $p < 0.0001$). Black dashed lines show the 1:1 relationship between estimated and actual mass, whereas colored solid lines show the regression for each method. Horizontal lines show the offsets between data points and the 1:1 line. 158

Figure 5.5. Boxplots of the percentage error for each estimation method with frequency distributions overlaid as dashed lines. Mass estimates from each method were not significantly different than actual mass in the Weddell seals. 159

List of Tables

	Page
Table 2.1. Descriptions and examples of main moulting strategies in birds and mammals. Strategies are colour coded to match Figure 2.1	32
Table 3.1. Information about molt surveys during 2013-2016, including quartiles for pupping dates and mean \pm standard deviation molt initiation dates for each year and reproductive category. Significant differences in molt initiation dates among years (by row, within a reproductive category) are denoted with Roman numerals.	74
Table 3.2. Parameter values used to estimate molt duration and molt initiation dates for all ages and sexes combined.	75
Table 3.3. Model selection for molt initiation date. The Repro_cat*Year interaction includes the two main effects and the interaction.	76
Table 3.4. Transition probabilities from pupping categories in the Year 1 pupping season (rows) and molting categories in the Year 1 molting season (columns) for previously parous females. The expected molt category outcomes are provided in the column headers and assume a random distribution of molt timing across pupping categories, calculated from the contribution of all pupping categories to each molting category. Each cell contains the number of individuals with that transition outcome (top value), the actual proportion of animals with that transition outcome (middle top value), the actual minus expected outcome (middle bottom value, green if positive, red if negative) and the p-value for the Markov simulation of actual versus expected outcome (bottom value, *** $p < 0.05$ with Bonferroni correction). Actual transition outcomes sum to 100% for each reproductive history (row).	77

Table 3.5. Transition probabilities of parous female Weddell seals from Year 1 molting categories (rows) to Year 2 pupping categories (columns). See Table 3.4 legend for description of values.	78
Table 3.6. Transition probability from pupping Year 1 to pupping Year 2 (ignoring the intermediate molt phenology). See Table 3.4 legend for description of values.	79
Table 3.7. Summary of molt durations for pinniped species.	80
Table 4.1. Species, group, and isotopic values ($\delta^{15}\text{N}$ and $\delta^{13}\text{C}$) of Weddell seal prey species along with the diet contribution estimated from a SIAR mixing model. Due to statistically indistinguishable isotopic values, prey species were combined into prey groups before using mixing models.....	113
Table 4.2. Annual mean date and depth of shallowest diving for all seals. Despite the 33-day range in ice break-out date across the four study years, the shallowest seal diving date consistently occurred 8-19 days before ice break-out. Data are provided as mean \pm standard deviation.....	114
Table 4.3. Linear mixed effects models demonstrate that bottom wiggles are positively associated with prey capture attempts and mass gain, which correspond to slower descent rates. PC = number of prey capture attempts per dive; W = number of bottom phase wiggles per dive; MG = mass gain per hour diving (calculated as mass gain between deployment and recovery divided by the total number of hours diving); DR = descent rates in meters per second (calculated as 5-day average before tag recovery).	115
Table 5.1. Comparison of actual mass, parameter estimations, and percent error across estimation methods given as mean \pm standard deviation for 56 animals. Mass was estimated	

using three methods: elliptical “cones”, “correction equation”, and “silhouette slice”. Percent error was calculated as $100 \times \frac{\text{the difference between the estimated mass and the actual mass}}{\text{the actual mass}}$. Superscript letters denote a significant difference in parameters across estimation methods. The sedation, equipment, and time requirements for all methods are noted..... 154

Preface

The fieldwork and research presented here was primarily funded by National Science Foundation grant ANT-1246463 to Drs. Jennifer Burns and J. Ward Testa. My salary was provided by the NSF grant (2013-14) along with a National Institutes of Health, IDeA Networks of Biomedical Research Excellence Fellowship (2014-15), and a National Science Foundation Graduate Research Fellowship (2015-18). Additional research funding for Chapter 4 was provided by a National Geographic Committee for Research and Exploration Grant (to JMB and RSB), LGL Graduate Student Research Award (to RSB), and UAF Erich Follman Memorial Student Research Support (to RSB). I am extremely grateful that these funding sources allowed me the time and flexibility to follow my dreams.

This project was made possible by logistical support from the National Science Foundation (NSF) United States Antarctic Program, Lockheed Martin Antarctic Support Contract, and support staff in Christchurch, New Zealand and McMurdo Station. Research activities were approved by National Marine Fisheries Service Marine Mammal permit #17411, University of Alaska IACUC protocols #419971 and #854089 and the Antarctic Conservation Act permit #2014-003 (Appendix). This material is based upon work supported by the National Science Foundation Graduate Research Fellowship Program (RSB) and while serving at the National Science Foundation (JMB). Any opinion, findings, and conclusions or recommendations expressed in this material are those of the authors and do not necessarily reflect the views of the National Science Foundation.

Additionally, I was graciously given many learning and science communication opportunities from the following travel funds: Japan National Institute of Polar Research Internship, LGL Graduate Student Research Award, NSF Graduate Research Internship

Program, Society for Ecological Modeling Travel Grant, AntEco Travel Grant, College of Natural Science & Mathematics Student Travel Grant, Alaska INBRE Student Travel Grant, Biomedical Learning and Student Training Travel Grant, Society for Marine Mammalogy Student Travel Grant, and Association for Polar Early Career Scientists Grant for the Alan Alda Center for Communicating Science Workshop.

Finally, with generous funding from the PADI Foundation Scholarship for Outreach and Education, Amy Kirkham and I co-founded an outreach program and visited over 4,000 K-12 students in Alaska. Traveling to Antarctica is a rare opportunity, and we were excited to share our experiences with these young scientists. We are grateful, too, to the University of Alaska Press who helped turn our story into a children's book, "A Seal Named Patches", that has brought children from all over the world on an imaginary adventure to Antarctica.

Acknowledgments

With gratitude to my graduate committee: to Brian Barnes and Diane O'Brien who encouraged me to dig deeper and to see the bigger picture; to Greg Breed, who took me under his wing and kept me honest with comments like "Sternal recumbency? I have absolutely no idea what part of a seal that is. Use less jargon"; to Ward Testa, thank you for introducing me to the magical islands in the Bering Sea and for the scientific banter at Staff Quarters; and to my Skypervisor Jenn, who was in the lab with the rest of us cleaning gear after every single day in the field. Thank you for choosing me, believing in me, being patient with me, and understanding my need to be home.

My dreams of traveling to Antarctica began when I was 7 years old, and it took an army of people to turn my dreams into reality. I am forever indebted to my teachers at High Tech High School, who showed me the value of experiential learning, and to my mentors at UC Santa Cruz, who took a curious kid and made her into a scientist. I am especially grateful to Colleen Reichmuth and Dan Costa who introduced me to seals and have supported me ever since.

To the contractors in Antarctica who made our science possible: Thank you for turning "the ice" into a home, making sure that we never ran out of disposable pipettes, organizing spur-of-the-moment helicopter pickups, keeping our snow machines running, and making sea ice maps so we wouldn't get lost.

To the B-292 team with whom I spent nearly 300 days on the ice: you know better than anyone the blood (literally), sweat, and tears that went into this dissertation. You were there for the shipping drama, the 1am blood centrifuging, the C130 boomerang flight, the missed dinners, the weather delays, and the endless cryovial labeling. We have shared the most breathtaking,

once-in-a-lifetime experiences. Thank you for always keeping a smile on my face and a chocolate bar in my inside pocket.

Over the past five years I have lived a long-distance life, and the lack of routine was never easy. My deepest gratitude goes to the friends that motivated me when I was stuck and encouraged me to rest when I was pushing myself too hard. To my Fairbanks friends: I hope that no matter where we all end up, we can manage to host family dinners every once in a while. To my Pribilof Islands friends: I will always cherish my memories of the fur seal wicker calls during our rookery lunch breaks. To my Santa Cruz triathlon friends, especially Jon, Gerardo, Jen, Shawn, and Crystal, who took a stressed-out grad student and turned her into an IRONMAN: thank you for showing me that anything is possible. There's Nothing That I Wouldn't Rather Do than chase you up hills for many years to come. And to my best friends Beth, Amy, Claire, Rachael, Ginger, and Matt, I am beyond grateful to have you all just a phone call away.

To my family (and family in-law) for constantly reminding me that I have amazing people in my corner. Thank you for encouraging my fascination with the natural world when I was growing up. Merci pour ton amour sans fin. To my mom and dad, who through thick and thin, victories and defeats, breakthrough moments and injuries, spent countless hours sitting together on the sidelines of soccer fields. Thank you for showing me how it feels to be proud of, and fulfilled by, the work that I do. Your stability has allowed me to explore the world at ease.

To my sweetheart Patrick, who amazes me each day with his kindness, empathy, intelligence, and dedication. Thank you for warming my cold feet, joining me on cooking adventures, science-ing with me, and being my biggest fan. I imagine it must be difficult to nest with the migratory bird that I have become, but you have found a way to keep me grounded, and for that I am endlessly thankful.

Dedication

*to mom and dad
the wind beneath my wings*

*and to “airplane”
our angel*

Chapter 1. General Introduction

Fitness can be maximized when the timing, or phenology, of an individual's life history events such as breeding, molting, and migrating align with high resource availability [1], match phenology of conspecifics [2], and avoid phenology of predators. This synchronization is evident in a diversity of taxa, including: hibernation timing in arctic mammals [3], migration in high-latitude birds [4], diurnal activities in arid ectotherms [5], and feeding patterns in tropical reptiles [6]. In response to environmental change, numerous species can shift the timing of life history events [7-9]; however, in some species, the pace of phenotypic plasticity may be slower than that of the changing climate: caribou *Rangifer tarandus* calving dates are advancing less quickly than onset of the plant growing season [10], great tit *Parus major* egg lay dates are shifting slower than peak resource availability for nestlings [11], and snowshoe hare *Lepus americanus* molt has shown limited plasticity relative to decreases in snow cover [12]. Global climate change has the potential to cause temporal mismatches between individuals and their environment [13-16]. In addition, the disparate rates at which trophic levels respond are concerning because they can result in cascading ecosystem consequences [17]. Thus, it is imperative to characterize the duration and phenology of life history events, both in isolation and in the context of other events.

At high latitudes, the extreme seasonality and narrow window of favorable conditions constrains the range of potential phenology of mammalian life history events [18]. Like other polar mammals, Antarctic Weddell seals *Leptonychotes weddellii* fit molting, pupping, and breeding into the short, intense summer season. In October and November each year, female Weddell seals give birth and nurse their pups for six to seven weeks [19] and then replace their worn fur during an annual molt in January and February [20]. Weddell seals have been the focus of a long-term research program in Erebus Bay, Antarctica [21] because they exhibit high site

fidelity, experience limited human disturbance, and haul out in accessible locations. As a result, ages and reproductive histories are known for most of the population [22]. Weddell seals have low reproductive rates (60-75%) relative to most pinniped species [21, 23, 24]. Each year, about one in every three sexually mature females skips pupping, although the rate of intermittent pupping is highly variable among individuals [25]. Sequential mass measurements of lactating Weddell seals have demonstrated that nursing is energetically expensive, as seals lose up to 40% of their body mass across the lactation period [19] despite exhibiting a mixed income-capital breeding strategy [26]. As compared to individuals that nurse pups, “Skip-Puppers” expend significantly less energy during early summer, but many questions remain about the downstream benefits of skipping a year’s reproductive output.

Relative to the pupping period, much less is known about seal behavior and energetics during the following mid-summer foraging period, when seals are thought to regain mass prior to the annual molt [20]. Underwater behavior is difficult to study at this time due to the guaranteed failure of gluing telemetry devices to molting seals; thus, diving and feeding behavior during mid-summer has not been characterized. The recent miniaturization of biologging devices has allowed for flipper attachments and thus retention throughout the summer foraging and molting periods.

Studying Weddell seal diving during mid-summer is particularly relevant to understanding ecosystem dynamics because it coincides with peak productivity, when sea ice break-out and solar radiation trigger the dramatic but short-lived phytoplankton bloom. The reproductive phenology of zooplankton [27], fishes [28], penguins [29], and seals [30] are known to align with the phytoplankton bloom. As a result, deviations from normal bloom phenology can have cascading effects on the vital rates of upper trophic levels via trophic mismatches [29, 31-

33]. It is currently unknown how Weddell seal foraging success during the highly productive summer compares to other seasons. In Chapter 4, I use flipper-attached time-depth recorders to provide the first insight into Weddell seal diving behavior during the annual phytoplankton bloom. Successful foraging and mass gain during summer could help seals recuperate mass lost during the lactation period in preparation for the subsequent molting period.

Of the major life history events, migration, mate acquisition, and offspring rearing have been studied extensively. By comparison, relatively little attention has been given to the regular replacement of hair and feathers, known as molt. The molt is challenging to study for several reasons. First, the fur/feather replacement process begins in the follicles and is externally visible only after animals begin to shed their old fur/feathers [34, 35]. Additionally, studying molt progression requires repeated sightings of uniquely identified individuals. As a result, most molt studies are restricted to broad descriptions of molt strategies in a single species. Characterizing molt strategies in this way is crucial for characterizing annual cycles and understanding how birds and mammals achieve critical tasks such as camouflage, mate attraction, thermoregulation, and flight [36-39]. In addition, a precise understanding of molt phenology can be used to effectively implement research programs: abundance surveys or capture procedures can be scheduled when the greatest number of molting individuals will be hauled out [40], biogeochemical or toxicological analysis can be placed within relevant timeframes [41, 42], and glue-attached biologging devices can be strategically deployed shortly after hair regrowth.

In the mammal and bird species that have been studied, a large number of molting strategies has been identified, from the week-long catastrophic molt in northern elephant seals *Mirounga angustirostris* [43], to the two-year feather replacement cycle in California condors *Gymnogyps californianus* [44], to the three-times-per-year molt in ptarmigan *Lagopus spp* [45].

Until now, there exists no comprehensive review of the interacting environmental and social selection pressures that drive the evolution of molt strategies [46]. In Chapter 2, I review this topic in birds and mammals.

While high-latitude seals (order *Pinnipedeae*, family *Phocidae*) rely primarily on blubber for thermoregulation, fur provides some thermoregulation, mechanical protection, and drag reduction [47]. Exposure to cold air and water temperatures diminishes the quality of their fur throughout the year, and as a result, all seals exhibit an annual molting strategy [20]. As the world's southernmost mammal [48], Weddell seals are exposed to particularly cold ambient temperatures that render the pelage faded and brittle by the end of the annual cycle [20]. The Weddell seal molt has been broadly described by Green et al. [20], but molt duration and phenology have yet to be quantified in individuals.

The energetic demands of the Weddell seal molt have not been quantified. Energetic models have predicted mass loss during molt (i.e., energetic expenditure exceeds energy gain from foraging activity) [49], whereas empirical studies on other phocid seals have provided conflicting information [43, 50]. Body mass is the ultimate metric for understanding energy dynamics across the summer period. Unfortunately, body mass measurements are difficult due to the logistical difficulties of weighing seals that frequently forage and have large body sizes [51-55]. As an alternative to body mass measurements, mass estimation via photographs (hereafter, photogrammetry) has been used extensively [56-58]; however, photogrammetry must first be validated with weighed animals [59]. In Chapter 5, I quantify the accuracies of several commonly-used photogrammetric and morphometric techniques. These techniques can be used in future studies to understand the energy balance during Weddell seal life history events and in turn characterize their importance to the Weddell seal annual cycle.

Given the quick succession of pupping, foraging, and molting events during the austral summer, it is important to understand how the phenology and energetics of one life history event relates to the next. In Weddell seals, the effect of reproductive success on the molt, and the effect of the molt on future reproductive attempts, are not well understood at this time. In other mammal and bird species, reproductively unsuccessful and sexually immature individuals usually begin to molt earlier than reproductively successful individuals [60-66]. This is thought to be driven by gonadal hormone levels, such as estrogen and prolactin, that may inhibit molt initiation when elevated [67, 68]. In birds, reproduction has been associated with a later molt [69, 70]; in turn, delayed bird molts are linked to lower reproductive success and later reproductive timing in the subsequent year [69]. In mammals, the links between offspring birth dates and molting dates, and the consequent impacts of molting dates on reproductive success, are unknown. In Chapter 3, I quantify the duration and start date of the Weddell seal molt and characterize the carry-over effects of molting and pupping phenology (and *vice versa*). Characterizing these links in Weddell seals provides insight into how tradeoffs in energy allocation are balanced and how the molt may be related to the intermittent breeding strategy.

The aims of this dissertation are to characterize the phenological links between molt and reproduction, and to evaluate the importance of feeding success and reproductive success to those links. To achieve those goals, I measure the pupping phenology, molting phenology, time-activity budgets, morphometrics, and photogrammetrics of adult, female Weddell seals. In combination, the chapters of my dissertation shed light on the ecological, physiological, and behavioral drivers of pupping and molting phenology in a mammal during polar summer.

1.2 Literature Cited

1. McNamara JM, Houston AI. Optimal annual routines: behaviour in the context of physiology and ecology. *Philosophical Transactions of the Royal Society of London B: Biological Sciences*. 2008;363(1490):301-19.
2. Sheriff MJ, Richter MM, Buck CL, Barnes BM. Changing seasonality and phenological responses of free-living male arctic ground squirrels: the importance of sex. *Phil Trans R Soc B*. 2013;368(1624):20120480.
3. Buck CL, Barnes BM. Annual cycle of body composition and hibernation in free-living arctic ground squirrels. *Journal of Mammalogy*. 1999;80(2):430-42.
4. Cotton PA. Avian migration phenology and global climate change. *Proceedings of the National Academy of Sciences*. 2003;100(21):12219-22.
5. Levy O, Dayan T, Porter WP, Kronfeld-Schor N. Foraging activity pattern is shaped by water loss rates in a diurnal desert rodent. *The American Naturalist*. 2016;188(2):205-18.
6. Wikelski M, Hau M. Is there an endogenous tidal foraging rhythm in marine iguanas? *Journal of Biological Rhythms*. 1995;10(4):335-50.
7. Rubolini D, Saino N, Møller AP. Migratory behaviour constrains the phenological response of birds to climate change. *Climate Research*. 2010;42(1):45-55.
8. Watson A, editor *The effect of climate on the colour changes of mountain hares in Scotland*. *Proceedings of the Zoological Society of London*; 1963: Wiley Online Library.
9. Flux JE. Life history of the Mountain hare (*Lepus timidus scoticus*) in north-east Scotland. *Journal of Zoology*. 1970;161(1):75-123.

10. Post E, Pedersen C, Wilmers CC, Forchhammer MC. Warming, plant phenology and the spatial dimension of trophic mismatch for large herbivores. *Proceedings of the Royal Society of London B: Biological Sciences*. 2008;275(1646):2005-13.
11. Visser ME, Holleman LJ, Gienapp P. Shifts in caterpillar biomass phenology due to climate change and its impact on the breeding biology of an insectivorous bird. *Oecologia*. 2006;147(1):164-72.
12. Mills LS, Zimova M, Oyler J, Running S, Abatzoglou JT, Lukacs PM. Camouflage mismatch in seasonal coat color due to decreased snow duration. *Proceedings of the National Academy of Sciences*. 2013;110(18):7360-5.
13. Kronfeld-Schor N, Visser ME, Salis L, van Gils JA. Chronobiology of interspecific interactions in a changing world. *Phil Trans R Soc B*. 2017;372(1734):20160248.
14. Hoffmann AA, Sgrò CM. Climate change and evolutionary adaptation. *Nature*. 2011;470(7335):479-85.
15. Parmesan C. Ecological and evolutionary responses to recent climate change. *Annu Rev Ecol Evol Syst*. 2006;37:637-69.
16. Visser ME. Keeping up with a warming world; assessing the rate of adaptation to climate change. *Proceedings of the Royal Society of London B: Biological Sciences*. 2008;275(1635):649-59.
17. Thackeray SJ, Henrys PA, Hemming D, Bell JR, Botham MS, Burthe S, et al. Phenological sensitivity to climate across taxa and trophic levels. *Nature*. 2016;535(7611):241-5.

18. Costa DP. Reproductive and foraging energetics of high latitude penguins, albatrosses and pinnipeds: implications for life history patterns. *American Zoologist*. 1991;31(1):111-30.
19. Wheatley KE, Bradshaw CJ, Davis LS, Harcourt RG, Hindell MA. Influence of maternal mass and condition on energy transfer in Weddell seals. *Journal of Animal Ecology*. 2006;75(3):724-33. doi: 10.1111/j.1365-2656.2006.01093.x. PubMed PMID: 16689955.
20. Green K, Burton HR, Watts DJ. Studies of the Weddell seal in the Vestfold Hills, east Antarctica: Australian Antarctic Division; 1995.
21. Cameron M, Siniff D. Age-specific survival, abundance, and immigration rates of a Weddell seal (*Leptonychotes weddellii*) population in McMurdo Sound, Antarctica. *Canadian Journal of Zoology*. 2004;82(4):601-15. doi: 10.1139/z04-025.
22. Hadley GL, Rotella JJ, Garrott RA, Nichols JD. Variation in probability of first reproduction of Weddell seals. *Journal of Animal Ecology*. 2006;75(5):1058-70.
23. Chambert T, Rotella JJ, Garrott RA. An evolutionary perspective on reproductive individual heterogeneity in a marine vertebrate. *J Anim Ecol*. 2014. doi: 10.1111/1365-2656.12211. PubMed PMID: 24673453.
24. Chambert T, Rotella JJ, Higgs MD, Garrott RA. Individual heterogeneity in reproductive rates and cost of reproduction in a long-lived vertebrate. *Ecology and Evolution*. 2013;3(7):2047-60. doi: 10.1002/ece3.615. PubMed PMID: 23919151; PubMed Central PMCID: PMC3728946.
25. Rotella JJ, Paterson JT, Garrott RA. Birth dates vary with fixed and dynamic maternal features, offspring sex, and extreme climatic events in a high-latitude marine mammal. *Ecology and Evolution*. 2016;6(7):1930-41.

26. Hindell MA, Harcourt R, Waas JR, Thompson D. Fine-scale three-dimensional spatial use by diving, lactating female Weddell seals *Leptonychotes weddellii*. Marine Ecology Progress Series. 2002;242:275-84.
27. Kawaguchi S, Yoshida T, Finley L, Cramp P, Nicol S. The krill maturity cycle: a conceptual model of the seasonal cycle in Antarctic krill. Polar Biology. 2007;30(6):689-98.
28. Vacchi M, Pisano E, Ghigliotti L. The Antarctic silverfish: a keystone species in a changing ecosystem. Cham, Switzerland: Springer; 2017. 314 p.
29. Chapman EW, Hofmann EE, Patterson DL, Fraser WR. The effects of variability in Antarctic krill (*Euphausia superba*) spawning behavior and sex/maturity stage distribution on Adélie penguin (*Pygoscelis adeliae*) chick growth: a modeling study. Deep Sea Research II. 2010;57(7):543-58.
30. Proffitt KM, Rotella JJ, Garrott RA. Effects of pup age, maternal age, and birth date on pre-weaning survival rates of Weddell seals in Erebus Bay, Antarctica. Oikos. 2010;119(8):1255-64.
31. Ropert-Coudert Y, Kato A, Meyer X, Pellé M, MacIntosh AJ, Angelier F, et al. A complete breeding failure in an Adélie penguin colony correlates with unusual and extreme environmental events. Ecography. 2015;38(2):111-3.
32. Paterson JT, Rotella JJ, Arrigo KR, Garrott RA. Tight coupling of primary production and marine mammal reproduction in the Southern Ocean. Proceedings of the Royal Society of London B: Biological Sciences. 2015;282(1806):20143137.
33. Chambert T, Rotella JJ, Garrott RA. Environmental extremes versus ecological extremes: impact of a massive iceberg on the population dynamics of a high-level Antarctic marine

- predator. Proceedings of the Royal Society of London B: Biological Sciences. 2012;279(1747):4532-41.
34. Stutz SS. Pelage patterns and population distributions in the Pacific harbour seal (*Phoca vitulina richardi*). Journal of the Fisheries Board of Canada. 1967;24(2):451-5.
 35. Ling JK. Pelage and molting in wild mammals with special reference to aquatic forms. Quarterly Review of Biology. 1970:16-54.
 36. Jovani R, Blas J. Adaptive allocation of stress-induced deformities on bird feathers. Journal of Evolutionary Biology. 2004;17(2):294-301.
 37. Swaddle JP, Lockwood R. Wingtip shape and flight performance in the European Starling *Sturnus vulgaris*. Ibis. 2003;145(3):457-64.
 38. Dawson TJ, Blaney CE, Munn AJ, Krockenberger A, Maloney SK. Thermoregulation by kangaroos from mesic and arid habitats: influence of temperature on routes of heat loss in eastern grey kangaroos (*Macropus giganteus*) and red kangaroos (*Macropus rufus*). Physiological and Biochemical Zoology. 2000;73(3):374-81.
 39. Smith HG, Montgomerie R. Sexual selection and the tail ornaments of North American barn swallows. Behavioral Ecology and Sociobiology. 1991;28(3):195-201.
 40. Daniel RG, Jemison LA, Pendleton GW, Crowley SM. Molting phenology of harbor seals on Tugidak Island, Alaska. Marine Mammal Science. 2003;19(1):128-40.
 41. Beltran R, Sadou M, Condit R, Peterson S, Reichmuth C, Costa D. Fine-scale whisker growth measurements can reveal temporal foraging patterns from stable isotope signatures. Marine Ecology Progress Series. 2015;523:243-53. doi: 10.3354/meps11176.

42. Brasso RL, Drummond BE, Borrett SR, Chiaradia A, Polito MJ, Rey AR. Unique pattern of molt leads to low intraindividual variation in feather mercury concentrations in penguins. *Environmental Toxicology and Chemistry*. 2013;32(10):2331-4.
43. Worthy G, Morris P, Costa D, Le Boeuf B. Moulting energetics of the northern elephant seal (*Mirounga angustirostris*). *Journal of Zoology*. 1992;227(2):257-65.
44. Snyder NF, Johnson EV, Clendenen DA. Primary molt of California condors. *Condor*. 1987;468-85.
45. Pyle P. Revision of molt and plumage terminology in ptarmigan (Phasianidae: *Lagopus* spp.) based on evolutionary considerations. *The Auk*. 2007;124(2):508-14.
46. Terrill RS. Evolutionary interactions of feather molt in birds 2017.
47. Erdsack N, Dehnhardt G, Witt M, Wree A, Siebert U, Hanke W. Unique fur and skin structure in harbour seals (*Phoca vitulina*)—thermal insulation, drag reduction, or both? *Journal of The Royal Society Interface*. 2015;12(104):20141206.
48. Stirling I. Ecology of the Weddell seal in McMurdo Sound, Antarctica. *Ecology*. 1969;573-86.
49. Beltran RS, Testa JW, Burns JM. An agent-based bioenergetics model for predicting impacts of environmental change on a top marine predator, the Weddell seal. *Ecological Modelling*. 2017;351:36-50.
50. Ashwell-Erickson SM, Elsner R. The energy cost of free existence for Bering Sea harbor and spotted seals: University of Alaska, Fairbanks; 1981.
51. Ozgul A, Childs DZ, Oli MK, Armitage KB, Blumstein DT, Olson LE, et al. Coupled dynamics of body mass and population growth in response to environmental change. *Nature*. 2010;466(7305):482-5.

52. Durban J, Parsons K. Laser metrics of free-ranging killer whales. *Marine Mammal Science*. 2006;22(3):735-43.
53. Shrader AM, Ferreira SM, Van Aarde RJ. Digital photogrammetry and laser rangefinder techniques to measure African elephants. *South African Journal of Wildlife Research*. 2006;36(1):1-7.
54. McDonald BI, Crocker DE, Burns JM, Costa DP. Body condition as an index of winter foraging success in crabeater seals (*Lobodon carcinophaga*). *Deep Sea Research Part II: Topical Studies in Oceanography*. 2008;55(3):515-22.
55. Ireland D, Garrott RA, Rotella J, Banfield J. Development and application of a mass-estimation method for Weddell seals. *Marine Mammal Science*. 2006;22(2):361-78.
56. Krause DJ, Hinke JT, Perryman WL, Goebel ME, LeRoi DJ. An accurate and adaptable photogrammetric approach for estimating the mass and body condition of pinnipeds using an unmanned aerial system. *PloS one*. 2017;12(11):e0187465.
57. Shero MR, Pearson LE, Costa DP, Burns JM. Improving the precision of our ecosystem calipers: a modified morphometric technique for estimating marine mammal mass and body composition. *PLOS ONE*. 2014;9(3):e91233.
58. Schwarz LK, Villegas-Amtmann S, Beltran RS, Costa DP, Goetsch C, Hückstädt L, et al. Comparisons and uncertainty in fat and adipose tissue estimation techniques: the northern elephant seal as a case study. *PLOS ONE*. 2015;10(6):e0131877.
59. de Bruyn PJN, Bester MN, Carlini AR, Oosthuizen WC. How to weigh an elephant seal with one finger: a simple three-dimensional photogrammetric application. *Aquatic Biology*. 2009;5:31-9. doi: 10.3354/ab00135.

60. Morton GA, Morton ML. Dynamics of postnuptial molt in free-living mountain white-crowned sparrows. *Condor*. 1990;813-28.
61. Newton I. The moult of the Bullfinch *Pyrrhula pyrrhula*. *Ibis*. 1966;108(1):41-67.
62. Flinks H, Helm B, Rothery P. Plasticity of moult and breeding schedules in migratory European Stonechats *Saxicola rubicola*. *Ibis*. 2008;150(4):687-97.
63. Pitelka FA. Timing of molt in Steller Jays of the Queen Charlotte Islands, British Columbia. *The Condor*. 1958;60(1):38-49.
64. Boily P. Metabolic and hormonal changes during the molt of captive gray seals (*Halichoerus grypus*). *American Journal of Physiology-Regulatory, Integrative and Comparative Physiology*. 1996;270(5):1051-8.
65. Kirkman S, Bester M, Pistorius P, Hofmeyr G, Jonker F, Owen R, et al. Variation in the timing of moult in southern elephant seals at Marion Island. *South African Journal of Wildlife Research*. 2003;33(2):79-84.
66. Badosa E, Pastor T, Gazo M, Aguilar A. Molt in the Mediterranean monk seal from Cap Blanc, western Sahara. *African Zoology*. 2006;41(2):183-92.
67. Raeside J, Ronald K. Plasma concentrations of oestrone, progesterone and corticosteroids during late pregnancy and after parturition in the harbour seal, *Phoca vitulina*. *Journal of Reproduction and Fertility*. 1981;61(1):135-9.
68. Boyd I. Changes in plasma progesterone and prolactin concentrations during the annual cycle and the role of prolactin in the maintenance of lactation and luteal development in the Antarctic fur seal (*Arctocephalus gazella*). *Journal of Reproduction and Fertility*. 1991;91(2):637-47.
69. Newton I. Molt and plumage. *Ringling & Migration*. 2009;24(3):220-6.

70. Dietz MW, Rogers KG, Piersma T. When the seasons don't fit: speedy molt as a routine carry-over cost of reproduction. *PLoS One*. 2013;8(1):e53890.

Chapter 2. Convergence of biannual moulting strategies across birds and mammals¹

2.1 Abstract

Birds and mammals have developed numerous strategies for replacing worn hair and feathers. Moulting usually occurs on an annual basis; however, moults that take place twice per year (biannual moults) also occur. Here, we review the forces driving the evolution of various moult strategies, focusing on the special case of the complete biannual moult as a convergence of selection pressures across birds and mammals. Current evidence suggests that harsh environmental conditions or seasonality (e.g. larger variation in temperatures) drive evolution of a biannual moult. In turn, the biannual moult can respond to secondary selection that results in phenotypic alteration such as colour changes for mate choice dynamics (sexual selection) or camouflage requirements (natural selection). We discuss the contributions of natural and sexual selection to the evolution of biannual moulting strategies in the contexts of energetics, niche selection, functionality, and physiological mechanisms. Finally, we suggest that moult strategies are directly related to species niche because environmental attributes drive the utility (e.g. thermoregulation, camouflage, social dynamics) of the hair or feathers. Functional efficiency of moult may be undermined if the pace of evolution fails to match that of the changing climate. Thus, future research should seek to understand the plasticity of moult duration and phenology, especially in the context of annual cycles.

¹ RS Beltran, JM Burns, GA Breed. Review: Convergence of biannual moulting strategies across birds and mammals. Proceedings of the Royal Society of London B. 20180318. <http://dx.doi.org/10.1098/rspb.2018.0318>

2.2 Introduction

Hair and feathers are non-living keratinous structures that degrade or fade through wear and breakage as they age. This reduced functionality can reduce individual fitness by compromising flight [1, 2], thermoregulation [3], and mating abilities [4]. Because the structures are non-living, the only mechanism for damage repair is complete replacement through shedding (a protracted, year-round replacement) or moult (a contracted, punctuated replacement) [5]. Though some species forgo migration and feeding events during the period when fur/feathers are replaced [6], no species has been documented to skip an entire moult cycle, suggesting its key importance to endotherm life cycles [7, 8]. Despite this importance, moulting is one of the most poorly studied life history events, particularly in mammals, but also in birds [9].

Birds and mammals exhibit a wide variety of moulting strategies [10, 11]. Most can be simplified and divided into two categories: replacement of fur or feathers after 12 months (hereafter, annual moult) and replacement of some or all fur or feathers twice per year (hereafter, incomplete or complete biannual moult). By definition, the first moult occurs after breeding and produces basic, non-breeding plumages (in birds, body and flight feathers replaced) or winter pelages (in mammals). The second moult of the year is almost always incomplete [8, 12], producing the alternate breeding plumage (in birds, body feathers replaced) or summer pelage (mammals). In some species, however, all feathers or fur are replaced during a complete second moult. In addition, some species can slow or halt a moult [13] due to nutritional deficiency or migration timing constraints and continue later (hereafter, facultative split moult) or in extreme cases, break the moult cycle (hereafter, partial moult) [14]. Still other species may replace fur during a

protracted, year-round process (hereafter, continuous moult) [15] or may take more than one year to perform a complete moult (hereafter, biennial moult) [16, 17]. Finally, some species exhibit a catastrophic or simultaneous moulting strategy where plumage or pelage function is temporarily compromised as feathers or fur are shed rapidly. The range of moulting strategies are subject to a wide range of selective forces (Table 2.1); understanding the factors underlying the variation in moult strategies is important for predicting future impacts of global change.

Here, we review contributions of natural and sexual selection to the frequency and timing of moult in birds and mammals in the context of energetics, ecological niches, functions, and physiological mechanisms. For simplicity, we limit the scope of our review to sexually mature adults (i.e. no juvenile plumages).

2.3 Functional roles and forms of pelage and plumage

The evolution of feathers and fur has allowed endothermic vertebrates to inhabit both land and sea [18, 19]. Plumages and pelages serve a variety of functions, such as providing thermal insulation by creating an air barrier between bare skin and surrounding ambient conditions [20], enhancing camouflage and/or mate attraction through coloration, providing mechanical protection, and altering fluid flow to minimize drag in flying and swimming species [13, 20, 21]. In mammals, fur generally includes long, coarse guard hairs, and numerous fine, short underhairs [22]. Birds have a more diverse set of above-skin coverings including several types of feathers (flight, down, tail, contour, semiplume, bristle, filoplume) that vary widely in their function and form. For example, flight feathers that provide thrust (primaries) and lift (secondaries) are characterized by

windproof surfaces of interlocking microstructures that allow birds to manoeuvre in the air. By contrast, down feathers have exceptional insulative properties that out-perform nearly all man-made materials.

Plumage and pelage morphologies of temperate/polar birds and mammals differ from those of tropical birds and mammals [13]. For example, tropical mammals rarely have fur longer than 20 mm [23], while arctic and high temperate mammals can have fur up to 70 mm, with relatively fine, abundant underhairs. Similarly, temperate and tropical birds have fewer down feathers and shorter contour feathers than those residing in polar areas [24]. While fur and feathers primarily provide insulation for animals in cool climates, they can also reflect solar radiation to reduce heat gain in hot climates. For instance, plumage reflectance is 65-69% higher for white plumage relative to black plumage and is thus beneficial for tropical birds nesting in open habitat [25]; however, white plumage may be less advantageous as wind speed increases, because white plumage limits convective cooling and thus retains a higher heat load [26]. Alternatively, white feathers and fur camouflage polar species such as snow petrels *Pagodroma nivea* and arctic foxes *Vulpes lagopus* in their snow-covered habitats.

2.4 Metabolic costs of moult

A biannual moult is expected when the energetic or fitness cost of producing a new pelage/plumage is less than the cost incurred by having suboptimal pelage/plumage coloration or insulation during different seasons. Although the sedentary nature of moulting animals minimizes transport costs [27], the moulting process (in combination, energy content of new tissue, production efficiency of new tissue, and compromised

thermoregulation) incurs considerable costs above those required for basal maintenance. In small terrestrial mammals, pelage accounts for between 4% [28] and 15% [29] of total body mass. These pelage proportions exceed those of large mammals (1.7% fur in Weddell seals [30]; 3.4% in fur and skin of northern elephant seals [31]; 4-4.5% in muskoxen [32]), likely because the smaller mammals have larger surface area (i.e. fur) to body mass ratios [33]. The energetics of moulting mammals has been studied almost exclusively in phocid seals (family *Phocidae*) with most studies reporting minimal [31] or no [34] added metabolic cost aside from the reduced activity. To our knowledge, no estimates exist for the energetic efficiency of fur production in mammals.

Moult energetics have been more extensively investigated in avian species. Plumages account for 4% [35] to 20% [36] of total body dry mass of birds. Less than 30% of energy used by moulting birds is thought to be incorporated into feathers [37]; the remaining energy is expended on the increases in thermoregulatory costs from the associated skin perfusion [30], increases in flight costs from reduced wing area [38], and production of tissues needed for feather synthesis [39]. It is difficult to disentangle the contributions of thermoregulation, protein deposition, and efficiency to the cost of the moult; as a result, most researchers report the overall metabolic increase during the moult. Moulting costs vary by species and can be large [40, 41], with metabolic rate increasing by 10% in red knots *Calidris canutus* [42], 12% in common eiders *Somateria mollissima* [27], 15-16% in blue jays *Cyanocitta cristata* and scrub jays *Aphelocoma californica* [43], 58% in white crowned sparrows *Zonotrichia leucophrys*, and 82% in white-plumed honeyeaters *Lichenostomus penicillatus* [44] relative to non-moulting individuals [45]. The energy cost of feather synthesis increases proportionally with basal

metabolic rate [45], such that small birds have higher mass-specific moult costs relative to large birds.

The highly variable moulting costs can be explained by interactions between moulting strategies, life histories, and environmental conditions. Rapid moults tend to occur in animals that experience greater mortality or energetic costs due to reduced functionality of fur or feathers [8, 10]. For instance, follicular growth requires perfusion to maintain skin temperature above a certain threshold [46], which could exacerbate heat loss during the moulting period in cold climates [47, 48]. Because the duration of favourable seasons decreases at high latitudes (e.g. “seasons of stress, seasons of opportunity”; [49]), moults in polar resident and breeding birds tend to be shorter than in tropical birds [50, 51]. In contrast, under less seasonal conditions (e.g. tropical regions), a more prolonged moult maximizes energetic efficiency because it avoids high daily costs of thermoregulation and fur growth [50]; as a result, tropical avian moults are usually slow [52]. We propose that the necessity of optimizing energetic expenditures coupled with the apparently high cost of moult provides a strong selection pressure for convergence of moulting durations within environmental niches.

2.5 Selection pressures and moulting strategies

Birds and mammals that inhabit comparable environmental niches must solve similar social, thermal, and energetic problems to survive and reproduce [53]. Because these selective pressures constrain moulting strategies, similar moulting strategies have evolved across avian and mammalian species where niches overlap [10]. For example, while an annual moult is usually sufficient to offset normal fur or feather degradation

rates, biannual moults are particularly common in species of birds and mammals that occupy harsh habitats or use seasonal plumages for territory defence or mate attraction [11, 13, 54]. It is important to consider differing moulting strategies may arise under ecological or social selection forces (Figure 2.1) [55].

The highly ornamented breeding plumages of many avian species are well known examples of sexual selection [56]. Many species (e.g. mandarin ducks *Aix galericulata*, Indian peacocks *Pavo cristatus*) have evolved colourful plumages because of female preference for more ornamented males [56]. The strong sexual selection for male birds to grow brightly coloured body feathers (i.e. alternate plumage) prior to the breeding season is usually facilitated by an incomplete second moult (i.e. biannual moult), which allows animals to return to a more cryptic plumage during the rest of the year [55]. Birds have tetrachromatic colour vision [57], which creates opportunities for heritable variations in plumage colour. Conversely, mammals generally have dichromatic vision with relatively poor colour sensitivity. Limited colour vision restricts the utility of colour in mating displays and thus minimizes sexual selective pressures for evolution of ornamental fur pigmentation in mammals [58]; here, the natural selective forces for crypsis dominate. As a result, coloration of most mammals is duller than many avian species and sexual dichromatism is nearly absent in mammals. Notable exceptions are primates and marsupials, which have retained trichromatic vision [59] and use bright colours (e.g. faces of mandrills *Mandrillus sphinx*, rumps of hamadryas baboons *Papio hamadryas*, and chests of geladas *Theropithecus gelada*) for intraspecific communication. However, these colours result from structural components in the skin rather than replaceable fur [59] and thus are independent from the pelage moult [60].

At least in mammals, some species with no sexual selection on pelage colour still undergo two complete moults per year. Strong seasonality in temperatures, such as occur in arctic, alpine, and temperate climates, require animals to either avoid temperature extremes through migration or to adapt to seasonal camouflage and insulation requirements. Thus, the selective forces of seasonal habitat transformations affect both migrants and residents, in different ways: requiring increased insulation, increased camouflage, or increased replacement due to degradation. We discuss each of these components below.

Many high latitude species have evolved behavioural strategies to cope with the extreme cold, including: hibernation in brown bears *Ursus arctos* [61], under-snow lairs in ruffed grouse *Bonasa umbellus* [62], “behavioural wintering” in European badgers *Meles meles* [63], and under-snow social aggregations in red-backed voles *Myodes gapperi* [64]. In contrast, species that are active above the snow rely heavily on insulation of the pelage or plumage during winter [22]. These species often have a biannual moult wherein a more insulative winter pelage or plumage replaces that of summer. In mammals, underfur from the winter pelage can vary in density, length, diameter, colour and texture, and guard hairs can be finer and longer to increase their insulation [22]. These anatomical changes have been observed in many species such as ferrets *Mustela putorius furo* [65], elk *Cervus canadensis* [66], mink *Mustela vison* [67], snow leopards *Panthera uncia* [68], white-tailed deer *Odocoileus virginianus* [69], moose *Alces alces* [70], grey squirrels *Sciurus carolinensis* [71], white-footed mice *Peromyscus leucopus* [72], and lesser white-toothed shrews *Crocidura suaveolens* [73]. Winter pelages can decrease the lower critical temperatures of red foxes *Vulpes vulpes* and porcupines

Erethizon dorsatum by $\sim 20^{\circ}\text{C}$ [22]. For these high latitude mammals, meeting insulation requirements does not require a colour change, so rather than a full second moult per year, these species typically grow a thicker pelage before the winter and then shed into their thinner summer pelage during spring to allow heat exchange. We consider this an incomplete moult because the summer shedding process is a partial loss of previous pelage (and occasional replacement of some fur) rather than growth of an entirely new pelage. Polar resident birds show a similar pattern of enhanced insulation in the basic (winter) plumage. During winter, non-migratory house sparrows *Passer domesticus* increase plumage weight 70% [49], and goldfinches *Carduelis carduelis* increase plumage weight up to 50% [74]. The purpose of the added winter pelage or plumage in these species is probably for thermoregulatory advantage rather than cryptic or breeding coloration.

When habitats are snow-covered, a combination of camouflage and thermoregulatory selection pressures have driven a biannual moult that facilitates an entirely white, thick winter pelage/plumage. Because summer pelage is usually brown, black, or grey, these species typically facilitate their fall and spring pelage changes by complete shedding of the previous pelage (i.e. complete biannual moult) rather than adding to the fur already grown. For example, to camouflage with seasonal snowfall in high latitude environments, rock, willow, and white-tail ptarmigan *Lagopus spp* alternate between pigmented, summer plumage and white, winter plumage [75], with longer winter feathers (42% longer contour feathers, 29% longer down feathers) than in summer [24]. Some terrestrial mammals such as Arctic, mountain, and snowshoe hares *Lepus spp* [76]; least, long-tailed, and short-tailed weasels *Mustela spp* [77]; Peary caribou *Rangifer*

tarandus pearyi [78]; collared lemmings *Dicrostonyx groenlandicus* [79]; Siberian hamsters *Phodopus sungorus* [80]; and arctic foxes *Vulpes lagopus* [81] complete an analogous biannual moult to grow a more insulative white pelage (Figure 2.2).

In addition to seasonal coloration and thermoregulation requirements, moulting strategies can also reflect the rate of degradation of features or fur. In temperate and tropical species, pelage or plumage degradation can result from abrasive vegetation, wind, and sand [22]. Likewise, the plumages of birds in humid climates are subject to feather-degrading bacteria [82]. The melanin associated with darker feathers increases feather keratin thickness (abrasion resistance) and solar absorption (above optimal temperature for microbe growth); thus, darker feathers tend to be found in more humid environments, termed Gloger's rule. In high latitude species, exposure to UV radiation during summer and to extreme cold during winter degrades pelage/plumage [54] by denaturing keratin and other structural proteins [83]. The ambient conditions and food availability of high latitude environments are inherently seasonal and thus provide strong selection pressures relative to tropical habitats that are relatively benign and homologous [84]. Thus, it is no surprise that the presence of the biannual moult can be explained more by environmental conditions than by phylogenetic relationships among birds and mammals.

2.6 Special considerations for aquatic species

Semi-aquatic animals have additional selection pressures from the increased thermal conductivity of water. When submerged, water replaces the insulating air layer between fur and reduces the thermal resistance of fur by 84-92% [85]. For diving animals

like phocid seals (family *Phocidae*), water pressure at depth diminishes the utility of fur insulation; instead, phocid seals rely almost exclusively on blubber for insulation. These blubber stores enable phocid seals to exploit seasonally available prey and withstand lower ambient temperatures than would be possible if they relied on fur alone; consequently, phocids have a wide niche and inhabit both polar and non-polar environments (10 polar species, 8 non-polar species). In contrast, sea lions and fur seals (family *Otariidae*) rely heavily on pelage for insulation and inhabit almost exclusively temperate and tropical environments (1 polar species, 13 non-polar species), with the Antarctic fur seals *Arctocephalus gazella* having denser fur than other species. These aquatic mammals are not required to coordinate pelages with seasonal changes due to the seasonally homogenous colour and temperature of their marine environments and thus only exhibit a single moult per year [10], with phocid seals moulting more rapidly than otariids. Sea otters *Enhydra lutris*, by contrast, replace fur continuously, likely due to their reliance on extremely thick pelage (up to 140,000 hairs/cm² [86]) for aquatic thermoregulation.

Some pinniped and avian species undergo an extreme annual moult that involves a rapid, nearly simultaneous shedding of all pelage or plumage [31, 87]. This is generally termed the “catastrophic moult” although a consistent definition has not yet been established. Northern elephant seals *Mirounga angustirostris*, southern elephant seals *Mirounga leonina*, Hawaiian monk seals *Neomonachus schauinslandi*, and penguins (order *Sphenisciformes*) are the only species described in the literature to moult this way [31, 87, 88]. In the pinniped literature, catastrophic moult refers to moulting of a thick epidermal layer in conjunction with hair loss (i.e. peeling skin sheets attached to hair

roots, in contrast to small flakes of skin as in some Weddell seals *Leptonychotes weddellii* [89]) [31, 88, 90], and all catastrophic moulting species are known to fast during hair replacement. In the avian literature, the distinction between catastrophic and non-catastrophic moult seems to be the duration of moult, with penguins moulting all feathers in 13-34 days (relative to a couple months [91] or more [92] in ordinary moult) while fasting [87]. The regeneration of skin and fur requires elevated skin temperature and surface blood flow [46] so concurrent moulting and feeding would result in drastic thermoregulatory losses in the highly thermally conductive marine environment. Similarly, moulting impedes the insulative, waterproof, and hydrodynamic functions of penguin plumage that are crucial for underwater foraging; as a result, these animals fast for the entire duration of the moult. Thus, across taxa, animals with catastrophic moults appear to meet two criteria: 1) they lose function of their pelage or plumage during the moult, and 2) they do not feed during the moult. To our knowledge, no terrestrial mammals undergo catastrophic moults.

Some birds, including common eiders *Somateria mollissima* (36 day moult [27]), lesser snow geese *Chen caerulescens caerulescens* (less than one month moult [93]), Hawaiian gallinules *Gallinula galeata sandvicensis* (21-54 day moult [94]), and grebes (order *Podicipedidae*, ~20 day moult [95]) undergo a quick simultaneous wing moult that renders them flightless; however, they do not fast during this moult, and the moult has not been referred to as “catastrophic” in the literature. The high energetic cost of the catastrophic and simultaneous moults [31] precludes a twice-per-year moult in these species; these strategies serve as interesting contrasts to the longer moults of many species in less thermally challenging environments.

Although hairless, at least four polar cetacean species undergo a similar catastrophic moult of their epidermis: killer whales *Orcinus orca* [96], southern right whales *Eubalaena australis* [97], belugas *Delphinapterus leucas* [98], and bowhead whales *Balaena mysticetus* [99]. All cetaceans experience selective pressures to deter ectoparasitic and commensal organisms (e.g. lice, barnacles, diatoms) from attaching to the skin [100] by continuously replacing their vascularized skin. For polar cetaceans, the extremely cold sea temperatures likely make prolonged skin perfusion energetically costly [96]. To avoid large heat loss associated with skin perfusion in cold water, these species migrate to warmer waters and replace/exfoliate their skin in a concentrated period [101]. In these cases, migration to moulting habitats can result in considerable metabolic costs.

2.7 Physiological mechanics of pelage and plumage replacement

Physiological drivers of avian and mammalian moults are generally similar, with age, sex, condition, and reproductive status affecting the timing and duration of moult [102, 103]. Internal factors (biological clocks, body condition) exert control via nervous and endocrine processes, and rely on external cues (zeitgebers, such as photoperiod and temperature cycles) for synchronization [104]. In combination, these mechanisms coordinate and sequence moult with other life history events, such as migration and reproduction, and align them with optimal environmental conditions [105].

A variety of hormones interact to regulate moult: thyroxine and progesterone promote hair and feather synthesis, whereas oestrogen and cortisol suppress it [102]. Corticosterone is downregulated during moult because it appears to negatively affect

feather quality [106]. Thyroxine influences moult onset [42] and duration by increasing metabolic activity of feather forming cells in a permissive rather than causal manner [107]. The timing of peak prolactin is linked to (and slightly precedes) moult start date [36], and prolactin and thyroxine appear mechanistically linked [108, 109]. Apart from species that exhibit moult-breeding overlap, moult initiation is inhibited by elevated levels of gonadal hormones such as oestrogen and testosterone. Consequently, sexually immature or reproductively unsuccessful individuals often initiate moult earlier than successful breeders, probably due to the reduction in levels of sex steroids. Moult timing is also influenced by body condition, which is driven by resource availability and reproductive output. Poor body condition, associated with increased cortisol levels, has been found to suppress thyroid hormones [110], causing slower and longer moult [106]. For instance, lower food abundance has been found to delay moult onset in harbour seals *Phoca vitulina* [102] while food abundance has been found to advance moult onset in swamp sparrows *Melospiza georgiana* [111]. Indeed, birds in superior body condition often advance moult timing and replace plumage more rapidly [112], possibly due to their lower circulating corticosterone. We note that endocrine control, which we have greatly simplified here, is not the only regulatory mechanism for moult. The roles of intrinsic and extrinsic factors for regulating moult phenology are topics of current research. See Payne et al. [113] and Zimova et al. [105] for detailed reviews.

Synthesis and secretion of hormones that regulate moult are coordinated in part by seasonal cues that affect the pituitary gland primarily through melatonin signalling and hypothalamic control. Experimental manipulations of temperature and photoperiod have both been found to induce changes in winter pelage [22]. In snowshoe hares *Lepus*

americanus, the winter moult was entirely suppressed when air temperature warmed by 7°C [76]. Conversely, cold exposure has delayed and shortened the spring moult in short-tailed weasels *Mustela erminea* [114] and accelerated the fall moult of the white-footed mouse *Peromyscus leucopus* [72].

The species-specific reliance on photoperiod or temperature cues has evolved based on environment. For instance, photoperiod appears to be the critical driver of moult in high latitude birds and mammals, while temperature and nutrition can modulate its timing. On the other hand, tropical residents and species that are subject to consistent annual daylength may rely heavily on non-photoperiodic cues such as temperature and rainfall [113]. Amphibious mammals such as pinnipeds apparently use a combination of cues for moult onset, including endogenous rhythms, changes in photoperiod, sea temperature, air temperature, and body condition [115]. In turn, moult onset cues decide how species respond to global change; for example, migratory birds that depend on photoperiod cues for moult onset are expected to respond with less phenotypic plasticity than those cued by temperature [116].

2.8 Feedbacks between moult and global change

By changing the colour or insulation of pelage and plumage, the biannual moult can increase seasonal functionality; however, a biannual moult may be maladaptive under global change scenarios. If the pace of evolution fails to match that of climate warming [117], the functional efficiency of moult may be undermined. For instance, phenological mismatches between snow presence and snowshoe hare *Lepus americanus* pelage coloration could compromise crypsis and lead to elevated predation risk [118]. In ambush

predators such as snow leopards *Panthera uncia*, similarly compromised crypsis could lead to diminished foraging success. For example, evidence for phenotypic plasticity to variable conditions has been found in mountain hares *Lepus timidus*, which tend to have slower spring moults (white to brown pelage coloration) in colder springs [119] and faster winter moults (brown to white) during colder falls [120]. Other studies have demonstrated that life histories can limit the flexibility of moult duration and phenology and thus limit adaptive capacities. For example, long-distance migrants have advanced their phenology less than short-distance migrants [116] because they have no information about phenology on the breeding grounds while in their wintering grounds [104]. Differential rates of phenological flexibility can lead to progressively mismatched seasonal timing between interacting species [104]. As a result, phenological plasticity can have population-level consequences under climate change.

2.9 Conclusion

In his seminal paper on mammalian moulting strategies in 1970, Ling [13] noted that “moult patterns... may be very different in closely related species ... and very similar in widely separated taxonomic groups”. Here, we synthesize evidence that environmental conditions are important in determining the frequency of moulting in birds and mammals. Because the functional roles of pelage and plumage are defined by environmental niches, moulting strategies across taxa converge as a function of environmental conditions [6]. In endotherms that inhabit higher latitudes, plumages and pelages play distinct seasonal roles [10] in camouflage (pelage colour polyphenism, [118]), insulation, and mate attraction. In birds, the biannual moult evolved from the

ancestral state of a single summer moult [11, 121, 122] as a response to energetic and environmental selection factors. We suggest that the same could be true in mammals, giving the moult similar adaptive functions across avian and mammalian taxa.




Comparative studies across taxa that share life history characteristics provide insight into the wide range of functional roles that have caused strategies to emerge. Researchers should take care to document species-typical moult routines and place these routines within the framework of other critical life history events and their environmental niches.

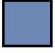
2.10 Acknowledgments

Thank you to Ryan S. Terrill, Claire Nasr, Parker Forman, and Amy Kirkham for reviewing previous drafts and to Diane O'Brien, Brian Barnes, and Ward Testa for helpful discussions. This work was supported by the National Science Foundation Graduate Research Fellowship Program under Grant No. DGE-1242789 to RSB. Any opinion, findings, and conclusions or recommendations expressed in this material are those of the authors and do not necessarily reflect the views of the National Science Foundation. The authors declare no competing interests.

Table 2.1. Descriptions and examples of main moulting strategies in birds and mammals.

Strategies are colour coded to match Figure 2.1.

Replacement Strategy	Description	Environmental conditions	Example mammal species	Example bird species
Continuous shedding 	Individuals replace fur or feathers during a protracted, year-round process.	This is typical in animals that experience limited seasonality in resource availability or ambient conditions.	Domestic dogs [15], sea otters [86].	Mousebirds [123].
Annual moult 	Individuals replace pelage/plumage once per year.	This is typical in seasonally homogenous areas.	Harbour seals [102], bent-winged bats [124].	Bullfinches [125], lesser redpolls [126].
	SUBSET: Catastrophic moult Individuals rapidly shed all pelage and plumage, such that pelage or plumage function is compromised, and feeding does not occur.	This is typical of species that reside in aquatic environments such that insulative, waterproof, and hydrodynamic functions of pelage and plumage are crucial.	Northern elephant seals [31], southern elephant seals [90], Hawaiian monk seals [88].	Adelie and emperor penguins [87].
	SUBSET: Simultaneous moult Individuals rapidly shed flight feathers, such that plumage function is compromised. Feeding does occur during this time.	Same as above.	To our knowledge, does not occur in mammals.	Common eiders [27], lesser snow geese [93].
Complete biannual moult 	Individuals replace pelage/plumage twice per year, usually to meet camouflage and insulation requirements.	This is typical or polar latitudes where conditions can be snowy and cold during the winter.	Arctic, mountain, and snowshoe hares [76] least, long-tailed, and short-tailed weasels [77], Peary caribou [127], collared lemmings [79], Siberian hamsters [80], ground	Rock, willow, and white-tailed ptarmigan [129], Willow warblers [130], black-chested Prinias [131].

			squirrels [128], and arctic foxes [81].	
<p>Incomplete biannual moult</p> 	<p>Individuals grow thicker winter pelage or plumage and then shed into their thinner summer pelage or plumage during spring to allow heat exchange. Thus, the covering is a composite of retained and new fur/feathers.</p>	<p>This is typical of temperate latitudes where it can be wet and cold in the winter but not snowy, and hot in the summer. Alternatively, species in high latitude environments that do not rely on snow camouflage for survival.</p>	<p>Ferrets [65], elk [66], mink [67], snow leopards [68], deer [69], moose [70], squirrels [71], white-footed mice [72], and shrews [73].</p>	<p>Grey-headed albatrosses [132], barred warblers [133], painted buntings [134].</p>
<p>Split moult</p>	<p>Animals can stop the moult and continue the moult later.</p>	<p>This is typical in areas where food supplies or weather conditions are unpredictable or periodic.</p>	<p>To our knowledge, does not occur in mammals.</p>	<p>Barred warblers [135], common whitethroats [20], spectacled warblers [136], see Appendix 1 in Norman [137].</p>

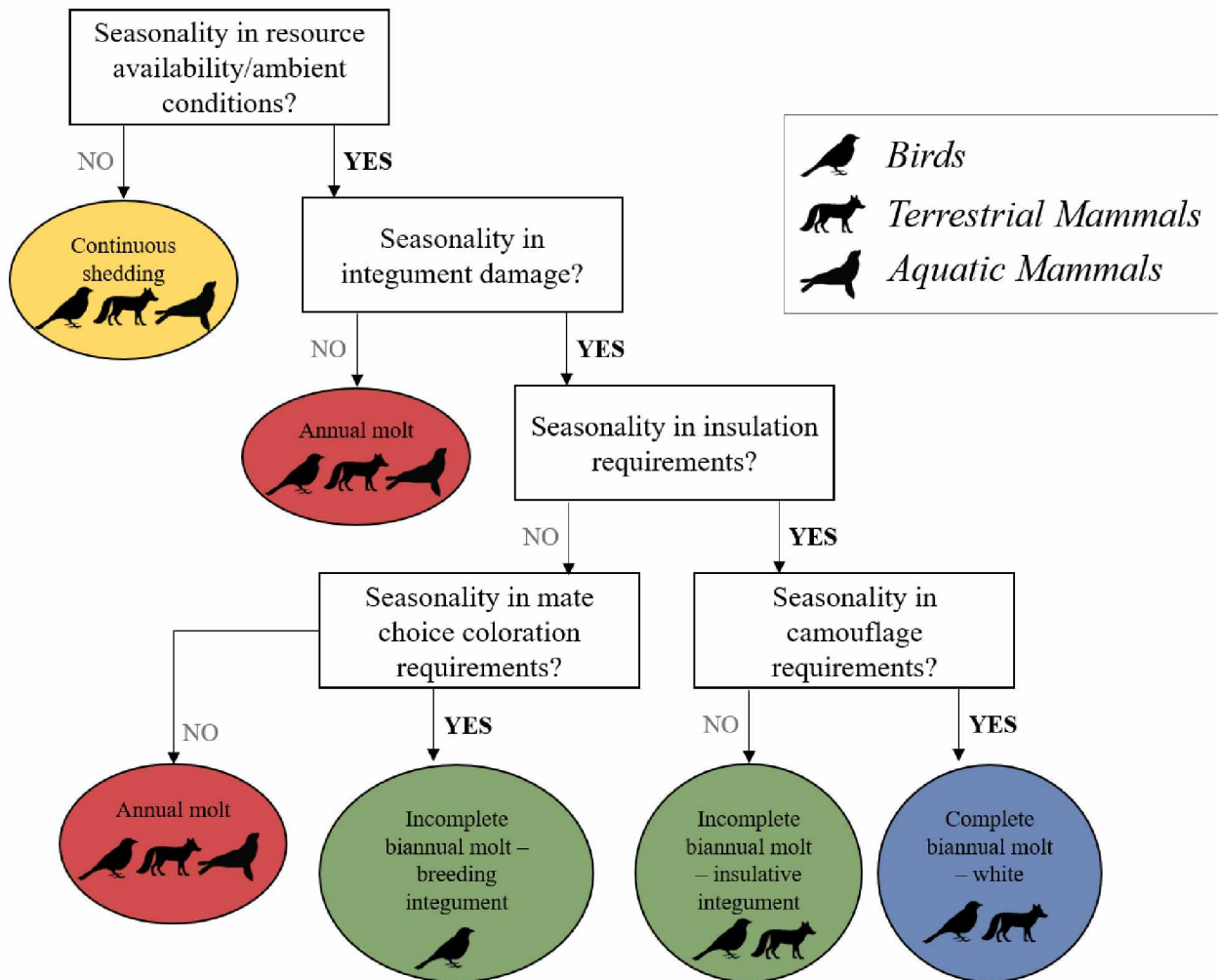


Figure 2.1. Selective pressures (squares) on moulting strategies (circles), including the group of endotherms that typically exhibits each strategy. Note that catastrophic moult is an extreme case of the annual moult.

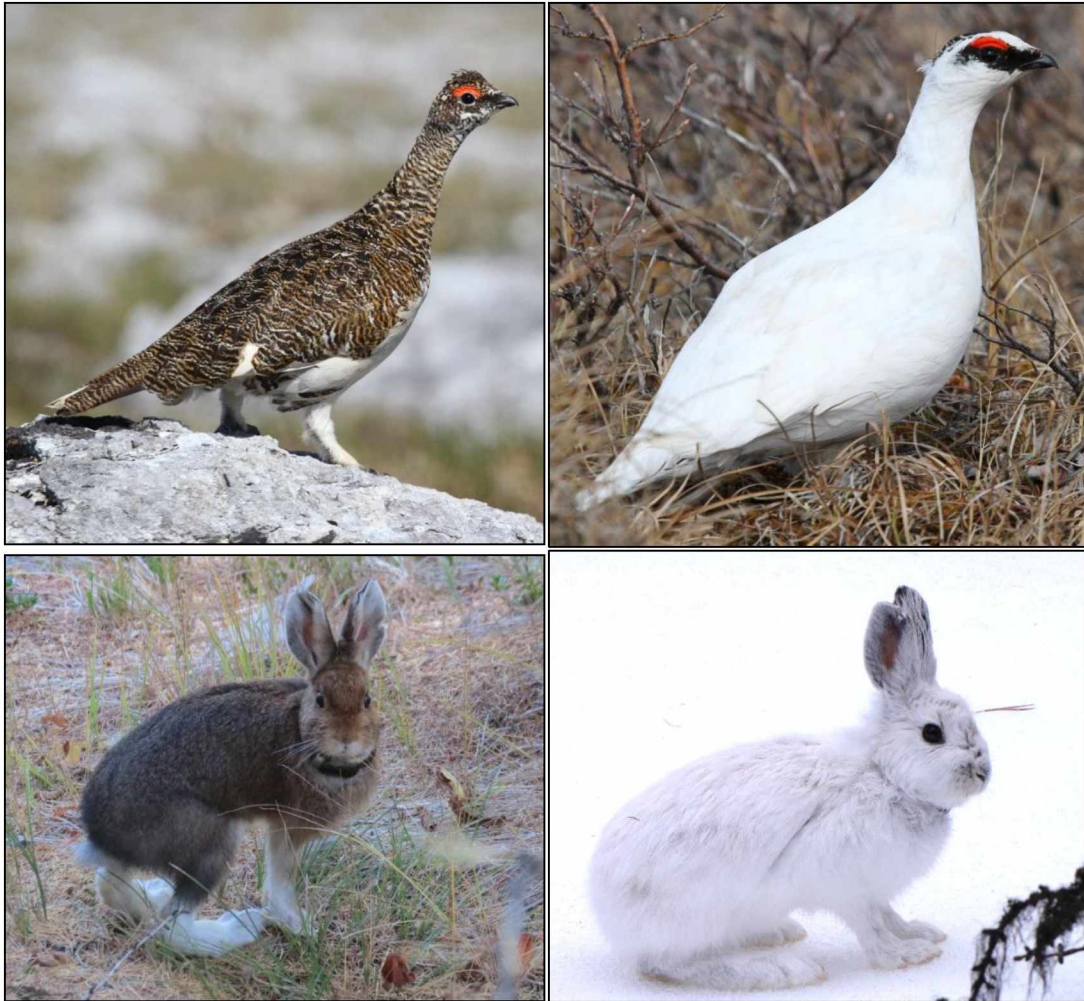


Figure 2.2. Rock ptarmigan *Lagopus muta* (top, photographs by Jared Hughey) and snowshoe hares *Lepus americanus* (bottom, research photographs by Mills lab) both undergo complete biannual moults, shedding into a thicker, white plumage/pelage before winter and a thinner, dark plumage/pelage before summer.

2.11 Literature Cited

1. Jovani R, Blas J. Adaptive allocation of stress-induced deformities on bird feathers. *Journal of Evolutionary Biology*. 2004;17(2):294-301.
2. Swaddle JP, Lockwood R. Wingtip shape and flight performance in the European Starling *Sturnus vulgaris*. *Ibis*. 2003;145(3):457-64.
3. Dawson TJ, Blaney CE, Munn AJ, Krockenberger A, Maloney SK. Thermoregulation by kangaroos from mesic and arid habitats: influence of temperature on routes of heat loss in eastern grey kangaroos (*Macropus giganteus*) and red kangaroos (*Macropus rufus*). *Physiological and Biochemical Zoology*. 2000;73(3):374-81.
4. Smith HG, Montgomerie R. Sexual selection and the tail ornaments of North American barn swallows. *Behavioral Ecology and Sociobiology*. 1991;28(3):195-201.
5. Boily P. Theoretical heat flux in water and habitat selection of phocid seals and beluga whales during the annual molt. *Journal of Theoretical Biology*. 1995;172(3):235-44.
6. Ryder TB, Parker PG, Blake JG, Loiselle BA. It takes two to tango: reproductive skew and social correlates of male mating success in a lek-breeding bird. *Proceedings of the Royal Society of London B: Biological Sciences*. 2009;276(1666):2377-84.
7. Pennycuik C. Mechanics of flight. *Avian Biology*. 1975;5:1-75.
8. Humphrey PS, Parkes KC. An approach to the study of molts and plumages. *The Auk*. 1959;76(1):1-31.

9. Bridge ES. Mind the gaps: what's missing in our understanding of feather molt. *The Condor*. 2011;113(1):1-4.
10. Ling J. Adaptive functions of vertebrate molting cycles. *American Zoologist*. 1972:77-93.
11. Svensson E, Hedenstrom A. A phylogenetic analysis of the evolution of moult strategies in Western Palearctic warblers (*Aves: Sylviidae*). *Biological Journal of the Linnean Society*. 1999;67(2):263-76.
12. Pyle P. Molt limits in North American passerines. *North American Bird Bander*. 1997;22(2):49-89.
13. Ling JK. Pelage and molting in wild mammals with special reference to aquatic forms. *Quarterly Review of Biology*. 1970:16-54.
14. Scheiman DM, Dunning Jr JB. A case of arrested molt in the Bobolink. *North American Bird Bander*. 2004;29(3).
15. Gunaratnam P, Wilkinson G. A study of normal hair growth in the dog. *Journal of Small Animal Practice*. 1983;24(7):445-53.
16. Snyder NF, Johnson EV, Clendenen DA. Primary molt of California condors. *Condor*. 1987:468-85.
17. Edwards AE. Large-scale variation in flight feather molt as a mechanism enabling biennial breeding in albatrosses. *Journal of Avian Biology*. 2008;39(2):144-51.
18. Smith HM. *Evolution of chordate structure: an introduction to comparative anatomy*: Holt, Rinehart and Winston; 1960.

19. Wu P, Hou L, Plikus M, Hughes M, Scehnet J, Suksaweang S, et al. Evo-Devo of amniote integuments and appendages. *The International Journal of Developmental Biology*. 2004;48:249.
20. Jenni L, Winkler R. *Moult and ageing of European passerines*: A&C Black; 1994.
21. Sokolov W. Adaptations of the mammalian skin to the aquatic mode of life. *Nature*. 1962;195(4840):464-6.
22. Marchand PJ. *Life in the cold: an introduction to winter ecology*: UPNE; 2014.
23. Davenport J. *Animal life at low temperature*: Springer Science & Business Media; 2012.
24. Nuttall M. *Encyclopedia of the Arctic*: Routledge; 2012.
25. Ellis HI. Metabolism and solar radiation in dark and white herons in hot climates. *Physiological Zoology*. 1980;53(4):358-72.
26. Walsberg G, Campbell G, King J. Animal coat color and radiative heat gain: a re-evaluation. *Journal of Comparative Physiology B: Biochemical, Systemic, and Environmental Physiology*. 1978;126(3):211-22.
27. Guillemette M, Pelletier D, Grandbois J-M, Butler PJ. Flightlessness and the energetic cost of wing molt in a large sea duck. *Ecology*. 2007;88(11):2936-45.
28. Sealander Jr JA. Survival of *Peromyscus* in relation to environmental temperature and acclimation at high and low temperatures. *American Midland Naturalist*. 1951:257-311.
29. McDevitt RM, Speakman JR. Central limits to sustainable metabolic rate have no role in cold acclimation of the short-tailed field vole (*Microtus agrestis*). *Physiological Zoology*. 1994;67(5):1117-39.

30. Beltran RS, Testa JW, Burns JM. An agent-based bioenergetics model for predicting impacts of environmental change on a top marine predator, the Weddell seal. *Ecological Modelling*. 2017;351:36-50.
31. Worthy G, Morris P, Costa D, Le Boeuf B. Moulting energetics of the northern elephant seal (*Mirounga angustirostris*). *Journal of Zoology*. 1992;227(2):257-65.
32. Adamczewski J, Flood P, Gunn A. Body composition of muskoxen (*Ovibos moschatus*) and its estimation from condition index and mass measurements. *Canadian Journal of Zoology*. 1995;73(11):2021-34.
33. Scholander P, Walters V, Hock R, Irving L. Body insulation of some arctic and tropical mammals and birds. *The Biological Bulletin*. 1950;99(2):225-36.
34. Ashwell-Erickson SM, Elsner R. The energy cost of free existence for Bering Sea harbor and spotted seals: University of Alaska, Fairbanks; 1981.
35. Turček FJ. On plumage quantity in birds: Państwowe Wydawnictwo Naukowe; 1966.
36. Dawson A. Control of molt in birds: association with prolactin and gonadal regression in starlings. *General and Comparative Endocrinology*. 2006;147(3):314-22.
37. Murphy ME. Energetics and nutrition of molt. *Avian Energetics and Nutritional Ecology*: Springer; 1996. p. 158-98.
38. Kiat Y, Izhaki I, Sapir N. Determinants of wing-feather moulting speed in songbirds. *Evolutionary Ecology*. 2016;30(4):783-95.
39. Dietz MW, Daan S, Masman D. Energy requirements for molt in the kestrel *Falco tinnunculus*. *Physiological Zoology*. 1992;65(6):1217-35.

40. King JR, Murphy ME. Periods of nutritional stress in the annual cycles of endotherms: fact or fiction? *American Zoologist*. 1985;25(4):955-64.
41. Murphy M, King J, editors. Nutritional aspects of avian molt. *Proceedings of the International Ornithological Congress*; 1991.
42. Vézina F, Gustowska A, Jalvingh KM, Chastel O, Piersma T. Hormonal correlates and thermoregulatory consequences of molting on metabolic rate in a northerly wintering shorebird. *Physiological and Biochemical Zoology*. 2009;82(2):129-42.
43. Bancroft GT, Woolfenden GE. The molt of scrub jays and blue jays in Florida. *Ornithological Monographs*. 1982;(29):iii-51.
44. Hoyer BJ, Buttemer WA. Inexplicable inefficiency of avian molt? Insights from an opportunistically breeding arid-zone species, *Lichenostomus penicillatus*. *PLoS One*. 2011;6(2):e16230.
45. Lindström Å, Visser GH, Daan S. The energetic cost of feather synthesis is proportional to basal metabolic rate. *Physiological Zoology*. 1993;66(4):490-510.
46. Feltz ET, Fay FH. Thermal requirements in vitro of epidermal cells from seals. *Cryobiology*. 1966;3(3):261-4.
47. Paterson W, Sparling CE, Thompson D, Pomeroy PP, Currie JI, McCafferty DJ. Seals like it hot: Changes in surface temperature of harbour seals (*Phoca vitulina*) from late pregnancy to moult. *Journal of Thermal Biology*. 2012;37(6):454-61.
doi: <http://dx.doi.org/10.1016/j.jtherbio.2012.03.004>.
48. Lustick S. Energy requirements of molt in cowbirds. *The Auk*. 1970;742-6.
49. Gill FB. *Ornithology*: Macmillan; 1995.

50. Helm B, Gwinner E. Timing of postjuvenal molt in African (*Saxicola torquata axillaris*) and European (*Saxicola torquata rubicola*) stonechats: effects of genetic and environmental factors. *The Auk*. 1999;589-603.
51. Holberton RL, Dufty Jr AM, Greenberg R, Marra P. Hormones and variation in life history strategies of migratory and non-migratory birds. *Birds of Two Worlds: the Ecology and Evolution of Migration*. 2005:290-302.
52. Fogden M. The seasonality and population dynamics of equatorial forest birds in Sarawak. *Ibis*. 1972;114(3):307-43.
53. Irving L. Arctic life of birds and mammals, including man. 1972.
54. Terrill RS. Evolutionary interactions of feather molt in birds 2017.
55. Ralph CL. The control of color in birds. *American Zoologist*. 1969;9(2):521-30.
56. Zahavi A. Mate selection—a selection for a handicap. *Journal of Theoretical Biology*. 1975;53(1):205-14.
57. Vorobyev M, Osorio D, Bennett AT, Marshall N, Cuthill I. Tetrachromacy, oil droplets and bird plumage colours. *Journal of Comparative Physiology A: Neuroethology, Sensory, Neural, and Behavioral Physiology*. 1998;183(5):621-33.
58. Caro T. The adaptive significance of coloration in mammals. *BioScience*. 2005;55(2):125-36.
59. Prum RO, Torres RH. Structural colouration of mammalian skin: convergent evolution of coherently scattering dermal collagen arrays. *Journal of Experimental Biology*. 2004;207(12):2157-72.

60. Vessey SH, Morrison JA. Molt in free-ranging rhesus monkeys, *Macaca mulatta*. Journal of Mammalogy. 1970;51(1):89-93.
61. Jacoby ME, Hilderbrand GV, Servheen C, Schwartz CC, Arthur SM, Hanley TA, et al. Trophic relations of brown and black bears in several western North American ecosystems. The Journal of Wildlife Management. 1999:921-9.
62. Garbutt A, Leatherland J, Middleton A. Seasonal changes in serum thyroid hormone levels in ruffed grouse maintained under natural conditions of temperature and photoperiod. Canadian Journal of Zoology. 1979;57(10):2022-7.
63. Maurel D, Coutant C, Boissin-Agasse L, Boissin J. Seasonal moulting patterns in three fur bearing mammals: the European badger (*Meles meles* L.), the red fox (*Vulpes vulpes* L.), and the mink (*Mustela vison*). A morphological and histological study. Canadian Journal of Zoology. 1986;64(8):1757-64.
64. West SD. Midwinter aggregation in the northern red-backed vole, *Clethrionomys rutilus*. Canadian Journal of Zoology. 1977;55(9):1404-9.
65. Harvey NE, Macfarlane W. The effects of day length on the coat-shedding cycles, body weight, and reproduction of the ferret. Australian Journal of Biological Sciences. 1958;11(2):187-99.
66. Parker KL, Robbins CT. Thermoregulation in mule deer and elk. Canadian Journal of Zoology. 1984;62(7):1409-22.
67. Martinet L, Mondain-Monval M, Monnerie R. Endogenous circannual rhythms and photorefractoriness of testis activity, moult and prolactin concentrations in mink (*Mustela vison*). Journal of Reproduction and Fertility. 1992;95(2):325-38.
68. Hemmer H. *Uncia uncia*. Mammalian Species. 1972;(20):1-5.

69. Silver H, Colovos N, Holter J, Hayes H. Fasting metabolism of white-tailed deer. *The Journal of Wildlife Management*. 1969;490-8.
70. Renecker LA, Hudson RJ. Seasonal energy expenditures and thermoregulatory responses of moose. *Canadian Journal of Zoology*. 1986;64(2):322-7.
71. Elton C, editor Some aspects of the biology of the grey squirrel (*Sciurus carolinensis*) in Great Britain. *Proceedings of the Zoological Society of London*; 1951: Wiley Online Library.
72. Lynch GR. Seasonal changes in thermogenesis, organ weights, and body composition in the white-footed mouse, *Peromyscus leucopus*. *Oecologia*. 1973;13(4):363-76.
73. Rood J. Observations on population structure, reproduction and molt of the Scilly shrew. *Journal of Mammalogy*. 1965;46(3):426-33.
74. Dawson WR, Carey C. Seasonal acclimatization to temperature in cardueline finches. *Journal of Comparative Physiology B: Biochemical, Systemic, and Environmental Physiology*. 1976;112(3):317-33.
75. Tickell WLN. White plumage. *Waterbirds*. 2003;26(1):1-12.
76. Hewson R, editor Moults and winter whitening in the mountain hare *Lepus timidus scoticus*, Hilzheimer. *Proceedings of the Zoological Society of London*; 1958: Wiley Online Library.
77. Bissonnette TH, Bailey EE. Experimental modification and control of molts and changes of coat-color in weasels by controlled lighting. *Annals of the New York Academy of Sciences*. 1944;45(1):221-60.

78. Choy CA, Popp BN, Kaneko JJ, Drazen JC. The influence of depth on mercury levels in pelagic fishes and their prey. *Proceedings of the National Academy of Sciences*. 2009;106(33):13865-9. doi: 10.1073/pnas.0900711106. PubMed PMID: 19666614; PubMed Central PMCID: PMC2728986.
79. Reynolds P, Lavigne D. Photoperiodic effects on post-weaning growth and food consumption in the collared lemming *Dicrostonyx groenlandicus*. *Journal of Zoology*. 1989;218(1):109-21.
80. Logan A. Pelage color cycles and hair follicle tyrosinase activity in the Siberian hamster. 1978.
81. Fuglei E, Ims RA. Global warming and effects on the arctic fox. *Science Progress*. 2008;91(2):175-91.
82. Burt Jr EH, Ichida JM. Gloger's rule, feather-degrading bacteria, and color variation among song sparrows. *The Condor*. 2004;106(3):681-6.
83. Blanco G, Frías O, Garrido-Fernández J, Hornero-Méndez D. Environmental-induced acquisition of nuptial plumage expression: a role of denaturation of feather carotenoproteins? *Proceedings of the Royal Society of London B: Biological Sciences*. 2005;272(1575):1893-900.
84. Barta Z, McNamara JM, Houston AI, Weber TP, Hedenström A, Fero O. Optimal moult strategies in migratory birds. *Philosophical Transactions of the Royal Society B: Biological Sciences*. 2008;363(1490):211-29.
85. Kvadsheim P, Aarseth J. Thermal function of phocid seal fur. *Marine Mammal Science*. 2002;18(4):952-62.

86. Kuhn RA, Ansorge H, Godynicki S, Meyer W. Hair density in the Eurasian otter *Lutra lutra* and the Sea otter *Enhydra lutris*. *Acta Theriologica*. 2010;55(3):211-22.
87. Davis LS, Darby JT. *Penguin biology*: Elsevier; 2012.
88. Kenyon KW, Rice DW. Life history of the Hawaiian monk seal. *Pacific Science*. 1959;13(3):215-52.
89. Green K, Burton HR, Watts DJ. *Studies of the Weddell seal in the Vestfold Hills, east Antarctica*: Australian Antarctic Division; 1995.
90. Ling J, Thomas C. The skin and hair of the southern elephant seal, (*Mirounga leonina* (L.) II. pre-natal and early post-natal development and moulting. *Australian Journal of Zoology*. 1967;15(2):349-65.
91. Holmgren N, Hedenström A. The scheduling of molt in migratory birds. *Evolutionary ecology*. 1995;9(4):354-68.
92. Bridge E. Influences of morphology and behavior on wing-molt strategies in seabirds. *Marine Ornithology*. 2006;34:7-19.
93. Ankney CD. Does the wing molt cause nutritional stress in Lesser Snow Geese? *The Auk*. 1979:68-72.
94. DesRochers DW, Butler LK, Silbernagle MD, Reed JM. Observations of molt in an endangered rallid, the Hawaiian Moorhen. *The Wilson Journal of Ornithology*. 2009;121(1):148-53.
95. Stout BE, Cooke F. Timing and location of wing molt in Horned, Red-necked and Western Grebes in North America. *Waterbirds*. 2003;26(1):88-93.

96. Durban J, Pitman R. Antarctic killer whales make rapid, round-trip movements to subtropical waters: evidence for physiological maintenance migrations? *Biology Letters*. 2012;8(2):274-7.
97. Reeb D, Best PB, Kidson SH. Structure of the integument of southern right whales, *Eubalaena australis*. *The Anatomical Record*. 2007;290(6):596-613.
98. Aubin DS, Smith TG, Geraci J. Seasonal epidermal molt in beluga whales, *Delphinapterus leucas*. *Canadian Journal of Zoology*. 1990;68(2):359-67.
99. Chernova O, Shpak O, Kiladze A, Azarova V, Rozhnov V, editors. Summer molting of bowhead whales *Balaena mysticetus* Linnaeus, 1758, of the Okhotsk Sea population. *Doklady Biological Sciences*; 2016: Springer.
100. Fish FE, Howle LE, Murray MM. Hydrodynamic flow control in marine mammals. *Integrative and Comparative Biology*. 2008;48(6):788-800. doi: 10.1093/icb/icn029. PubMed PMID: 21669832.
101. Fortune SM, Koski WR, Higdon JW, Trites AW, Baumgartner MF, Ferguson SH. Evidence of molting and the function of “rock-nosing” behavior in bowhead whales in the eastern Canadian Arctic. *PloS one*. 2017;12(11):e0186156.
102. Daniel RG, Jemison LA, Pendleton GW, Crowley SM. Molting phenology of harbor seals on Tugidak Island, Alaska. *Marine Mammal Science*. 2003;19(1):128-40.
103. Morales J, Moreno J, Merino S, Tomas G, Arriero E, Lobato E, et al. Early moult improves local survival and reduces reproductive output in female pied flycatchers. 2009.

104. Helm B, Ben-Shlomo R, Sheriff MJ, Hut RA, Foster R, Barnes BM, et al., editors. Annual rhythms that underlie phenology: biological time-keeping meets environmental change. Proceedings of the Royal Society of London B: Biological Sciences; 2013: The Royal Society.
105. Zimova M, Hackländer K, Good JM, Melo-Ferreira J, Alves PC, Mills LS. Function and underlying mechanisms of seasonal colour moulting in mammals and birds: what keeps them changing in a warming world? Biological Reviews. 2018.
106. Romero LM, Storchlic D, Wingfield JC. Corticosterone inhibits feather growth: potential mechanism explaining seasonal down regulation of corticosterone during molt. Comparative Biochemistry and Physiology Part A: Molecular & Integrative Physiology. 2005;142(1):65-73.
107. Jenni-Eiermann S, Jenni L, Piersma T. Temporal uncoupling of thyroid hormones in Red Knots: T3 peaks in cold weather, T4 during moult. Journal für Ornithologie. 2002;143(3):331-40.
108. Goldsmith A, Nicholls T. Changes in plasma prolactin in male starlings during testicular regression under short days compared with those during photorefractoriness. Journal of Endocrinology. 1984;102(3):353-6.
109. Goldsmith A, Nicholls T, Plowman G. Thyroxine treatment facilitates prolactin secretion and induces a state of photorefractoriness in thyroidectomized starlings. Journal of Endocrinology. 1985;104(1):99-103.

110. St. Aubin D, Geraci J. Capture and handling stress suppresses circulating levels of thyroxine (T4) and triiodothyronine (T3) in beluga whales *Delphinapterus leucas*. *Physiological Zoology*. 1988;61(2):170-5.
111. Danner RM, Greenberg RS, Danner JE, Walters JR. Winter food limits timing of pre-alternate moult in a short-distance migratory bird. *Functional Ecology*. 2015;29(2):259-67.
112. Saino N, Rubolini D, Ambrosini R, Romano M, Scandolara C, Fairhurst GD, et al. Light-level geolocators reveal covariation between winter plumage molt and phenology in a trans-Saharan migratory bird. *Oecologia*. 2015;178(4):1105-12.
113. Payne RB, Farner D, King J. Mechanisms and control of molt. *Avian Biology*. 1972;2:103-55.
114. Rust CC. Temperature as a modifying factor in the spring pelage change of short-tailed weasels. *Journal of mammalogy*. 1962;43(3):323-8.
115. Schop J, Aarts G, Kirkwood R, Cremer JS, Brasseur SM. Onset and duration of gray seal (*Halichoerus grypus*) molt in the Wadden Sea, and the role of environmental conditions. *Marine Mammal Science*. 2017.
116. Rubolini D, Saino N, Møller AP. Migratory behaviour constrains the phenological response of birds to climate change. *Climate Research*. 2010;42(1):45-55.
117. Stocker T. Climate change 2013: the physical science basis: Working Group I contribution to the Fifth assessment report of the Intergovernmental Panel on Climate Change: Cambridge University Press; 2014.

118. Mills LS, Zimova M, Oyler J, Running S, Abatzoglou JT, Lukacs PM.
Camouflage mismatch in seasonal coat color due to decreased snow duration.
Proceedings of the National Academy of Sciences. 2013;110(18):7360-5.
119. Watson A, editor The effect of climate on the colour changes of mountain hares in
Scotland. Proceedings of the Zoological Society of London; 1963: Wiley Online
Library.
120. Flux JE. Life history of the Mountain hare (*Lepus timidus scoticus*) in north-east
Scotland. Journal of Zoology. 1970;161(1):75-123.
121. Guallar S, Figuerola J. Factors influencing the evolution of moult in the non-
breeding season: insights from the family *Motacillidae*. Biological Journal of the
Linnean Society. 2016.
122. Pyle P, Leitner WA, Lozano-Angulo L, Avilez-Teran F, Swanson H, Limón EG,
et al. Temporal, spatial, and annual variation in the occurrence of molt-migrant
passerines in the Mexican monsoon region. The Condor. 2009;111(4):583-90.
123. Moreau R, Wilk A, editors. The moult and gonad cycles of three species of birds
at five degrees south of the equator. Proceedings of the Zoological Society of
London; 1947: Wiley Online Library.
124. Dwyer P. Seasonal changes in Pelage of *Miniopterus schreibersi blepotis*
(*Chiroptera*) in north-eastern NSW. Australian Journal of Zoology.
1963;11(3):290-300.
125. Newton I. The moult of the Bullfinch *Pyrrhula pyrrhula*. Ibis. 1966;108(1):41-67.
126. Evans P. Autumn movements, moult and measurements of the Lesser Redpoll
Carduelis flammea cabaret. Ibis. 1966;108(2):183-216.

127. Gunn A, Miller F, Thomas D. The current status and future of Peary caribou *Rangifer tarandus pearyi* on the Arctic Islands of Canada. *Biological Conservation*. 1981;19(4):283-96.
128. Butterworth BB. Molt patterns in the barrow ground squirrel. *Journal of Mammalogy*. 1958;39(1):92-7.
129. Cramp S. *Handbook of the birds of Europe, the Middle East and North Africa*: Oxford University Press; 1980.
130. Underhill L, Prys-Jones R, Dowsett R, Herroelen P, Johnson D, Lawn M, et al. The biannual primary moult of willow warblers *Phylloscopus trochilus* in Europe and Africa. *Ibis*. 1992;134(3):286-97.
131. Herremans M. Biannual complete moult in the Black-chested Prinia *Prinia flavicans*. *Ibis*. 1999;141(1):115-24.
132. Prince P, Rodwell S, Jones M, Rothery P. Molt in Black-browed and Grey-headed Albatrosses *Diomedea melanophris* and *D. chrysostoma*. *Ibis*. 1993;135(2):121-31.
133. Hasselquist D, Hedenström A, Lindström Å, Bensch S. The Seasonally Divided Flight Feather Molt in the Barred Warbler *Sylvia nisoria*: A New Molt Pattern for European Passerines. *Ornis Scandinavica*. 1988:280-6.
134. Thompson CW. The sequence of molts and plumages in Painted Buntings and implications for theories of delayed plumage maturation. *Condor*. 1991:209-35.
135. Lindström Å, Pearson DJ, Hasselquist D, Hedenström A, Bensch S, Akesson S. The molt of Barred Warblers *Sylvia nisoria* in Kenya—evidence for a split wing-molt pattern initiated during the birds' first winter. *Ibis*. 1993;135(4):403-9.

136. Talabante C. Atypical moult of the secondary feathers in Spectacled Warbler *Sylvia conspicillata*. *Ringling & Migration*. 2014;29(1):44-6.
137. Norman S. Suspended split-moult systems-an alternative explanation for some species of Palearctic migrants. 1991.

Chapter 3. Reproductive success influences molt phenology and subsequent colony attendance in Weddell seals ²

3.1 Abstract

While strong ties between molt and reproductive timing (hereafter, phenology) have been described in avian taxa, the impact that molt has on subsequent life history events in mammals is poorly understood. Our aim was to determine the linkages between pupping and molting phenology in a polar marine mammal. To do so, we conducted demographic surveys of 4,252 flipper-tagged Weddell seals (*Leptonychotes weddellii*) in Erebus Bay, Antarctica (77°S, 165°E) during the austral summers of 2013-2017. At each sighting, seals were assigned a molt code based on the visible presence of new fur, and the start date of each animal's molt was back-calculated based on duration estimates. On average, Weddell seal molt duration was 29 ± 8 days. Pupping success and parturition dates were obtained for the breeding season prior to and after the molt. Non-parturient females started to molt 16 days earlier than parturient females (molt start date January 06 ± 12 days vs. January 22 ± 13 d, t-test $p < 0.0001$). Among parturient seals, molt timing mirrored parturition timing, with females that gave birth earlier initiating and completing molt earlier. Missing individuals were 10% more likely than expected to remain missing the following year, although 76% of missing individuals did return to breeding colonies. The physiological and behavioral differences between attendant and non-attendant skip-puppers should be quantified in future studies.

² RS Beltran, AL Kirkham, GA Breed, JW Testa, JM Burns. Reproductive success influences molt phenology and subsequent colony attendance in a high latitude mammal. Prepared for submission to Functional Ecology.

3.2 Introduction

Animals can respond to stressors through phenological plasticity of life history events [1, 2]. However, changes in one part of the annual cycle can impact subsequent processes (i.e. carry-over effects; [3, 4]) and these shifts can in turn diminish success in foraging, breeding, or surviving [5-7]. Among most vertebrates, it is uncommon for molt and reproduction, two key elements of the annual cycle, to overlap due to the high energetic costs of both [8-10]. Because peak food availability [11, 12] and suitable climate [13] are important to the success of both life history events [14, 15], an adaptive balance exists between breeding and molting phenology [16]. Thus, it is important to study phenological variation in the larger context of annual cycles [17] and survival rates [14, 18] in order for the ecological implications of stressors to be understood [19, 20].

Documenting molt progression is a prerequisite for understanding the carry-over effects of phenological disruptions. In previous work, the role of the molt as an intermediate life history event between two reproductive episodes has been studied almost exclusively in avian taxa [15, 21]. Mammalian molt studies have been restricted to basic descriptions of when molt starts and how it influences animal behavior [22, 23]. Here, molt initiation is difficult to identify because follicle growth precedes visible hair loss [24]. Histology can reveal subcutaneous molt start [25]; however, this method requires invasive biopsy techniques. Instead, molt start dates have been estimated based on when animals lose fur dye marks or biologging devices glued to fur [26]. As a result, progression of the molt has been primarily documented in species where repeated measures are possible [18], such as free-ranging animals with high site fidelity and sighting frequency (e.g. pinnipeds), domestic species kept for fur or wool harvesting (e.g. fox, mink, sheep), and species with discernable molting patterns (e.g. elephant seals with a “catastrophic

molt” [25]). Relative to the molt, much more is known about reproductive success and phenology due to the relative ease of determining the presence/absence of dependent offspring.

In true seals (family *Phocidae*), the annual molt follows pup weaning and precedes pup birth the following year. Phenological links between pupping and molting have been noted, particularly a delayed molt phenology in parturient individuals relative to non-parturient conspecifics (approximately 60 days later in gray seals *Halichoerus grypus* [27], 14 days later in southern elephant seals *Mirounga leonina* [28], 6 months later in Mediterranean monk seals *Monachus monachus* [29], and 28 days later in Hawaiian monk seals *Monachus schauinslandi* [30]). Until now, no pinniped research has characterized the carry-over effects between molting and pupping phenology in the same season, how molt timing affects pupping success the following season, or how molt duration is related to reproductive outcomes or phenology. Given the apparent role of reproductive hormones in delaying molt onset [31], we hypothesize that later pupping will result in later molting, and in turn reduce pupping success in the following year.

The Weddell seal population in Erebus Bay, Ross Sea, Antarctica, is ideal for studying the linkages between molt and reproduction. A large fraction of this population has been tagged and resighted annually because animals show high site fidelity and are not disturbed by close observation [32]. Resighting efforts occur in October to early December each year, when females haul out on the ice to give birth and nurse their pups for 6-7 weeks [33], so the timing and success of each reproductive cycle is well documented. Shortly thereafter, seals of all ages and sexes begin an annual molt [22], with adult females spending an average of 15 hours per day resting on the ice (Beltran et al., *in prep*) to replace worn fur with new fur. The Weddell seal molt has been described at the population level by Green et al. [22]: seals replace their fur in a characteristic pattern beginning at the head, continuing down the back and finally wrapping

around the sides [22]. Until now, individual molt duration and phenology have not been quantified in Weddell seals.

In this study, we had three specific aims: 1) To describe the duration and phenology of the Weddell seal molt across age, sex, and reproductive categories; 2) To analyze the relationship between pupping phenology (October-November, Year 1) and subsequent molting phenology (January-March, Year 1) in reproductive females; 3) To understand the relationship between molting phenology and pupping phenology in the following season (Oct-Nov, Year 2); and 4) To evaluate the role of skipped reproductive cycles in mediating molt phenology and future reproductive outcomes.

3.3 Methods

3.3.1 Fieldwork methods

In 2013-2017, we conducted semi-weekly surveys of Weddell seals (*Leptonychotes weddellii*) in Erebus Bay, Antarctica (77°S, 165°E). Each seal was approached and its flipper tag identification number, age class, and sex were recorded along with a qualitative molt code based on the visible presence of new fur (Figure 3.1): code 0 - molt had not begun, no new fur visible; code 1 - head molted and/or a thin stripe of new fur visible along the spine; code 2 - head completely molted and connected to a wide swath of new fur along the spine; code 3 - only small patches of unmolted fur remained laterally between the front and rear flippers; and code 4 - fully molted, no old fur visible. If the molt code could not be assigned because the animal was wet, covered in snow, or laying in such a way that their dorsal pelage was not visible, molt state was noted as unknown. Ages and sexes were obtained for tagged individuals based on a long-term demographic study [32, 34, 35]. Year is given as the austral summer each seal was observed

molting (e.g., AS13 is the 2013-14 austral summer season, including the October 2013-December 2013 pupping and December 2013-March 2014 molting periods) (Table 3.1). For each year, ice break-out date was obtained using methods described in Chapter 4 of this dissertation.

Adult females were assigned a reproductive category for the pupping period preceding the molt season in which they were observed (October-December, hereafter Year 1 pupping period) and the pupping period following the molt (hereafter Year 2 pupping period). If adult females were observed with a dependent pup, they were considered to have pupped successfully (hereafter, parous). Each colony was visited every two to three days throughout the birthing period, which allowed pupping success and precise birth dates of newborn pups (those with visible umbilical cord stumps) to be determined for many adult females per year. However, inclement weather and logistical constraints occasionally reduced visitation frequency. For the analyses presented here, we only used data from pups whose birth dates could be precisely determined based on appearance of the pup, placenta, and/or umbilical stump [36]. Using the pupping date distribution for newborns to estimate the quantiles of pupping dates for each year, we categorized parturient females as follows: Early-Puppers, who gave birth before the 25th percentile of the pupping distribution; Middle-Puppers, who gave birth between (or on) the 25th and 75th percentile of the pupping distribution; and Late-Puppers, who gave birth after the 75th percentile of the pupping distribution (Figure 3.2).

In 2013, the United States government shutdown delayed the start of annual pup tagging efforts until October 29, typically the median of the pupping distribution (Table 3.1). As a result, pup birthdates are more uncertain in AS13 for pups born before October 29. To estimate birth dates for AS13 with the highest accuracy possible, we estimated birthdates based on the visual presence of an umbilical cord on each pup: the birthdate was considered six days prior to first

sighting if there was no umbilical cord, four days prior to sighting if there was an umbilical cord but the pup was estimated to be older than two days based on size, or one day prior to sighting if the pup was noted as newborn. Because the number of pups born in AS13 ($n=544$) was known, we assumed that the pupping distribution was normally distributed as in other years [36]. Thus, we assigned the median date when half the pups had been born (272nd pup; October 29th) and the 75th percentile when three quarters of the pups had been born (408th pup; November 02nd; [36]). Due to the uncertainty in pupping dates prior to the median, we calculated the categories for AS13 parturient females as follows: Early-Puppers, who gave birth before the 50th percentile of the pupping distribution (32% of individuals); Middle-Puppers, who gave birth between (or on) the 50th and 75th percentile of the pupping distribution (48%); and Late-Puppers, who gave birth after the 75th percentile of the pupping distribution (20%).

For those females seen during a given molting season, but who did not give birth or who were not observed during the lactation season, the categories were as follows: “Seen Immature” if seen during the breeding season without a pup and never recorded with a pup in any previous year (i.e. no pups produced yet in life); “Seen Skip-Pupper” if seen during the breeding season without a pup but recorded with a pup in any previous year; “Missing Parous” if not seen during the breeding season but recorded with a pup in previous years; and “Missing Immature” if not seen during the breeding season and never recorded with a pup in previous years. Given that there are no known pupping colonies near our study colony, we suspect that Missing individuals skipped pupping and temporarily emigrated, as described by Chambert et al. [37]. Additionally, the proportion of sexually mature females that became Skip-Puppers, Missing Parous, and Skip-Puppers in Year 2 was calculated for each study year (Table 3.1). Because male breeding

behavior is difficult to assess, we did not attempt to link breeding and molting phenology in males.

3.3.2 Analytical methods

To estimate the duration of molt, we created a custom function in *R* (*R* Development Core Team 2017, version 3.3.2) that evaluated molt progression based on subsequent sightings of a series of molt codes in each individual. Encounter histories for each animal were sorted by date and filtered to exclude repeated observations of the same animal on the same day, or cases in which molt code at time $[t]$ was not less than or equal to the molt code at time $[t+1]$ (i.e. the molt progression was biologically impossible). This led to the removal of 5.5% of sightings. We use a count of elapsed day in each year (Day 0 is January 1) as the temporal scale in analyses and figures but show calendar date in tables.

3.3.3 Estimating molt stage durations

The molt stage durations τ_n were calculated as the amount of time that passed between that molt code (n) and the molt codes preceding ($n-1$) and following ($n+1$), using a midpoint approach (see Figure 3.3). The molt codes 0,1,2,3, and 4 were used to calculate molt durations τ_n for codes $n=1,2,3$ as follows:

$$(1) \quad \tau_n = \left(\frac{First_{n+1} + Last_n}{2} \right) - \left(\frac{First_n + Last_{n-1}}{2} \right)$$

where *First* is the first sighting in a given molt code n , and *Last* is the last sighting in a given molt code n . For instance, the molt stage 1 duration τ_1 is the difference between [the midpoint of

the first code 2 sighting and the last code 1 sighting] and [the midpoint of the first code 1 sighting and the last code 0 sighting]. Stage durations were calculated for all seals that were observed in three consecutive molt codes (e.g. codes 0, 1, 2 in the case of τ_1), and the distributions of those durations was tested for normality using Lilliefors tests. The duration of each molt stage was not significantly different across years, sexes, or reproductive histories (unpaired t-test, $p > 0.05$ for each stage); thus, data were combined to calculate a mean and standard deviation duration τ_n for each stage. Total molt duration T was then calculated as the sum of τ_1 , τ_2 , and τ_3 (Figure 3.3). We acknowledge that the existence of a negative co-variance between the duration of τ_n and τ_{n+1} results in a conservative estimate of T .

3.3.4 Estimating molt initiation dates

Of the 4252 unique seal-year combinations that were observed during the study, 1208 were observed in both molt codes 0 and 1 (i.e., beginning of molt was known to occur between two set dates. For these individuals, we estimated the molt initiation date as the midpoint between the last code 0 sighting and the first code 1 sighting). Of the remaining individuals, 681 were first observed in molt code 1, 681 in molt code 2, 444 in molt code 3, and 749 in molt code 4. To include the animals in our molt phenology analysis that had not been observed at molt initiation, we back-calculated molt initiation dates for each remaining animal based on their molt code k at first sighting $First_k$. Estimating the beginning of a stage required that we first estimate the mean difference Δ_k between [the midpoint of the first code $n+1$ sighting and the last code n sighting] and [the subsequent code n sighting] (Figure 3.3), using:

$$(2) \quad \Delta_n = First_n - \left(\frac{First_{n+1} + Last_n}{2} \right)$$

for all seals that were observed in two consecutive molt codes (e.g. codes 0,1 to calculate Δ_1).

Using a Lilliefors test, the Δ_n distributions were found to be normal. This resulted in average difference Δ_n values of 5.4 ± 3.9 days ($n=347$ animals) for Δ_1 , 4.5 ± 2.9 days ($n=347$ animals) for Δ_2 , 4.3 ± 2.9 days ($n=226$ animals) for Δ_3 , 5.1 ± 3.7 days ($n=213$ animals) for Δ_4 (Table 3.2). Finally, to back-calculate an initiation date for each animal based on their molt code k at first sighting $First_k$, we subtracted the difference value Δ_k and the sum of the stage durations τ for each molt stage n in which the animal was not observed:

$$(3) \quad InitiationDate = First_k - \Delta_k - \sum_{n=1}^{k-1} \tau_n$$

To control for inter-annual variation in molt timing, individuals were assigned to molt categories based on the molt initiation date relative to the initiation dates of the other animals in the year of sighting: Early-Molters, who initiated molting before the 25th percentile of the molt initiation dates; Middle-Molters, who initiated molting between (or on) the 25th and 75th percentile of the molt initiation dates; or Late-Molters, who initiated molt after the 75th percentile of the molt initiation dates.

3.3.5 Accounting for error propagation

Molt duration values are presented as mean $\mu \pm$ standard deviation σ . To account for the propagation of error resulting from summing τ_n components with separate standard deviation terms, we calculated an overall molt duration standard deviation σ_T using the following equation:

(4)

$$\sigma_T = \sqrt{\sum_{n=0}^k (\sigma_{\tau_n})^2}$$

Similarly, we calculated a cumulative error value for the molt initiation date of each seal as follows:

(5)

$$\sigma_{Date_{init}} = \sqrt{(\sigma_{\Delta_k})^2 + \sum_{n=0}^k (\sigma_{\tau_n})^2}$$

where σ_m is the standard deviation of molt duration for molt code n , summed from molt code 0 ($n=0$) to the molt code k at first sighting ($n=k$). In this way, the extrapolated molt start date for animals that were first sighted in molt code 4 would have a larger estimated error than for animals that were first sighted in molt code 1.

3.3.6 Drivers of molt phenology

To evaluate relationships between molt phenology and sex, year, and reproductive category, we constructed biologically plausible models and then selected the best models using an information-theoretic approach (Table 3.3). Mixed-effects models were constructed using the package *lme4* and selected using *AIC* [38, 39] in *R* (R Core Team 2017). The global model was $Date_init \sim Repro_cat * Year * Age + (1|ID)$ where $1|ID$ is the random effect of individual and $Repro_cat$ is a combined sex/reproductive history category that includes males, and females in several categories (Seen Skip-Pupper, Seen Immature, Seen Pupper, Missing Immature, Missing Parous). Age differed by reproductive category (mean ages for Immatures = 4.45 years old (yo),

Males = 8.73 yo, Puppies = 14.03 yo, Skip-Puppies = 15.12 yo; ANOVA, Tukey HSD post-hoc, $p < 0.05$ for all, except Puppies:Skip-Puppies $p > 0.05$). However, the model AIC was higher when Age was included in the global model (Table 3.3); as a result, all ages within a single reproductive category were combined for the remaining analyses. For parturient females, the relationship between pup birth date and molt initiation date was also examined using a linear mixed-effects model with year as a fixed effect and individual as a random effect using the package *lme4* in R.

3.3.7 Interactions between pupping success/phenology and molt phenology

For sexually mature females (i.e., those that had reproduced at least once prior to the year in which we collected molt data for the individual), we calculated the transition probabilities from all pupping categories into each molting category (Table 3.4; transition probabilities 26% Early-Molters, 48% Mid-Molters, and 26% Late-Molters). These values were used as the null “expected” transition probabilities and compared against the “observed” transition probabilities from each of the five reproductive categories separately to each molting category using a Markov simulation on 10,000 multinomial draws. P-values were adjusted to account for table-wide Type I errors using a Bonferonni-type correction [40]. An adjusted test-wise critical value α_A was calculated for each cell using $\alpha_A = \alpha_{PF}/C$ where α_{PF} is the family-wise critical value of 0.05 and C is the number of significant cells. Unadjusted α_U values were ranked from smallest to largest and evaluated against α_A values corrected for that many cells ($C=n$). If the unadjusted α_U value was still less than the adjusted α_A value, it was retained (***) in Tables 3.4-3.6); otherwise it was considered non-significant. The next highest unadjusted α_U value was then compared to the next adjusted α_A for $C=n-1$ cells, and so on for each subsequent α_U value. The same analysis was

performed from molting categories into pupping categories in the following reproductive year (Table 3.5; expected transition probabilities 24% Skip-Puppers, 16% Early-Puppers, 32% Mid-Puppers, 17% Late-Puppers, 12% Missing Parous) and from year one reproductive categories into year two reproductive categories (Table 3.6; expected transition probabilities 22% Skip-Puppers, 16% Early-Puppers, 31% Mid-Puppers, 16% Late-Puppers, 14% Missing Parous).

3.4 Results

3.4.1 Demography of molting animals

Survey frequencies and counts for each study year are provided in Table 3.1. We observed 2% of animals during all four study years, 11% during three years, 25% during two years, and 62% during one year. Tagged animals (all ages and sexes) were observed an average of 2.1 ± 1.4 times within a molting season (minimum 1, maximum 15, median 2, mode 1). Of the 4252 seals seen during the molt, 63% of animals had been seen during the lactation period several weeks earlier. For females, the composition of Immatures, Puppers, and Skip-Puppers seen during the molting period stayed relatively consistent within and across years, averaging 23%, 51%, and 26%, respectively.

3.4.2 Molt duration

Molt stage durations were 10.2 ± 5.3 days for τ_1 (stage 1), 9.4 ± 4.0 days for τ_2 (stage 2), and 9.6 ± 3.8 days for τ_3 (stage 3) (Table 3.2). Using these average stage durations, the entire visible molt duration T was 29.2 ± 7.7 (mean \pm standard deviation) days for Weddell seals. Using Equation 5, animals first seen in molt codes 1 (i.e. $k=1$), 2, 3, and 4 had σ_{Date_init} values of 3.90 days ($n=1007$), 6.04 days ($n=503$), 7.25 days ($n=251$), and 8.50 days ($n=369$), respectively. Note

that animals with only sightings at code 0 were excluded ($n=182$) such that the total number of animals assigned initiation dates was 2130.

3.4.3 Links between pupping phenology and molting phenology in one season

Molt initiation date ranged from Dec 09 to Feb 28 with a mean start date of January 15 ± 13.5 (SD) days. Based on the lowest AIC value and Akaike weight, the best mixed-effects model included the interaction between *Repro_cat* and *Year* (Table 3.3). Thus, the wide range (81 days) of molt initiation dates likely resulted from influences of year and reproductive categories.

The resulting transition probabilities from pupping categories to molting categories in each year are provided in Table 3.4. Skip-Puppers had the earliest average molt initiation dates (range December 28 to January 12 across study years) followed by Immatures (January 04 to January 15), Males (January 09 to January 24), and females that had given birth (Puppers; January 15 to January 29) (Figure 3.4). Given that eight of fifteen transition outcomes differ significantly from expected, the data strongly suggest that molt phenology is not independent from pupping phenology in a given year (Table 3.4). Specifically, the Early-Molt category is more likely to be comprised of Skip-Puppers (28% greater than expected) than Early-, Mid-, or Late-Puppers (13%, 13%, and 15% less than expected, respectively). Animals in the Mid-Molt category were disproportionately composed of animals that had been Missing during the previous pupping period (14% greater than expected). Animals that pupped contributed significantly more than expected to the Late-Molt category, with Late-Puppers (46%) contributing more than Mid-Puppers (39%), or Early-Puppers (36%). For Puppers, the molt initiation date was significantly related to when the pup was born (linear mixed effects model,

$R^2=0.24$). Thus, molt phenology is delayed in Puppies relative to Skip-Puppies, and there is a direct relationship between date of pupping and molt onset.

3.4.4 Inter-annual variation in ice dynamics, molt phenology, and colony attendance

Among most reproductive categories, the molt began earliest in AS13 (mean molt initiation date January 08±13 days) and latest in AS16 (January 22±14 days) with the two intermediate years in between, although this pattern was not always significant across reproductive categories (January 11±11 days in AS14 and January 14±10 days in AS15; Figure 3.4, Table 3.1). Sea ice break-out date varied by 33 days across the study years and both ice break-out and molt initiation dates were later in AS16 than other years (Table 3.1). Additionally, the proportion of Missing animals in Year 2 was higher (and proportion of Puppies lower) when Year 1 ice break-out was early (AS15, 22% missing, 60% pupped) and late (AS16, 20% missing, 55% pupped) relative to more normal ice break-out (AS13, 10% missing, 68% pupped and AS14, 6% missing, 72% pupped) (Table 3.1).

These inter-annual differences in molt initiation dates were supported by the raw survey data. In the first survey of AS13, 33% of observed seals had yet to begin molting (molt code 0) and only 12% had completed the molt (molt code 4), whereas in an AS16 survey on that same date, 47% of seals had yet to begin molting, and only 1% had completed the molt. The one exception was Puppies, in which molt initiation began significantly earlier in AS14 (January 15) than AS13 (January 19) and AS14 (January 18) (Figure 3.4, Table 3.1, TukeyHSD on ANOVA, $p<0.05$). While the AS16 molt surveys extended later than other years (Table 3.1), this would not have impacted molt initiation dates, as most seals seen after February 13-15 (final survey dates of AS13, AS14, and AS15) had started to molt (and thus molt start date would have already been

detected prior to the end of surveys). Indeed, removing the AS16 sightings after February 15 still resulted in significantly later AS16 molt start dates as compared to other years for all reproductive categories.

3.4.5 Links between pupping and molting phenology in one season and pupping in the next

For sexually mature females, the Year 2 pupping categories (Pupping, Skip-Pupping, or Missing) were significantly related to when the molt started (chi-square test, $\chi^2 = 18.923$, $p=0.0153$): Early-Molters contributed 4% less than expected to the Missing-Parous category whereas Late-Molters showed the opposite trend, contributing 6% more than expected to Missing-Parous (Table 3.5). The Year 2 pupping categories were more strongly related to the Year 1 pupping categories ignoring the intervening molt (chi-square test, $\chi^2 = 130.52$, $p<0.0001$, Table 3.6). In general, individuals in a given pupping category in year 1 were more likely to remain in the same category in year 2 than would be expected from random transition probabilities (Table 3.6). Thus, it appears that Year 1 pupping categories are more important than Year 1 molting categories in driving transitions to the Year 2 pupping categories.

3.5 Discussion

Weddell seals provided a unique opportunity to document molt duration and phenology due to their high inter-annual site fidelity on land-fast ice [35]. Using 8,915 sightings of 4,252 unique individuals, we found that parturient females tend to molt later, especially those with late parturition dates. Our findings echo the strong ties between molting and reproduction that have been described in avian taxa [14, 41]. Sexually mature, post-reproductive individuals have been found to molt later than sexually mature but non-reproductive white-crowned sparrows

Zonotrichia leucophrys oriantha (18 days later [42]), bullfinches *Pyrrhula pyrrhula* ([43]), European stonechats *Saxicola rubicola* (10 days later [44]), and Steller jays *Cyanocitta stelleri* [13].

Previous studies have found that duration of the molt also appears to vary as a function of reproductive success, such that successful offspring rearing increases the rate of the molt (e.g., 29% faster in European starlings *Sturnus vulgaris* [18], 22% faster in red knot *Calidris canutus islandica* [14]), which can compromise the integrity of the plumage and affect future survival and reproduction [17, 18, 42, 45]. In our study, we found no effect of sex, reproductive category, or year on molt duration. We estimated the Weddell seal molt duration to be 29.2 ± 7.7 (mean \pm standard deviation) days. The Weddell seal molt duration aligns well with the published estimates from other phocid seals, being longer than most catastrophic molts and similar in duration to non-catastrophic molts (Table 3.7). In contrast, phocid molt durations are notably longer than those of otariids (Table 3.7).

3.5.1 Reproductive history affects molt phenology

We found a striking effect of skipped reproduction on molt initiation date. During all study years, sexually mature females that did not produce a pup (Skip-Puppers) molted earlier than all other reproductive categories. In contrast, sexually mature females that produced a pup (Puppers) tended to molt later than sexually immature females (Immatures) and Males. Similar delays in molt phenology of post-parturient females have been found in all pinniped species studied during the molt [27-30]. In post-parturient females, molt initiation is likely inhibited by elevated circulating cortisol [46] and prolactin [47] levels during lactation. Similarly, in males,

testosterone is elevated during the breeding season [48]. These endocrine controls likely delay molt onset in Puppies and Males relative to Skip-Puppies and Immatures [49].

Within Puppies, molt timing loosely mirrored pup birth timing, with females that gave birth later initiating molt later (see Table 3.4). The relationship between pup birth date and molt initiation date may have been stronger if our study had included factors that are known to affect pupping and molting dates, including pup sex [36], maternal body condition [30], and circulating hormone concentrations [49]. Future studies should use these variables to explain life history event phenology.

Although the causal mechanisms in this study are unknown, we hypothesize that energetics may mediate carryover effects between pupping and molt; specifically, reduced body condition following lactation may delay molt onset until seals can regain sufficient energy stores by foraging; late molt phenology could increase energetic expenditure. In our study, the molt initiation date of Skip-Puppies (January 06 ± 12 days) aligned with the warmest air temperatures of the year (January 03-05 [50]); in contrast, Puppies initiated molt on average 16 days later (in up to 5°C colder temperatures) than Skip-Puppies (see Table 3.1). Because seal epidermal cells may have a minimum temperature threshold for mitotic division [51], mismatches between molt phenology and ambient conditions could lead to higher temperature differentials between skin and ambient temperatures (i.e. higher heat loss). Thus, by molting later, Puppies may experience increased molt costs and may need to gain more energy from foraging. These costs, in addition to the high energetic costs of lactation [33], may result in Puppies beginning the next reproductive cycle at poorer body conditions. It is currently unknown whether the energetic cost of delayed molt phenology relates more to the cellular molt stage (i.e. follicle activation period, start of hair growth) or the visible molt stage.

3.5.2 Inter-annual variation in ice dynamics, molt phenology, and colony attendance

We found a significant effect of year on molt initiation dates, with molt starting earliest in AS13 and latest in AS16 (see Table 3.1, Figure 3.4) in most reproductive categories. The marked inter-annual differences in molting phenology across AS13 and AS16 may be associated with differences in sea ice break-out phenology: in AS16, the McMurdo Sound ice break-out occurred 21 days later [52] and the molt occurred 10-15 days later than in AS13. Each year, the ice break-out triggers the annual phytoplankton bloom and enhances productivity for seals via trophic linkages [53]. Extremely limited pack ice retreat has been found to stunt (as much as 44% lower) and delay (up to 2 months) the annual phytoplankton bloom [54] which would likely impact the food resources of Weddell seals [55]. Indeed, similar ice perturbations delay Weddell seal pupping dates [36]. Lower food abundance has been found to delay molt onset in harbor seals [23] and higher food abundance has been found to advance molt onset in birds [8]. We suggest that a similar mechanism may be acting in this system: it is possible that low resource availability and consequently poor body condition delay molt via increased cortisol levels and suppressed thyroid hormones [31, 56].

3.5.3 Cross-year carryover effects between molting and pupping

In general, parous seals were likely to remain in the same pupping categories across Year 1 and Year 2 (Table 3.6); however, we found that Late-Puppers were more likely than expected to become Missing the following year. In turn, Missing individuals were 10% more likely than expected to remain missing (Table 3.6), although 76% of individuals returned to breeding colonies the subsequent year, suggesting that Missing seals were predominantly temporary

emigrants. Our evidence suggests that Year 2 reproductive outcomes are driven primarily by Year 1 pupping success/phenology rather than Year 1 molting phenology (Tables 3.5, 3.6).

While colony attendance provides breeding opportunities and predator avoidance, it also increases conspecific conflict and food competition [57]. In immature Weddell seals, increased sea ice extent has been found to result in more frequent emigration, probably because larger sea ice extent corresponds to lower primary production and lower presumed foraging success [58], and in turn there exists a threshold body condition that is necessary for attending colonies [59]. Indeed, the probability of colony attendance appeared related to the ice dynamics in a given year, as colony attendance was lower in the years following early or late summer ice break-out (Table 3.1).

It is common for sexually mature birds and mammals to intermittently skip reproduction [60] because it takes individuals more than one calendar year to acquire the capital needed for future reproduction [61]. In support of this mechanism, non-breeding individuals are often in poorer quality due to stress, starvation, diseases, or parasites [62]. We suggest that energetics may be responsible for the increased probability of Late-Puppers becoming Missing: individuals with lower energy reserves are commensurately less likely to attend breeding colonies [58]. Similar effects have been seen in other species. In red voles, for example, females that successfully reproduce and consequently molt later have lower overwinter survival due to delayed winter preparation [63, 64]. Recent evidence suggests that Weddell seal life history events fill nearly an entire year, with embryonic diapause being very short or non-existent [65], gestation lasting 10 months [66], visible molt lasting 29 days (this study), and lactation lasting 45 days [67]; however, some Weddell seals produce pups in many sequential years [36] so a >365 day life history cycle is unlikely, at least for the best performing individuals.

3.5.4 Implications of links between pupping and molting phenology

Phenological disruptions are increasingly likely under predicted environmental changes [68] and have already been documented in several species; for instance, breeding phenology advancement in birds has been associated with spring temperature increases [69-71]. These phenology disruptions may carry-over to other life history events or other years [72], and have larger impacts on population health than predicted if treated in isolation. In this way, phenology links are important to incorporate into predictions of global change. These carry-over effects are particularly concerning in high-latitude environments [73] because annual phenology impacts survival and reproduction more directly due to the shorter ‘benign’ season [74]. Furthermore, species may differ in their phenological plasticity, which can lead to mismatches between interacting species such as predators and prey. Here we have shown that to fully understand the ecological impacts of changing environments, researchers must first characterize the full annual cycle, including how molt and reproduction interact.

3.6 Acknowledgements

We thank the B-009 team members, especially Robert Garrott, Terrill Paterson and Jay Rotella for contributing information on many birth dates and on female ages and reproductive states, as it was crucial to our paper. We also thank B-292 field members Michelle Shero, Rachel Bergartt, Linnea Pearson, Patrick Robinson, Skyla Walcott, Gregg Adams, and Rob McCorkell for data collection; Marm Kilpatrick and Tim Tinker for statistical advice; and Matt Cameron, Rachel Holser, and Joe Eisaguirre for helpful comments on previous drafts. NCEP Reanalysis air temperature data provided by the NOAA/OAR/ESRL PSD, Boulder, Colorado, USA. Ice break-out date from the US National Snow and Ice Data Center NASA Bootstrap SMMR-SSM/I combined dataset. This project was made possible by logistical support from the United States National Science Foundation (NSF) through the U.S. Antarctic Program, Lockheed Martin Antarctic Support Contract, and support staff in Christchurch, New Zealand and McMurdo Station. Research activities were approved by National Marine Fisheries Service Marine Mammal permit #17411, University of Alaska IACUC protocols #419971 and #854089 and the Antarctic Conservation Act permit #2014-003. Research was conducted with financial support from NSF grant ANT-1246463 to JMB and JWT and an NSF graduate research fellowship to RSB (Grant No. 2015174455). This material is based upon work supported by the National Science Foundation Graduate Research Fellowship Program (RSB) and while serving at the National Science Foundation (JMB). Any opinion, findings, and conclusions or recommendations expressed in this material are those of the authors and do not necessarily reflect the views of the National Science Foundation.

Table 3.1. Information about molt surveys during 2013-2016, including quartiles for pupping dates and mean \pm standard deviation molt initiation dates for each year and reproductive category. Significant differences in molt initiation dates among years (by row, within a reproductive category) are denoted with Roman numerals.

	AS13	AS14	AS15	AS16
Sighting Metadata				
# Sightings	1810	1470	2212	3423
# Seals	1038	866	937	1411
# Survey Days	19	10	11	26
First Molt Survey Date	Jan 13	Jan 17	Jan 18	Jan 18
Last Molt Survey Date	Feb 13	Feb 14	Feb 15	Mar 8
Pupping Quartiles				
Minimum	*	Oct 11	Oct 13	Oct 14
25 th percentile	*	Oct 22	Oct 22	Oct 24
Median	Oct 29	Oct 26	Oct 27	Oct 28
75 th percentile	Nov 02	Oct 30	Oct 30	Nov 02
Maximum	Nov 15	Nov 26	Nov 13	Nov 19
Molt Initiation Dates				
Skip-Puppers	Dec 28 \pm 11.9 ⁱ	Jan 05 \pm 10.7 ⁱⁱ	Jan 07 \pm 9.9 ⁱⁱ	Jan 12 \pm 9.8 ⁱⁱⁱ
Missing Immatures	Jan 06 \pm 11.6 ⁱ	Jan 07 \pm 13.7 ⁱ	Jan 11 \pm 9.7 ⁱ	Jan 17 \pm 12.1 ⁱⁱ
Seen Immatures	Jan 04 \pm 11.3 ⁱ	Jan 11 \pm 6.7 ⁱⁱ	Jan 15 \pm 8.3 ⁱⁱ	Jan 15 \pm 14.6 ⁱⁱ
Missing Parous	Jan 07 \pm 14.5 ⁱ	Jan 11 \pm 11.8 ⁱ	Jan 17 \pm 11.7 ⁱ	Jan 19 \pm 9.6 ⁱ
Seen Puppers	Jan 19 \pm 8.4 ⁱ	Jan 15 \pm 11.1 ⁱⁱ	Jan 18 \pm 9.2 ⁱ	Jan 29 \pm 13.2 ⁱⁱⁱ
Males	Jan 09 \pm 13.1 ⁱ	Jan 13 \pm 10.6 ⁱⁱ	Jan 16 \pm 8.1 ⁱⁱ	Jan 24 \pm 12.9 ⁱⁱⁱ
Ice break-out date**				
	Jan 14	Jan 14	Jan 02	Feb 04
Colony attendance***				
Skip-Puppers	22%	22%	18%	24%
Missing-Parous	10%	6%	22%	20%
Seen Puppers	68%	72%	60%	55%

* In AS13, the United States government shut down delayed the Weddell seal research program by several weeks, and pup tagging began only after 50% of the pups were born; as a result, the dates of the earlier quartiles are not known (see methods).

** Date when 7-day running mean of ice concentration falls below 50%, see Chapter 4 for details.

*** Colony attendance proportions for the following year.

Table 3.2. Parameter values used to estimate molt duration and molt initiation dates for all ages and sexes combined.

Parameter	Molt duration (mean $\mu \pm \text{SD } \sigma$)	Number of Individuals
τ_n ; duration of molt stage n		
τ_1	10.2 \pm 5.3 days	70
τ_2	9.4 \pm 4.0 days	73
τ_3	9.6 \pm 3.8 days	50
T ; entire molt duration		
	29.2 \pm 7.7 days	
Δ_n ; difference between first sighting at stage n and previous midpoint		
Δ_1	5.4 \pm 3.9 days	347
Δ_2	4.5 \pm 2.9 days	347
Δ_3	4.3 \pm 2.9 days	226
Δ_4	5.1 \pm 3.7 days	213

Table 3.3. Model selection for molt initiation date. The `Repro_cat*Year` interaction includes the two main effects and the interaction.

Model	K	AIC	Δ AIC	AIC Weight
<code>Repro_cat*Year</code>	5	16312.7	0	1
<code>Repro_cat+Year</code>	4	16392.78	80.08	4.08E-18
<code>Repro_cat*Year*Age</code>	7	16514.2	121.42	1.75E-44
<code>Year</code>	3	16719.9	407.2	3.78E-89
<code>Repro_cat</code>	3	16815.74	503.04	5.8E-110
<code>Intercept</code>	2	17134.43	821.73	3.7E-179

Table 3.4. Transition probabilities from pupping categories in the Year 1 pupping season (rows) and molting categories in the Year 1 molting season (columns) for previously parous females. The expected molt category outcomes are provided in the column headers and assume a random distribution of molt timing across pupping categories, calculated from the contribution of all pupping categories to each molting category. Each cell contains the number of individuals with that transition outcome (top value), the actual proportion of animals with that transition outcome (middle top value), the actual minus expected outcome (middle bottom value, green if positive, red if negative) and the p-value for the Markov simulation of actual versus expected outcome (bottom value, *** $p < 0.05$ with Bonferroni correction). Actual transition outcomes sum to 100% for each reproductive history (row).

		Molt Year 1		
		Early-Molter (expected 26%)	Mid-Molter (expected 48%)	Late-Molter (expected 26%)
Pupping Year 1	Skip-Pupper	144 54% +28% ***	114 43% -5%	9 3% -23% ***
	Early-Pupper	18 13% -13% ***	72 51% +4%	50 36% +9%
	Mid-Pupper	35 13% -13% ***	129 48% +1%	103 39% +12% ***
	Late-Pupper	16 11% -15% ***	62 43% -5%	66 46% +20% ***
	Missing Parous	23 27% +1%	53 62% +14%	10 12% -15% ***

Table 3.5. Transition probabilities of parous female Weddell seals from Year 1 molting categories (rows) to Year 2 pupping categories (columns). See Table 3.4 legend for description of values.

		Pupping Year 2				
		Skip Pup (expected 24%)	Early Pup (expected 16%)	Mid Pup (expected 32%)	Late Pup (expected 17%)	Missing Parous (expected 12%)
Molt Year 1	Early Molt	82 28% +5%	53 18% +3%	87 30% -2%	45 16% -1%	23 8% -4% ***
	Mid Molt	118 23% -1%	70 14% -2%	169 33% +1%	90 18% +1%	61 12% 0%
	Late Molt	48 19% -4%	39 16% 0%	76 31% -1%	40 16% -1%	44 18% +6% ***

Table 3.6. Transition probability from pupping Year 1 to pupping Year 2 (ignoring the intermediate molt phenology). See Table 3.4 legend for description of values.

		Pupping Year 2				
		Skip-Puppers (expected 22%)	Early-Puppers (expected 16%)	Mid-Puppers (expected 31%)	Late-Puppers (expected 16%)	Missing Parous (expected 14%)
Pupping Year 1	Skip-Puppers	72 27% +5%	56 21% +4%	81 30% -1%	31 12% -5%	27 10% -4%
	Early-Puppers	37 27% +5%	43 31% +14% ***	41 29% -2%	7 5% -11% ***	11 8% -6%
	Mid-Puppers	47 18% -4%	32 12% -4%	103 39% +8% ***	45 17% +1%	36 14% -1%
	Late-Puppers	22 15% -6%	4 3% -14% ***	32 22% -9%	52 36% +20% ***	33 23% +9% ***
	Missing Parous	16 19% -3%	13 15% -1%	24 28% -3%	12 14% -2%	21 24% +10%

Table 3.7. Summary of molt durations for pinniped species.

Species	Family	Molt Duration (Days)	Molt Type	Citation
Hawaiian monk seal	<i>Phocidae</i>	8-9	Catastrophic	[30]
Southern elephant seal	<i>Phocidae</i>	7-14	Catastrophic	[75]
Mediterranean monk seal	<i>Phocidae</i>	14	Catastrophic	[29]
Weddell seal	<i>Phocidae</i>	29±8	Gradual	This study
Harbor seal	<i>Phocidae</i>	33-35	Gradual	[49, 76]
New Zealand sea lion	<i>Otariidae</i>	60	Gradual	[77]
Northern fur seal	<i>Otariidae</i>	105	Gradual	[78]






	Molt Code 0 Molt had not begun, no new fur visible.
	Molt Code 1 Head was molted and/or a thin stripe of new fur was visible on the dorsum.
	Molt Code 2 Head was completely molted and connected to a wide dorsal stripe .
	Molt Code 3 Most of the body was molted aside from small patches of fur remaining laterally between the front and rear flippers.
	Molt Code 4 Fully molted, with no old fur visible.

Figure 3.1. During surveys, each individual was assigned a molt code: 0 (unmolted), 1 (head or dorsal stripe molted), 2 (head and wide dorsal stripe molted), 3 (flank starting to molt), or 4 (completely molted).

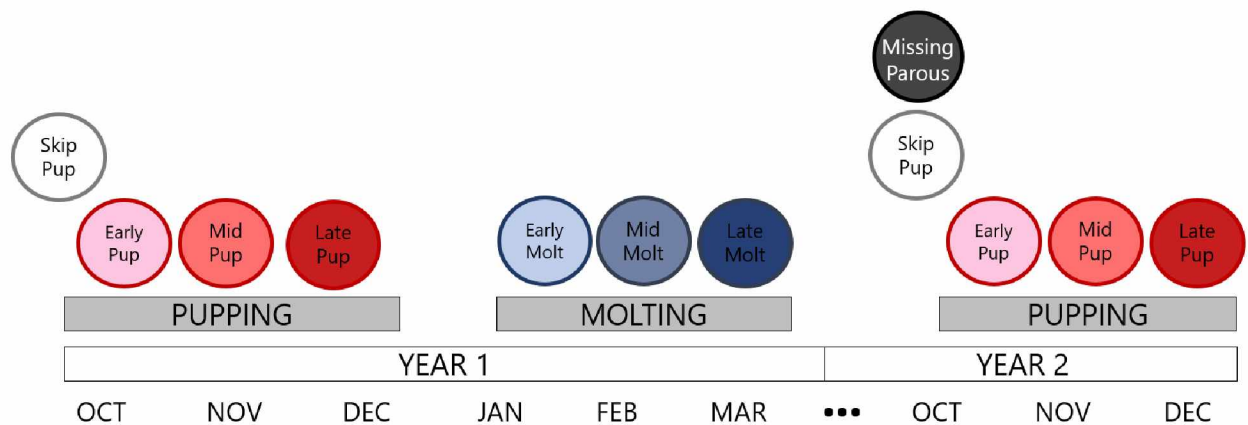


Figure 3.2. Based on individual sightings, adult female Weddell seals were assigned a phenology category for three life history events: pupping in Year 1, molting in Year 1, and pupping in Year 2. During the pupping season, Early-Puppers gave birth before the first 25%ile of the pupping distribution; Mid-Puppers gave birth on or between the 25-75%ile of the pupping distribution; Late-Puppers gave birth after the last 75%ile of the pupping distribution; Skip-Puppers had previously pupped but were not parturient in a given year; and Missing-Parous had been seen during the Year 1 pupping and molting season but were missing during the Year 2 pupping season. During the molting season, Early-Molters began molting before the first 25%ile of the molt start date distribution; Mid-Molters began molting on or between the 25-75%ile of the molting distribution; and Late-Molters gave began molting after the last 75%ile of the molt start date distribution.

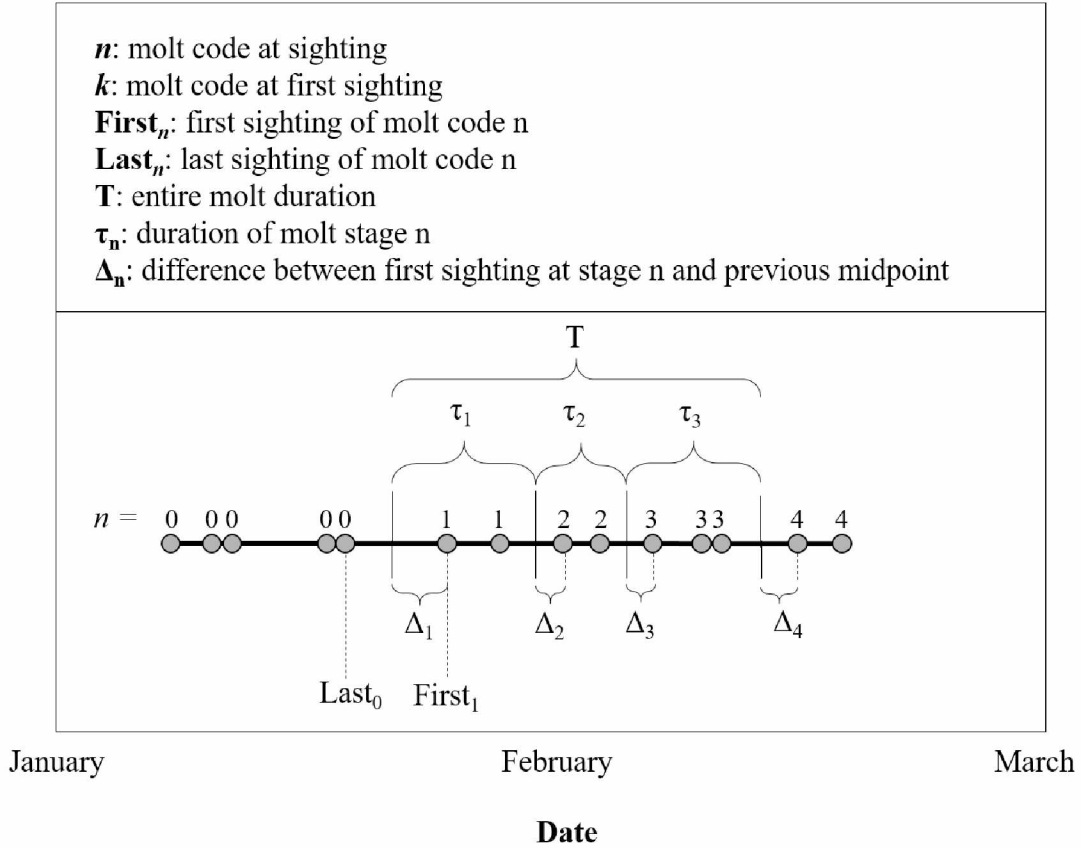


Figure 3.3. Molt sighting data from a theoretical animal with molt code n shown as numbers along the date axis. Each sighting is represented as a grey circle with molt code n shown. Mean molt stage durations τ_n were used to back-calculate a start date for each individual when the animal was not observed in a molt code n . A glossary of parameters is shown in the top panel.

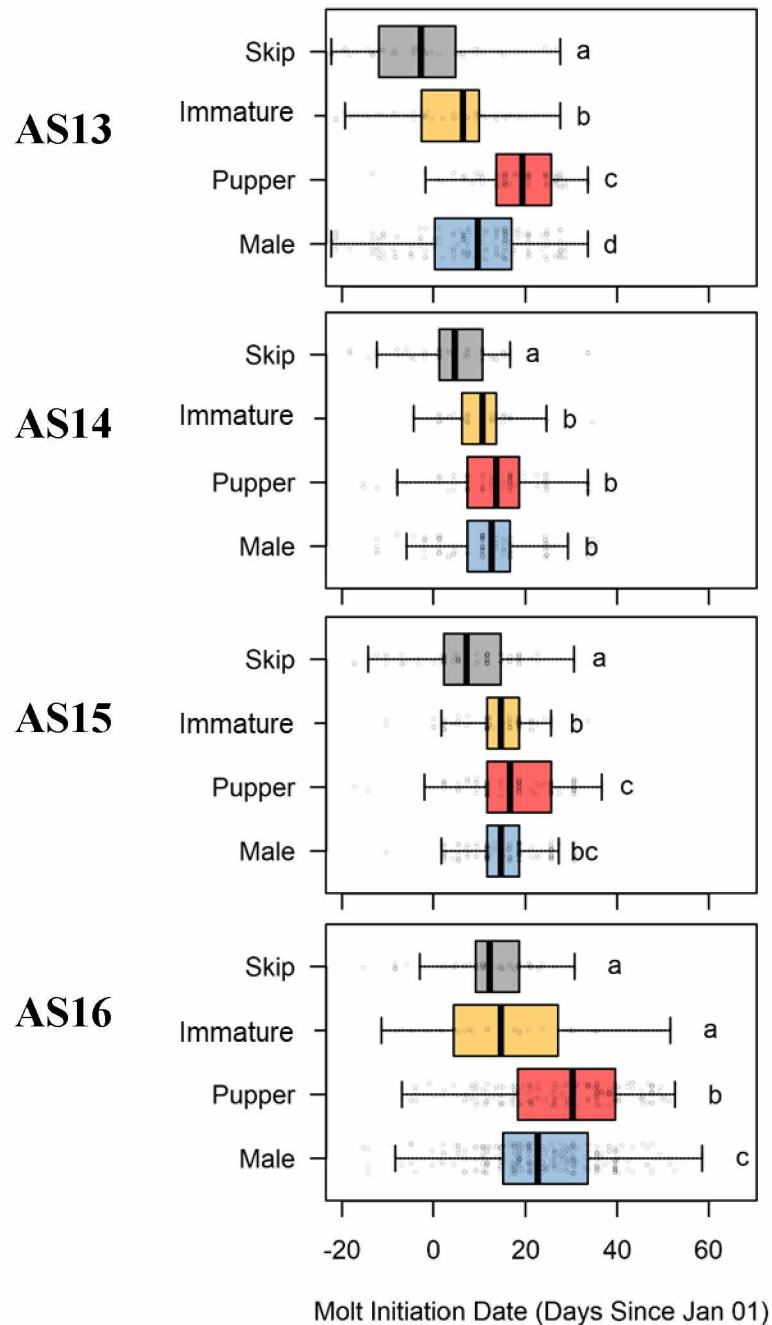


Figure 3.4. Molt initiation dates across reproductive categories and years (panels; AS13 is the 2013 Austral Year including the December 2013 – February 2014 molt). Within each year, different letters denote significantly different molt initiation dates across reproductive categories (Tukey's HSD, $p < 0.05$). During all study years, sexually mature females that did not produce a pup (Skips) molted earlier than all other reproductive categories. On the contrary, sexually

mature females that produced a pup (Puppers) tended to molt later than sexually immature females (Immatures, significant difference in AS13, AS15, AS16), and Males (significant difference in AS13, AS16).

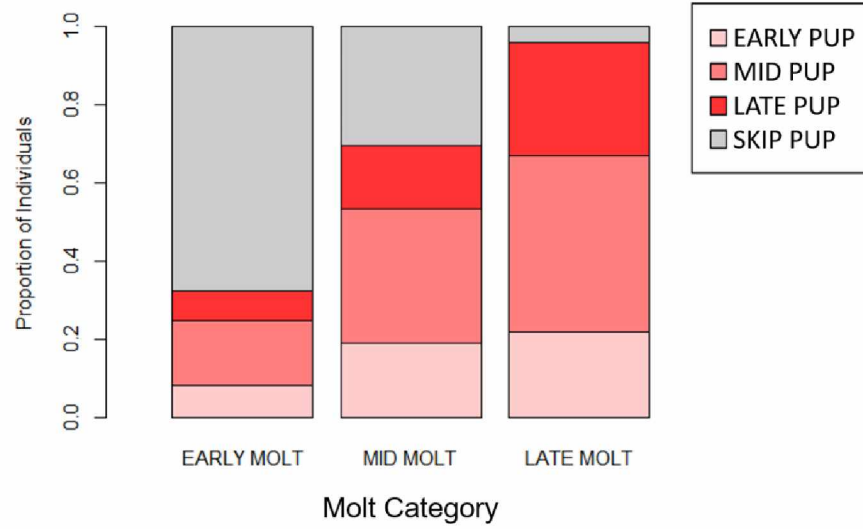


Figure 3.5. Proportion of seals in each molt category in Year 1 comprised of different reproductive categories from Year 1. Molt phenology was not independent of pupping phenology: the Early-Molters category was predominated by Skip-Puppers, whereas the Late-Molters category was predominated by Puppers.

3.7 Literature Cited

1. Barbraud C, Weimerskirch H. Antarctic birds breed later in response to climate change. *Proceedings of the National Academy of Sciences*. 2006;103(16):6248-51.
2. Gordo O. Why are bird migration dates shifting? A review of weather and climate effects on avian migratory phenology. *Climate Research*. 2007;35(1-2):37-58.
3. Morrison CA, Baillie SR, Clark JA, Johnston A, Leech DI, Robinson RA. Flexibility in the timing of post-breeding moult in passerines in the UK. *Ibis*. 2015;157(2):340-50.
4. Harrison XA, Blount JD, Inger R, Norris DR, Bearhop S. Carry-over effects as drivers of fitness differences in animals. *Journal of Animal Ecology*. 2011;80(1):4-18.
5. Watanuki Y, Ito M, Deguchi T, Minobe S. Climate-forced seasonal mismatch between the hatching of rhinoceros auklets and the availability of anchovy. *Marine Ecology Progress Series*. 2009;393:259-71.
6. Miller-Rushing AJ, Høye TT, Inouye DW, Post E. The effects of phenological mismatches on demography. *Philosophical Transactions of the Royal Society of London B: Biological Sciences*. 2010;365(1555):3177-86.
7. Hipfner JM. Matches and mismatches: ocean climate, prey phenology and breeding success in a zooplanktivorous seabird. *Marine Ecology Progress Series*. 2008;368:295-304.
8. Danner RM, Greenberg RS, Danner JE, Walters JR. Winter food limits timing of pre-alternate moult in a short-distance migratory bird. *Functional Ecology*. 2015;29(2):259-67.

9. Hemborg C, Lundberg A. Costs of overlapping reproduction and moult in passerine birds: an experiment with the pied flycatcher. *Behavioral Ecology and Sociobiology*. 1998;43(1):19-23.
10. Payne RB, Farner D, King J. Mechanisms and control of molt. *Avian Biology*. 1972;2:103-55.
11. Carey C. The impacts of climate change on the annual cycles of birds. *Philosophical Transactions of the Royal Society of London B: Biological Sciences*. 2009;364(1534):3321-30.
12. Gaston AJ, Gilchrist HG, Mallory ML, Smith PA. Changes in seasonal events, peak food availability, and consequent breeding adjustment in a marine bird: a case of progressive mismatching. *The Condor*. 2009;111(1):111-9.
13. Pitelka FA. Timing of molt in Steller Jays of the Queen Charlotte Islands, British Columbia. *The Condor*. 1958;60(1):38-49.
14. Dietz MW, Rogers KG, Piersma T. When the seasons don't fit: speedy molt as a routine carry-over cost of reproduction. *PLoS One*. 2013;8(1):e53890.
15. Helm B, Gwinner E. Timing of molt as a buffer in the avian annual cycle. *Current Zoology*. 2006;52:703-6.
16. Ling J. Adaptive functions of vertebrate molting cycles. *American Zoologist*. 1972:77-93.
17. McNamara JM, Houston AI. Optimal annual routines: behaviour in the context of physiology and ecology. *Philosophical Transactions of the Royal Society of London B: Biological Sciences*. 2008;363(1490):301-19.

18. Dawson A, Hinsley S, Ferns P, Bonser RC, Eccleston L. Rate of moult affects feather quality: a mechanism linking current reproductive effort to future survival. *Proceedings of the Royal Society of London B: Biological Sciences*. 2000;267(1457):2093-8.
19. Forcada J, Trathan PN, Murphy EJ. Life history buffering in Antarctic mammals and birds against changing patterns of climate and environmental variation. *Global Change Biology*. 2008. doi: 10.1111/j.1365-2486.2008.01678.x.
20. Fraser WR, Hofmann EE. A predator's perspective on causal links between climate change, physical forcing and ecosystem. *Marine Ecology Progress Series*. 2003;265:1-15.
21. Newton I, Rothery P. The timing, duration and pattern of moult and its relationship to breeding in a population of the European greenfinch *Carduelis chloris*. *Ibis*. 2005;147(4):667-79.
22. Green K, Burton HR, Watts DJ. Studies of the Weddell seal in the Vestfold Hills, east Antarctica: Australian Antarctic Division; 1995.
23. Daniel RG, Jemison LA, Pendleton GW, Crowley SM. Molting phenology of harbor seals on Tugidak Island, Alaska. *Marine Mammal Science*. 2003;19(1):128-40.
24. Stutz SS. Pelage patterns and population distributions in the Pacific harbour seal (*Phoca vitulina richardi*). *Journal of the Fisheries Board of Canada*. 1967;24(2):451-5.
25. Ling JK. Pelage and molting in wild mammals with special reference to aquatic forms. *Quarterly Review of Biology*. 1970:16-54.
26. Melchior HR, Iwen FA. Trapping, restraining, and marking arctic ground squirrels for behavioral observations. *The Journal of Wildlife Management*. 1965:671-8.

27. Boily P. Metabolic and hormonal changes during the molt of captive gray seals (*Halichoerus grypus*). American Journal of Physiology-Regulatory, Integrative and Comparative Physiology. 1996;270(5):1051-8.
28. Kirkman S, Bester M, Pistorius P, Hofmeyr G, Jonker F, Owen R, et al. Variation in the timing of moult in southern elephant seals at Marion Island. South African Journal of Wildlife Research. 2003;33(2):79-84.
29. Badosa E, Pastor T, Gazo M, Aguilar A. Molt in the Mediterranean monk seal from Cap Blanc, western Sahara. African Zoology. 2006;41(2):183-92.
30. Johanos TC, Becker BL, Ragen TJ. Annual reproductive cycle of the female Hawaiian monk seal (*Monachus schauinslandi*). Marine Mammal Science. 1994;10(1):13-30.
31. Romero LM, Storchlic D, Wingfield JC. Corticosterone inhibits feather growth: potential mechanism explaining seasonal down regulation of corticosterone during molt. Comparative Biochemistry and Physiology Part A: Molecular & Integrative Physiology. 2005;142(1):65-73.
32. Cameron M, Siniff D. Age-specific survival, abundance, and immigration rates of a Weddell seal (*Leptonychotes weddellii*) population in McMurdo Sound, Antarctica. Canadian Journal of Zoology. 2004;82(4):601-15. doi: 10.1139/z04-025.
33. Wheatley KE, Bradshaw CJ, Davis LS, Harcourt RG, Hindell MA. Influence of maternal mass and condition on energy transfer in Weddell seals. Journal of Animal Ecology. 2006;75(3):724-33. doi: 10.1111/j.1365-2656.2006.01093.x. PubMed PMID: 16689955.

34. Chambert T, Rotella JJ, Higgs MD, Garrott RA. Individual heterogeneity in reproductive rates and cost of reproduction in a long-lived vertebrate. *Ecology and Evolution*. 2013;3(7):2047-60. doi: 10.1002/ece3.615. PubMed PMID: 23919151; PubMed Central PMCID: PMC3728946.
35. Rotella JJ, Link WA, Chambert T, Stauffer GE, Garrott RA. Evaluating the demographic buffering hypothesis with vital rates estimated for Weddell seals from 30 years of mark-recapture data. *Journal of Animal Ecology*. 2012;81(1):162-73. doi: 10.1111/j.1365-2656.2011.01902.x. PubMed PMID: 21939440.
36. Rotella JJ, Paterson JT, Garrott RA. Birth dates vary with fixed and dynamic maternal features, offspring sex, and extreme climatic events in a high-latitude marine mammal. *Ecology and Evolution*. 2016;6(7):1930-41.
37. Chambert T, Rotella JJ, Garrott RA. Female Weddell seals show flexible strategies of colony attendance related to varying environmental conditions. *Ecology*. 2015;96(2):479-88.
38. Akaike H. Information theory and an extension of the maximum likelihood principle. *Selected Papers of Hirotugu Akaike*: Springer; 1998. p. 199-213.
39. Burnham KP, Anderson DR. *Model selection and multimodel inference: a practical information-theoretic approach*: Springer Science & Business Media; 2003.
40. Hochberg Y. A sharper Bonferroni procedure for multiple tests of significance. *Biometrika*. 1988;75(4):800-2.
41. Newton I. Molt and plumage. *Ringed & Migration*. 2009;24(3):220-6.
42. Morton GA, Morton ML. Dynamics of postnuptial molt in free-living mountain white-crowned sparrows. *Condor*. 1990:813-28.

43. Newton I. The moult of the Bullfinch *Pyrrhula pyrrhula*. Ibis. 1966;108(1):41-67.
44. Flinks H, Helm B, Rothery P. Plasticity of moult and breeding schedules in migratory European Stonechats *Saxicola rubicola*. Ibis. 2008;150(4):687-97.
45. Johnson EI, Stouffer PC, Bierregaard Jr RO. The phenology of molting, breeding and their overlap in central Amazonian birds. Journal of Avian Biology. 2012;43(2):141-54.
46. Raeside J, Ronald K. Plasma concentrations of oestrone, progesterone and corticosteroids during late pregnancy and after parturition in the harbour seal, *Phoca vitulina*. Journal of Reproduction and Fertility. 1981;61(1):135-9.
47. Boyd I. Changes in plasma progesterone and prolactin concentrations during the annual cycle and the role of prolactin in the maintenance of lactation and luteal development in the Antarctic fur seal (*Arctocephalus gazella*). Journal of Reproduction and Fertility. 1991;91(2):637-47.
48. Bartsh SS, Johnston SD, Siniff DB. Territorial behavior and breeding frequency of male Weddell seals (*Leptonychotes weddelli*) in relation to age, size, and concentrations of serum testosterone and cortisol. Canadian Journal of Zoology. 1992;70(4):680-92.
49. Thompson P, Rothery P. Age and sex differences in the timing of moult in the common seal, *Phoca vitulina*. Journal of Zoology. 1987;212(4):597-603.
50. Kanamitsu M, Ebisuzaki W, Woollen J, Yang S-K, Hnilo JJ, Fiorino M, et al. NCEP–DOE AMIP-II Reanalysis (R-2). Bulletin of the American Meteorological Society. 2002;83(11):1631-43. doi: 10.1175/bams-83-11-1631.
51. Feltz ET, Fay FH. Thermal requirements in vitro of epidermal cells from seals. Cryobiology. 1966;3(3):261-4.

52. Comiso J. Bootstrap Sea Ice Concentrations from Nimbus-7 SMMR and DMSP SSM/I-SSMIS, Version 3. Boulder, Colorado USA: NASA National Snow and Ice Data Center Distributed Active Archive Center; 2017.
53. Ainley D, Fraser W, Sullivan C, Torres J, Hopkins T, Smith W. Antarctic mesopelagic micronekton: evidence from seabirds that pack ice affects community structure. *Science*. 1986;232:847-50.
54. Arrigo KR, Worthen D, Schnell A, Lizotte MP. Primary production in Southern Ocean waters. *Journal of Geophysical Research: Oceans*. 1998;103(C8):15587-600.
55. Seibel BA, Dierssen HM. Cascading trophic impacts of reduced biomass in the Ross Sea, Antarctica: Just the tip of the iceberg? *The Biological Bulletin*. 2003;205(2):93-7.
56. St. Aubin D, Geraci J. Capture and handling stress suppresses circulating levels of thyroxine (T4) and triiodothyronine (T3) in beluga whales *Delphinapterus leucas*. *Physiological Zoology*. 1988;61(2):170-5.
57. Siniff D, DeMaster D, Hofman R, Eberhardt L. An analysis of the dynamics of a Weddell seal population. *Ecological Monographs*. 1977;47(3):319-35.
58. Stauffer GE, Rotella JJ, Garrott RA. Variability in temporary emigration rates of individually marked female Weddell seals prior to first reproduction. *Oecologia*. 2013;172(1):129-40. doi: 10.1007/s00442-012-2472-z. PubMed PMID: 23053233.
59. Laws RM. Growth and sexual maturity in aquatic mammals. *Nature*. 1956;178:193-4.
60. Baron JP, Galliard JF, Ferrière R, Tully T. Intermittent breeding and the dynamics of resource allocation to reproduction, growth and survival. *Functional Ecology*. 2013;27(1):173-83.

61. Shaw AK, Levin SA. The evolution of intermittent breeding. *Journal of Mathematical Biology*. 2013;66(4-5):685-703.
62. Bradley J, Wooller R, Skira I. Intermittent breeding in the short-tailed shearwater *Puffinus tenuirostris*. *Journal of Animal Ecology*. 2000;69(4):639-50.
63. Viitala J. The red vole, *Clethrionomys rutilus*(Pall.), as a subordinate member of the rodent community at Kilpisjaervi, Finnish Lapland. *Acta Zoologica Fennica*. 1984.
64. Ylönen H. Vole cycles and antipredatory behaviour. *Trends in Ecology & Evolution*. 1994;9(11):426-30.
65. Shero MR, Adams GP, Burns JM. Field use of ultrasonography to characterize the reproductive tract and early pregnancy in a phocid, the weddell seal (*Leptonychotes weddellii*). *The Anatomical Record*. 2015;298(12):1970-7.
66. Shero M, Adams G, McCorkell R, Kirkham A, Burns J. Minimally-invasive ultrasonography reveals a pinniped that may not have an embryonic diapause. *Society for Marine Mammalogy; Canada*2017.
67. Tedman R, Green B. Water and sodium fluxes and lactational energetics in suckling pups of Weddell seals (*Leptonychotes weddellii*). *Journal of Zoology*. 1987;212(1):29-42.
68. Vegvari Z, Bokony V, Barta Z, Kovacs G. Life history predicts advancement of avian spring migration in response to climate change. *Global Change Biology*. 2010;16(1):1-11.
69. Crick HQ, Dudley C, Glue DE, Thomson DL. UK birds are laying eggs earlier. *Nature*. 1997;388(6642):526-.
70. Both C, Bouwhuis S, Lessells C, Visser ME. Climate change and population declines in a long-distance migratory bird. *Nature*. 2006;441(7089):81-3.

71. Both C, Visser ME. Adjustment to climate change is constrained by arrival date in a long-distance migrant bird. *Nature*. 2001;411(6835):296-8.
72. Fayet AL, Freeman R, Shoji A, Kirk HL, Padgett O, Perrins CM, et al. Carry-over effects on the annual cycle of a migratory seabird: an experimental study. *Journal of Animal Ecology*. 2016;85(6):1516-27.
73. Fretwell SD. *Populations in a seasonal environment*: Princeton University Press; 1972.
74. Reed TE, Schindler DE, Waples RS. Interacting effects of phenotypic plasticity and evolution on population persistence in a changing climate. *Conservation Biology*. 2011;25(1):56-63.
75. Boyd I, Arnborn T, Fedak M. Water flux, body composition, and metabolic rate during molt in female southern elephant seals (*Mirounga leonina*). *Physiological Zoology*. 1993;43-60.
76. Scheffer VB, Slipp JW. The harbor seal in Washington State. *The American Midland Naturalist*. 1944;32(2):373-416.
77. McConkey S, Lallas C, Dawson S. Moulting and changes in body shape and pelage in known-age male New Zealand sea lions (*Phocarctos hookeri*). *New Zealand Journal of Zoology*. 2002;29(1):53-61.
78. Scheffer VB, Johnson AM. *Molt in the northern fur seal*: US Department of Interior, Fish and Wildlife Service; 1963.

Chapter 4. Seal diving behavior suggests shallowing of fish distributions during sea-ice driven phytoplankton blooms ³

4.1 Abstract

In Antarctica, the short duration of optimal environmental conditions constrains the timing of biological processes. Summer sea ice break-out and the resulting phytoplankton bloom drastically impact trophic interactions; however, little is known about the resulting changes in vertical space utilization of organisms, from zooplankton to marine mammals. Data from time-depth recorders placed on 59 adult female Weddell seals *Leptonychotes weddellii* over four years revealed a previously undocumented seasonal shallowing of dive depths. Dives gradually shallowed from >300 m to less than 200 m during the seasonal phytoplankton bloom and returned to >300 m after the bloom apparently dissipated several weeks later. Inter-annual variability in the seasonal timing of this pattern was explained by ice break-out phenology, as later ice break-out correlated with later dive shallowing. Seal feeding effort and success, as measured by jaw accelerometers and vertical transit rates, were significantly higher during the phytoplankton bloom; however, stable isotope analysis revealed no seasonal diet shifts. Taken together, results suggest that during the phytoplankton bloom that follows ice break-out, zooplankton and fishes aggregate in shallower waters, and top predators adjust their foraging behaviour to take advantage of the increased prey availability at these shallower depths.

³ RS Beltran, GA Breed, T Adachi, A Takahashi, Y Naito, PW Robinson, WO Smith Jr., AM Kilpatrick, AL Kirkham, JM Burns. Seal diving behavior suggests shallowing of fish distributions during sea-ice driven phytoplankton blooms. Prepared for submission to the Proceedings of the National Academy of Sciences.

4.2 Introduction

The co-evolution of predators and their prey causes distribution patterns to vary predictably as a function of space and time. In the ocean, the ubiquitous diel vertical migrations (DVMs) of zooplankton comprise the largest daily biomass movement on the planet [1].

Zooplankton avoid visual predators by moving closer to the surface in the dark of night and returning to depth during the light of day. In response, seals, whales, and penguins track the vertical movements of zooplankton and their fish predators [1-3], often diving deeper during the day and shallower at night [2, 4]. This vertical coupling (“cascading migration” [5]) has been studied extensively on a daily scale; however, it is unclear if DVMs of zooplankton occur at high latitudes with seasonally variable photoperiods.

Polar regions are characterized by high resource availability and constant photoperiod during summer, when retreating sea ice and increased solar radiation trigger a rapid increase in phytoplankton biomass in the ocean’s upper 50 m [6, 7]. Behavioural plasticity in vertical movements by zooplankton has been shown to occur when food supply and photoperiodic cues change [8]. When increased algal concentrations provide food resources and shade to the water column, zooplankton [9] and their fish predators [10] prioritize feeding and spawning within the surface layer over remaining at depth to avoid predators [9, 11-14]. For example, adult zooplankton come to the surface to spawn [15], larval zooplankton undergo a developmental ascent to surface waters seeking food [16], and fish larvae inhabit near-surface waters to feed on zooplankton [17]. During this brief period of increased resource availability, zooplankton and fishes may forgo DVMs in favour of constant, shallow distributions [8]. The influences of these seasonal DVM patterns on vertical ecosystem coupling are poorly understood due to the

logistical challenges of studying ecosystem dynamics in both continuous time and 3-dimensional space.

The aim of this study was to examine how variation in the timing of ice break-out controls trophic interactions and vertical space use by fishes and the top predators that consume them. We combined measurements of vertical foraging behaviour with feeding activity measured by jaw accelerometers and diet assessed via stable isotope analyses in an Antarctic top predator, the Weddell seal *Leptonychotes weddellii*. Understanding the vertical dimension of these seasonal trophic dynamics is essential to a complete understanding of the ecology of the Ross Sea [18], the Southern Ocean's most productive region [19, 20] that supports a third of the world's Adélie penguins *Pygoscelis adeliae* and emperor penguins *Aptenodytes forsteri* and half of its killer whales *Orcinus orca* [21].

4.3 Methods

4.3.1 Field methods

Adult female Weddell seals ($n=95$) were captured in Erebus Bay, Ross Sea, Antarctica (77.6°S 167.0°E) during austral summers 2013-2016. Throughout this manuscript the study years are referred to by the year in which the summer started: i.e. AS13 refers to the 2013-14 austral summer season that extended from November 2013 through February 2014. All females were between the ages of 10 and 20 years and had given birth at least once prior to inclusion in this study. Each individual was chemically immobilized as described in Mellish et al. [22] and instrumented with a time-depth recorder (hereafter TDR, manufactured by LOTEK, model LAT1800, 6 second sampling interval) and VHF tag for relocation (manufactured by SIRTRACK) during the lactation period (November/December). In AS13 and AS14, one

whisker was plucked from each of 19 seals, and the follicle number recorded [23]. Whiskers were selected based on the following criteria: 1) The whisker was at asymptotic length (e.g. similar in length to its adjacent whiskers [24]) ; and 2) The whisker was fully intact (e.g. tapered at end, with no clear breakage or splintering). In AS16, four seals were also instrumented with raw acceleration loggers (Little Leonardo, 2-axis acceleration at 20Hz) that were affixed to the jaw with Loctite epoxy, and recovered 2-4 days later. If the seal had given birth to a pup, the birth date was calculated as described in Chapter 3 of this dissertation.

During the molting period (January/February), seals were recaptured and their molt start dates were calculated as described in Chapter 3 of this dissertation. Of the 95 instrumented seals, 59 were recaptured (57 ± 13 days later) with their TDRs that contained complete dive records used in this analysis. If applicable, the regrown whisker was plucked from the recorded whisker follicle location [25]. Additionally, seal mass was measured at tag deployment and recovery using an electronic scale (MSI-7300 Dyna-Link 2, resolution ± 0.25 kg) suspended from a tripod [26].

4.3.2 Diving data analysis

Zero-offset correction and dive identification were accomplished using the IKNOS toolbox in MATLAB (Y. Tremblay, unpublished, as used in Kuhn et al. [27], Robinson et al. [28]). For each dive (defined as an excursion from the surface to a minimum depth of 10 meters and a minimum duration of 30 seconds, $n=138,506$), the maximum dive depth, total duration, the duration of the bottom phase (defined as 80% of maximum dive depth), rate of ascent, rate of descent, and number of vertical excursions in the bottom phase (wiggles; e.g. [27, 28]), were

calculated. Using the raw acceleration data, prey capture attempts were identified based on a 0.3g amplitude surge acceleration threshold in IGOR PRO [29] (Figure 4.1).

Each dive was classified as either benthic or pelagic based on parameter thresholds adapted from Robinson et al. [30]. Dives were considered benthic if they had (1) minimal bottom phase vertical excursions and (2) square corners. To characterize the bottom phase vertical excursions, we calculated a kernel density of bottom phase vertical rate for each dive. If the peak fell within the range of ± 0.08 meters per second (nearly flat bottom) and the height of the peak exceeded a density of 1.5 (consistent vertical rate), it was classified as a benthic dive.

Additionally, best-fit lines were drawn for the descent phase and the bottom phase, and the intersection between the two lines was checked against the animal's actual trajectory. If the actual trajectory was less than 15 meters from the intersection point (i.e. switch from descent phase to bottom phase was sharp), it was identified as a benthic dive ($n=1,423$). We used a linear mixed-effects model in R (package "lmer") to determine whether benthic dive depths varied predictably across the summer. Benthic dives were then excluded from all remaining analyses because we were interested in quantifying seasonal changes in mid-water dives. All other dives (those with gradual changes from descent to bottom phase, variable vertical rates) were considered pelagic and were included in all analyses ($n=137,083$, or 99% of all dives).

Figure 4.2B was produced by calculating averages of the maximum depth of each pelagic dive. Using a Generalized Additive Mixed Model (GAMM) fit to the 95th quantile of dive depth on each day for each seal ($n=2,941$)(Figure 4.3), we characterized the deep-shallow-deep seasonal diving pattern. We chose to fit the 95th quantile of dive depth for two reasons: 1) we were interested in quantifying the seasonal change in mid-water (not under-ice) dive depths; and 2) seals primarily encounter prey near the maximum dive depth [31]. To evaluate the inter-

annual differences in the deep-shallow-deep diving pattern, we fit a 5th order GAMM with individual as a random effect to the 95th quantile dive depths (per individual per day) separately for each study year.

To differentiate the shallow period from the deep periods preceding and following, we calculated the full time duration at 25% minimum depth (adapted from full-width-at-half-maximum waveform analysis) using the following equation:

$$Cutoff = Y_{max} - \left[(Y_{max} - Y_{min}) * \frac{1}{4} \right]$$

where Y_{max} is the shallowest 95th quantile daily depth value (171 meters) and Y_{min} is the deepest 95th quantile daily depth value (410 meters). The cutoff was found to be 231 meters, and days where 95th quantile dive depth was shallower than the cutoff were considered the “shallow period”. To determine whether seals dove deeper during daytime (1200 to 1300 local time) than nighttime (2400 to 0100 local time) across the summer, we ran two sets of linear mixed-effects model (R package “lme” with individual as random effect; model1= *divedepth~icecorrecteddate*; model2=*divedepth ~ icecorrecteddate + timeofday*, where *timeofday* is a dummy variable for daytime and nighttime). AIC values were compared between m1 and m2 for each of the three behavioral periods: “deep before break-out”, “shallow”, “deep after break-out”.

4.3.3 Percent ice cover

To compare diving patterns with interannual ice dynamics, we computed daily sea ice concentrations (% cover between Nov 01 and Feb 28) from the NASA Bootstrap SMMR-SSM/I combined dataset courtesy of the US National Snow and Ice Data Center for each year (spatial resolution 25km x 25km). Daily averaged sea ice concentration data were extracted for latitude 77.32°S and longitude 165.84°E (station 71904), which is in Wohlschlag Bay, McMurdo Sound,

just north of our study site in Erebus Bay. The date of ice melt/break-out was defined as the first occurrence of a 7-day running mean ice concentration of <50% [32]. The ice break-out date was taken as the approximate start date of *in situ* primary production. This is a conservative estimate of primary production, as phytoplankton advection and sea-ice microalgae release precede *in situ* production [19, 33] (see Discussion).

4.3.4 Diet analysis

To infer Weddell seal diet across the summer period, we analyzed whisker carbon and nitrogen stable isotopes ($\delta^{13}\text{C}$ and $\delta^{15}\text{N}$ values, respectively) in whiskers grown between the lactation and molting periods. Each whisker was measured and then washed for 30 minutes in a reciprocal shaking ultrasonic bath (20°C, 180 rpm; Thermo Fisher Scientific, Waltham, MA, USA) with petroleum ether to remove exogenous lipids. The base of each whisker (0.8 ± 0.3 cm) was removed in order to avoid the ^{15}N bias associated with the sub-dermal whisker portion [34]. The remaining whisker was then subsampled into 0.45-0.55 mg sequential segments and placed into tin boats for analysis. In addition, the distance of each subsample from the whisker tip was recorded so that growth dates could be estimated. Samples were analyzed for $\delta^{13}\text{C}$ and $\delta^{15}\text{N}$ using an ECS 4010 elemental analyzer (Costech, Valencia, CA, USA) coupled to a ThermoFinnigan Delta V Advantage continuous-flow isotope ratio mass spectrometer (Thermo Scientific, Bremen, Germany) at the University of Alaska Anchorage Environment and Natural Resources Institute Stable Isotope Laboratory. Homogenized peach leaf (NIST 1547, $\delta^{13}\text{C}=-25.89\text{‰}$, $\delta^{15}\text{N}=1.89\text{‰}$), bowhead whale baleen (University of Alaska; $\delta^{13}\text{C}=-18.37\text{‰}$, $\delta^{15}\text{N}=14.44\text{‰}$) and purified methionine (Alfa Aesar, Heysham, UK; $\delta^{13}\text{C}=-34.58\text{‰}$, $\delta^{15}\text{N}=-0.94\text{‰}$) were used as internal standards. All values are reported in parts per thousand deviations

from the standard value (‰) using the equation $\delta^hX = [((R_{\text{sample}} - R_{\text{standard}}) / R_{\text{standard}}) * 1000]$ where X represents the element, h is the heavy atomic mass number, and R is the heavy-to-light isotope ratio found in the sample or standard ($^{13}\text{C}/^{12}\text{C}$ or $^{15}\text{N}/^{14}\text{N}$).

Because tissue catabolism (i.e. mass loss) can elevate tissue $\delta^{15}\text{N}$ values independently of dietary changes [35], we limited our analysis to the nine seals that gained mass across the deployment period out of 19 seals sampled. Average whisker $\delta^{13}\text{C}$ and $\delta^{15}\text{N}$ values for each seal (mean \pm SD, 5 \pm 2 segments, range 3 to 8) were incorporated into a stable-isotope mixing model using R package SIAR [36] along with bulk isotope values from five prey groups (values from [37], Table 4.1), the $\Delta^{13}\text{C}$ trophic enrichment factor (TEF) used in Goetz et al. [37] (mean \pm SD 0.8 \pm 0.12‰), and the $\Delta^{15}\text{N}$ TEF from Beltran et al. [38] (mean \pm SD 3.2 \pm 0.5‰).

We then examined $\delta^{13}\text{C}$ and $\delta^{15}\text{N}$ values across date from deployment to recovery by assigning timestamps to each whisker segment. To estimate the dates during which each segment was grown, we first calculated a growth rate for each whisker using the asymptotic growth equations appropriate for phocid seals [24, 25]. The curvature constant k was calculated for each whisker using $k = -(\log(1 - (L / L_{\infty})) / T)$ where L is the total length of the whisker upon recovery (cm), T is the duration of whisker growth (i.e. number of days between the first handling and recapture), and L_{∞} is the asymptotic length of the whisker (cm), which was assumed to be the length of the first whisker from that follicle when it was plucked during the first handling in November/December [24]. The ages of segments along each whisker were then calculated using $\text{Age} = (-1/k) * \log(1 - \text{Distance} / L_{\infty})$ where k is the previously determined curvature constant, Distance is the distance of each regrown whisker segment from the tip of the whisker (cm), and L_{∞} is the previously determined asymptotic length of each whisker (cm). The age of each whisker subsample was thus the number of days since the whisker had started growing (i.e.,

initiation date). The tip of the whisker (i.e., oldest growth) was treated as day zero, and the base of the whisker (i.e., newest growth) represented the maximum age of growth that also corresponded to the number of days between the first handling and recapture. The date of starting growth for each whisker was calculated by subtracting the age of the subsample closest to the base from the date of the recovery procedure. Finally, the starting date of growth for each whisker segment was calculated as the difference between the starting growth date of each whisker and the age of each subsample. Linear mixed-effects models were used to characterize the relationship between date (days since January 01) and isotopic values in whiskers ($\delta^{13}\text{C}$ and $\delta^{15}\text{N}$ values) with individual as a random effect.

4.4 Results and discussion

4.4.1 Seal dives become shallower in summer

Our analysis of time-depth records from 59 female Weddell seals in the Ross Sea, Antarctica (137,083 pelagic dives ≥ 30 seconds duration and ≥ 10 meters depth) demonstrated that maximum dive depths become predictably shallower during the mid-summer phytoplankton bloom (Figure 4.2). During mid-summer, Weddell seal maximum daily dive depth shallowed to less than 200 m, which is notably different from the ~ 300 m depth of dives during early- and late-summer (Figure 4.2B).

4.4.2 Shallow dives are unrelated to pupping or molting

The date of shallowest diving varied by 69 days among seals; however, pupping date and molt start date did not explain the date of shallowest diving identified with the GAMM fits (linear regressions, $R^2=0.0015$ and $R^2=0.0078$, respectively). Benthic dives did not exceed 638 m

(mean \pm SD 321 \pm 75 m) which matches the bathymetry of the McMurdo Sound area [39] and is consistent with seals staying relatively close to the breeding colonies. Further, benthic dive depth exhibited no seasonal pattern across the summer (i.e. seals did not appear to transit to deeper areas during mid-summer). Testa [40] also found that Weddell seals tend to remain within the Erebus Bay region until April, probably due to the seasonal presence of killer whales *Orcinus orca* in the more open waters of greater McMurdo Sound.

4.4.3 No evidence that diet changes during shallow diving period

Stable isotopes in regrown whiskers from the nine seals that gained mass over summer ($n=47$ whisker segments, mean \pm SD; $\delta^{15}\text{N}$ 13.0 \pm 0.5‰ and $\delta^{13}\text{C}$ -23.2 \pm 0.3‰) suggested a reliance on mid-water silverfish *Pleurogramma antarcticum* supplemented with under-ice *Trematomus newnesi* (total diet proportion mode 72%, 95% confidence interval 34% to 86%) (Table 4.1, Figure 4.4). Whisker isotopes fluctuated across summer but did not show a distinct pattern, suggesting that no diet shift occurred during the summer. The limited frequency of benthic dives (mean 1.03% of dives across all individuals, ranging from 0% to 16% in a single individual) provides supporting evidence that seals focused their foraging efforts on pelagic or under-ice fishes. Further, jaw acceleration loggers deployed in AS16 ($n=4$, 20 Hz sampling interval, deployment duration 2-4 hours, 500 total dives) on a separate set of seals demonstrated that jaw motion events often occurred as a single surge of acceleration, suggesting distinct, quick feeding events on smaller fishes such as silverfish rather than chewing large fishes such as Antarctic toothfish *Dissostichus mawsoni* [29]. Antarctic silverfish are a keystone species in the Ross Sea, accounting for more than 90% of mid-water fish biomass [41], and have been reported to be the main prey of Weddell seals (especially during midwater dives > 300 m [42]) [43].

4.4.4 Ice-driven physical-biological coupling

The significant effect of year on the date (ANOVA, $F_{3,55}=10.92$ $p<0.0001$) and depth (ANOVA, $F_{3,55}=4.145$, $p=0.0101$) of shallowest diving suggests that seal diving depth is driven by extrinsic factors (Table 4.2). The inter-annual differences in shallowing dates match ice break-out dates, which varied by 33 days across study years (Figure 4.5, Table 4.1). In AS16, ice break-out and the shallow-diving period occurred significantly later than other years (Figure 4.6). There was a significant relationship between the annual average date of shallowest diving (DSD) and the date of ice break-out (DOB) ($R^2=0.97$, $p=0.02$, $(DSD=0.6*DOB-5.5)$) (Figure 4.6, Table 4.2). A GAMM demonstrated that 95th-quantile dive depth was better explained by ice break-out date (AIC=34,543) than calendar date (AIC=35,266), further suggesting that the seasonal variation in seal dive depth is driven by ice dynamics. Across years, the “shallow period” of seal diving lasted approximately 23 days, from 19 days before ice break-out to 3 days after break-out, when seal dives began to deepen again.

4.4.5 Summer shallowing of ocean biomass

We infer that observed Weddell seal diving patterns are due to aggregation of prey items at shallower depths during a brief phytoplankton bloom associated with sea ice break-out (Figure 4.2A). In the Southern Ross Sea, phytoplankton communities are dominated by diatoms [44] which are effectively grazed by zooplankton [45], and *Phaeocystis* haptophytes that are not. Crystal krill *Euphausia crystallorophias* spawn during the phytoplankton bloom [15] and the positively buoyant krill eggs and larvae remain in surface waters [46]. After the phytoplankton

bloom has begun, krill larvae and other species of copepods and amphipods are typically found at depths less than 100m and feed on phytoplankton [9, 46]. Similarly, Antarctic silverfish eggs float under the ice [47] and once they hatch, larval and juvenile silverfishes consume small zooplankton and zooplankton eggs [48] in the upper 50m of the water column [49]. Adult silverfish are known to prey primarily on krill [50]. Thus, our data are consistent with silverfish moving into shallower water to feed and spawn, concurrent with the phytoplankton bloom and krill ascent. Because ice break-out mediates photoperiodic control of when female krill spawn [51, 52], the late ice break-out in AS16 may have delayed the krill reproductive cycle and therefore resulted in later observations of seal shallowing.

We use ice break-out (ice cover $\leq 50\%$) as a metric for *in situ* phytoplankton growth [32] (Figure 4.2); however, this is likely a conservative estimate of the date of primary production initiation. Each summer, three sequential processes occur: sea ice microalgae are released into the water column during ice melt, phytoplankton is advected into the study area from the Ross Sea polynya (77.0°S 175.0°E), and *in situ* phytoplankton production increases [19] (Figure 4.2). Sea-ice microalgae are capable of net photosynthesis at very low irradiance levels [53], but contribute little to the chlorophyll concentration; instead, their main impact is reducing light penetration deeper into the water column. Based on the current speeds of $\sim 8 \text{ cm s}^{-1}$ [54] and the distance between our study area and the Ross Sea polynya, advected phytoplankton probably reach our study area approximately two weeks earlier than when *in situ* water column productivity markedly increases. These advective inputs are thought to be quantitatively more important than *in situ* production for the Erebus Bay region [33]. Thus, the vertical distribution shift of zooplankton and fishes proposed here could begin as soon as water column chlorophyll begins to increase, which likely precedes ice break-out.

While crystal krill [46] and silverfish [55] are typically strong diurnal migrators, this behavior has been found to cease during phytoplankton blooms when food availability is high [46]. Using a mixed effects model of dive depth across ice-corrected date, we found that seals more strongly tracked a DVM (deeper dives during noon than midnight) during the “deep before break-out” (AIC improved by $\Delta 45$ over null model when time of day factor was included), and this DVM was less evident during the “shallow” period (AIC improved by $\Delta 28$ over null model) and the following “deep after break-out” period (AIC improved by $\Delta 11$ over null model). Surface-feeding seabirds in the Weddell Sea and Scotia Sea (including snow petrels *Pagodroma nivea* and Antarctic petrels *Thalassoica antarctica*) have been found to consume mesopelagic fishes during mid-summer phytoplankton blooms [56], suggesting that the fishes may cease DVMs and shallow their distribution during this time [57].

In combination, these findings suggest that the accumulation of phytoplankton biomass at depths <50m occurs over eight weeks, reaching a maximum in late December [6]. Bloom dissipation occurs over a few days [6] as a result of iron limitation [58] and rapid sinking of phytoplankton biomass [59]. Following the seasonal reduction of phytoplankton biomass in February, we propose that silverfish [17] and krill [15] return back to the deeper depths at which they are usually found (Figure 4.2) and Weddell seal dive depths deepen (Figure 4.6). Adélie penguin *Pygoscelis adeliae* dives have been found to deepen during bloom dissipation [60], probably as a response to shallow water prey depletion due to the seasonal influx of large vertebrates such as killer whales [61]. As suggested by Ainley et al. [61], we believe that competition between Weddell seals, killer whales, and penguins may be playing a role in the deeper post-bloom vertical distribution of silverfish that occurs in late January. This seasonal

deepening of water column biomass occurs when day length remains long and the phytoplankton bloom dissipates.

4.4.6 Effect of the shallow diving period on foraging efficiency

Because our knowledge of mass gain is limited to the difference between seal mass measured at deployment and recovery, we used three metrics for evaluating foraging success throughout the summer: jaw motion events, bottom wiggles (vertical excursions in dive bottom phase) and vertical transit (ascent and descent) rates. Weddell seal buoyancy and dive descent rates have been shown to vary predictably when body composition changes [62]. In our study animals, slower descent rates were associated with higher body mass (Table 4.3). Because diving depth is similar between beginning and end of summer (Figure 4.7A), we believe that changes in vertical transit rates largely reflect mass gain rather than depth. Thus, in the absence of body condition data throughout the instrument deployment period, we use descent rate as a proxy for body condition changes [63, 64].

Based on data from the jaw accelerometers, prey capture attempt frequency could be explained by the number of bottom wiggles in each dive, and in turn, bottom wiggles were a strong predictor of mass gain per hour diving (Table 4.3). The number of bottom wiggles per minute bottom time was higher during the shallow-period than the deep-periods preceding and following (Figure 4.7B), suggesting higher presumed feeding effort during this time. Additionally, descent rate tended to decrease relative to ascent rate during the shallow-period (Figure 4.7C), suggesting that body condition (increased proportion of buoyant adipose tissue; [65]) improved most quickly during that time.

A vertical shift of biomass confers an energetic advantage to air-breathing vertebrates such as birds, seals, and whales because it requires less transit time [12]. The higher presumed feeding effort during this shallow-diving period provides an energetic benefit to Weddell seals that would facilitate mass recuperation after the pup nursing period. The energetic advantages of shallow diving during the polar summer is also suggested by the fact that concurrent with seal dive shallowing, the proportion of Adélie penguin diet comprised of energetically-dense silverfish (relative to lower energy krill) increases from 7% to 56% [66]. This proposed phytoplankton-zooplankton-fish coupling could also explain the shallower and more successful elephant seal feeding dives below higher phytoplankton concentrations in the sub-Antarctic [12]. A similar phenomenon occurs in the northern hemisphere, where grey seals forage shallower and more successfully during summer [67] when prey aggregate in shallower water [68].

4.4.7 Conclusions

This study is the first to identify a gradual shallowing in the vertical distributions of several associated trophic levels during polar summer that leads to improved feeding success in a top predator. Future predictions in the Ross Sea include decreased ice that may negatively impact ice-dependent intermediate trophic levels [69] and alter the phenology of ice, phytoplankton, zooplankton, and fishes [70]. Furthermore, interannual variation in the timing of sea ice break-out may have cascading effects on upper trophic levels [71]. For example, penguin fledgling mass is lower when krill spawning (controlled by ice break-out phenology [51]) occurs later [72]. Likewise, seals experience reduced reproductive success [73] and recruitment [74] in ice-heavy years with delayed phytoplankton blooms. The repercussions of potential de-coupling

between top predators and their prey must not be overlooked when describing polar ecosystems in the context of predicted global change.

4.5 Acknowledgments

We thank the B-292 team members for assistance with fieldwork, C. Woolner for labwork assistance, C. Youngflesh and T. Tamura for providing analytical assistance, and researchers from Japan's National Institute of Polar Research and Little Leonardo for helpful feedback. This project was made possible by logistical support from the National Science Foundation (NSF) United States Antarctic Program, Lockheed Martin Antarctic Support Contract, and support staff in Christchurch, New Zealand and McMurdo Station. Research activities were approved by National Marine Fisheries Service Marine Mammal permit #17411, University of Alaska IACUC protocols #419971 and #854089 and the Antarctic Conservation Act permit #2014-003. This research was conducted with financial support from NSF grant ANT-1246463 to JMB and JWT; National Geographic grant #9802-15 to JMB and RSB; NSF graduate research fellowship #2015174455 to RSB. This material is based upon work supported by the NSF Graduate Research Fellowship Program (RSB) and while serving at the NSF (JMB). Any opinion, findings, and conclusions or recommendations expressed in this material are those of the authors and do not necessarily reflect the views of the NSF.

Table 4.1. Species, group, and isotopic values ($\delta^{15}\text{N}$ and $\delta^{13}\text{C}$) of Weddell seal prey species along with the diet contribution estimated from a SIAR mixing model. Due to statistically indistinguishable isotopic values, prey species were combined into prey groups before using mixing models.

Prey Group	Prey Species	$\delta^{15}\text{N}$ mean \pm SD ‰	$\delta^{13}\text{C}$ mean \pm SD ‰	Diet Contribution mode (min-max) %
a	<i>Dissostichus mawsoni</i>	13.5 \pm 0.5	-23.6 \pm 0.5	0.01 (0.00-0.10)
b	<i>Trematomus hansonii</i>	12.3 \pm 0.3	-24.8 \pm 0.2	0.01 (0.00-0.13)
c	<i>Pagothenia borchgrevinki</i> <i>Trematomus nicolai</i> <i>Trematomus bernacchii</i> <i>Trematomus pennellii</i>	10.7 \pm 0.3	-22.8 \pm 0.5	0.20 (0.06-0.39)
d	<i>Trematomus newnesi</i> <i>Pleurogramma antarcticum</i>	9.7 \pm 0.4	-24.4 \pm 0.1	0.72 (0.34-0.86)
e	<i>Neopagetopsis ionaha</i>	11.1 \pm 0.7	-26.1 \pm 0.1	0.02 (0.00-0.16)

Table 4.2. Annual mean date and depth of shallowest diving for all seals. Despite the 33-day range in ice break-out date across the four study years, the shallowest seal diving date consistently occurred 8-19 days before ice break-out. Data are provided as mean \pm standard deviation.

Year	Number of Seals	Shallowest Depth (m)*	Shallowest Date	Ice Break-out Date	Difference between Shallowest Date and Ice Break-out
AS13	9	200 \pm 64	Jan 06 \pm 16 days	Jan 14	8 days
AS14	17	145 \pm 57	Jan 03 \pm 13 days	Jan 14	11 days
AS15	17	134 \pm 39	Dec 25 \pm 7 days	Jan 02	8 days
AS16	16	158 \pm 30	Jan 16 \pm 9 days	Feb 04	19 days

* *These values are derived from the 95th Quantile models, and as such, represent the 95th quantile of depth (benthic dives excluded) during the shallowest day of diving.*

Table 4.3. Linear mixed effects models demonstrate that bottom wiggles are positively associated with prey capture attempts and mass gain, which correspond to slower descent rates. PC = number of prey capture attempts per dive; W = number of bottom phase wiggles per dive; MG = mass gain per hour diving (calculated as mass gain between deployment and recovery divided by the total number of hours diving); DR = descent rates in meters per second (calculated as 5-day average before tag recovery).

Variable 1	Variable 2	Relationship	Equation	R ² Value
Prey capture attempts	Wiggles	Positive	$PC=1.8*W+7.4$	0.42
Mass gain	Wiggles	Positive	$MG=0.002*W-0.010$	0.43
Descent rate	Mass	Negative	$DR = -0.0026*M+1.6677$	0.30

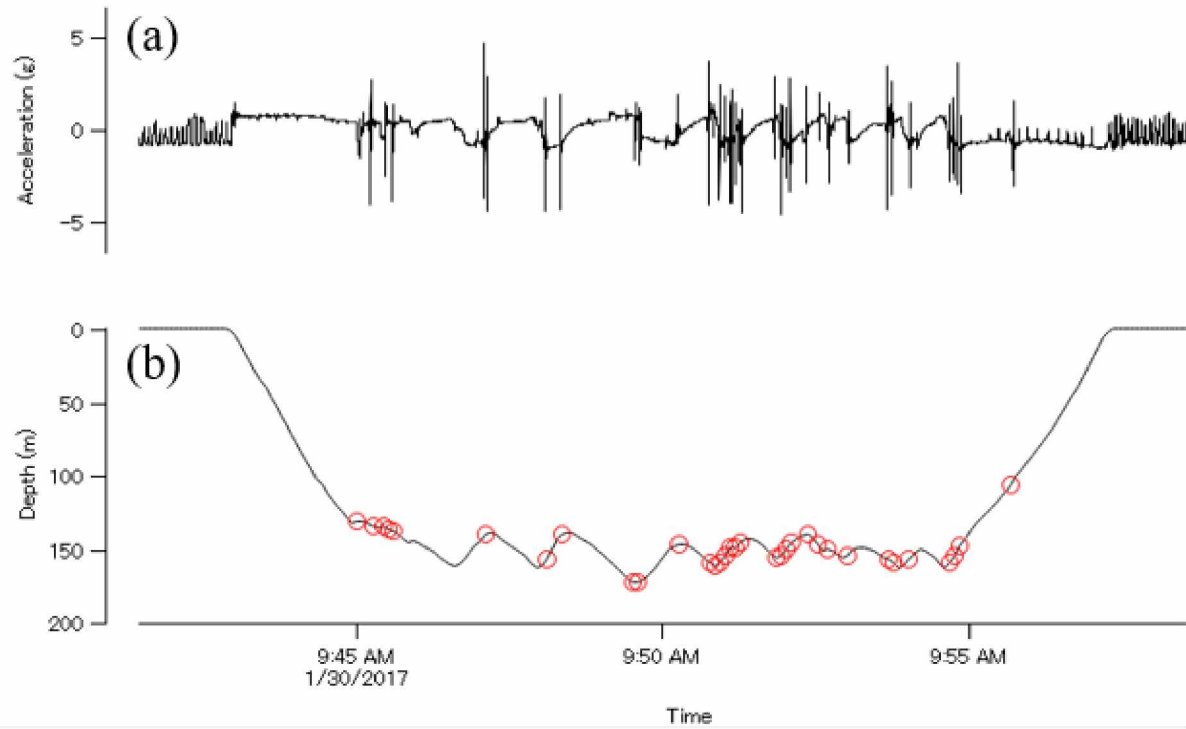


Figure 4.1. Jaw motion events (b, red circles) were identified using a 0.3g amplitude threshold for surge acceleration based on the raw acceleration data (a). The number of wiggles per dive were also characterized as vertical excursions during the bottom phase (b).

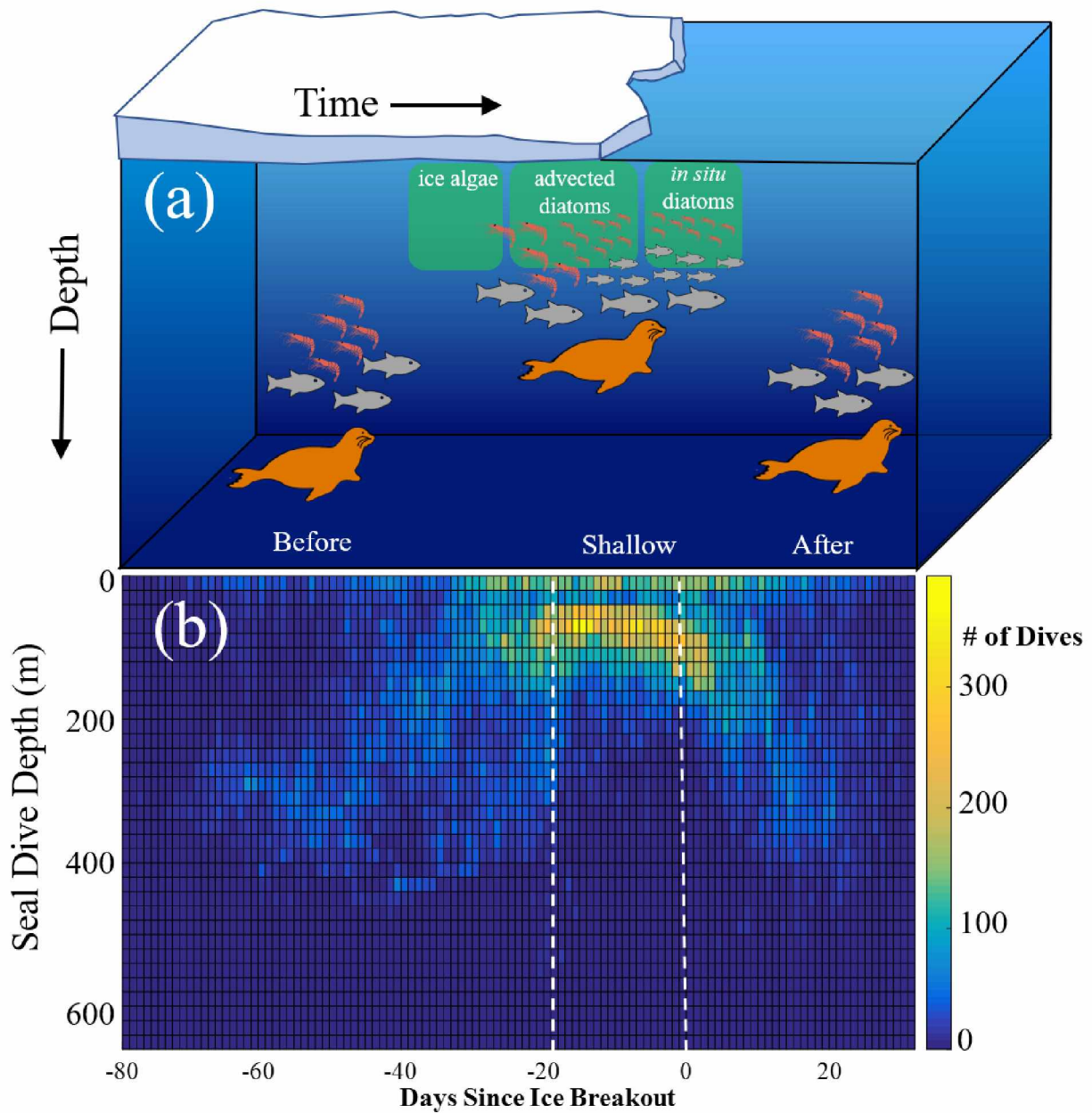


Figure 4.2. Conceptual figure of deep-shallow-deep diving pattern (a) and empirical diving data from Weddell seals that exhibited that pattern (b). Dashed reference lines represent the start and end of “shallow” period, denoted as mean dive depth ≤ 200 meters. The ice break-out is coupled to the annual phytoplankton bloom, and larval krill undergo a developmental ascent to surface waters seeking food [15], adult krill come to the surface to spawn [15], and fish larvae inhabit

near-surface waters to feed on zooplankton [17]. We hypothesize that this aggregates seal prey into shallower waters and thus causes seals to dive shallower during the phytoplankton bloom.

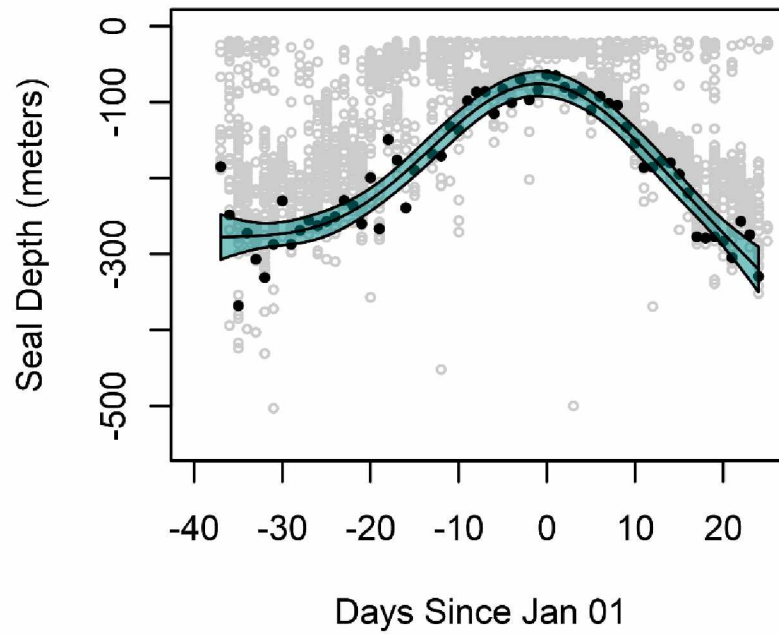


Figure 4.3. Maximum depth of each dive (grey open circles) plotted against time for one seal (#13468, gained 1.48kg/day), with results from the Generalized Additive Mixed Model (blue polygon) on 95th quartile of maximum dive depth (black closed circles).

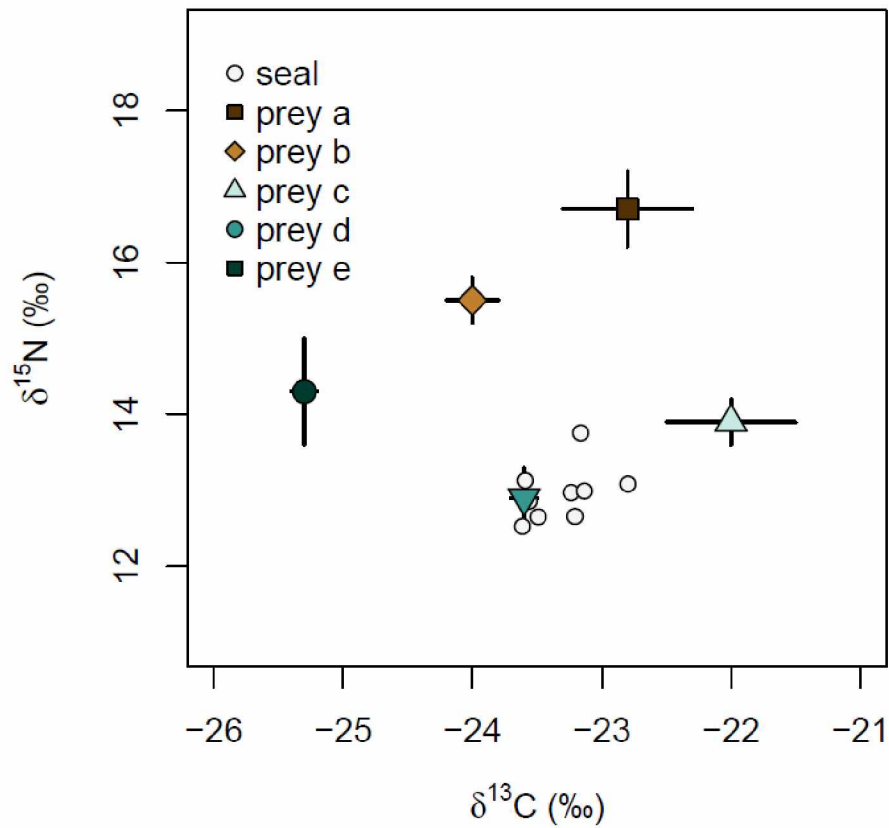


Figure 4.4. Mean and standard deviation stable isotope values of Weddell seal prey groups (colored shapes) adjusted for trophic enrichment factors, along with Weddell seal whisker samples (white circles).

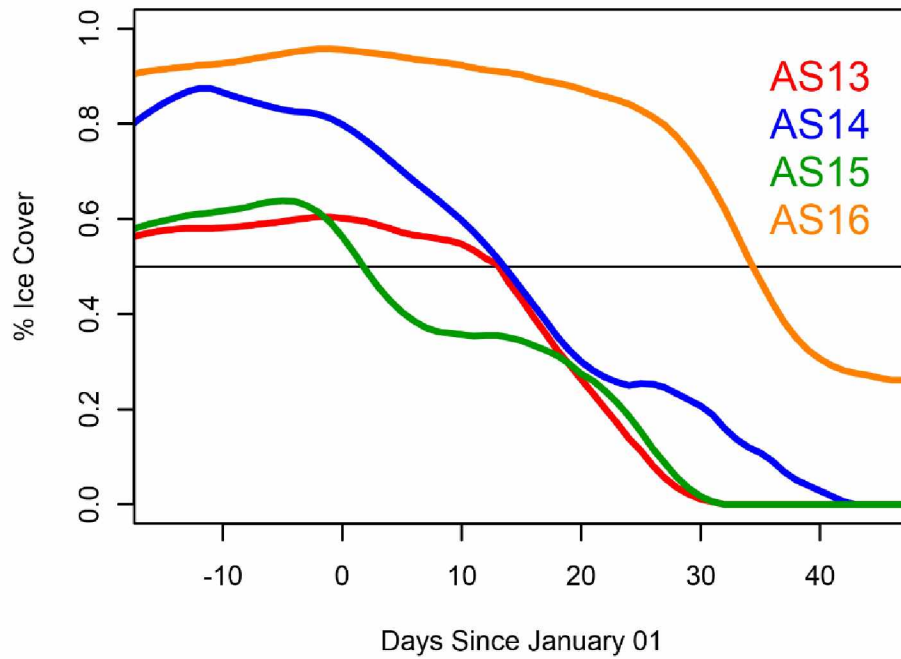


Figure 4.5. Seven-day running mean of percent ice cover for the four study years in McMurdo Sound, Ross Sea, Antarctica (satellite-derived sea ice concentration courtesy of the US National Snow and Ice Data Center; NASA Bootstrap SMMR-SSM/I combined dataset). The ice break-out (defined as <50% ice cover, red line) occurred earliest in AS15 and latest in AS16.

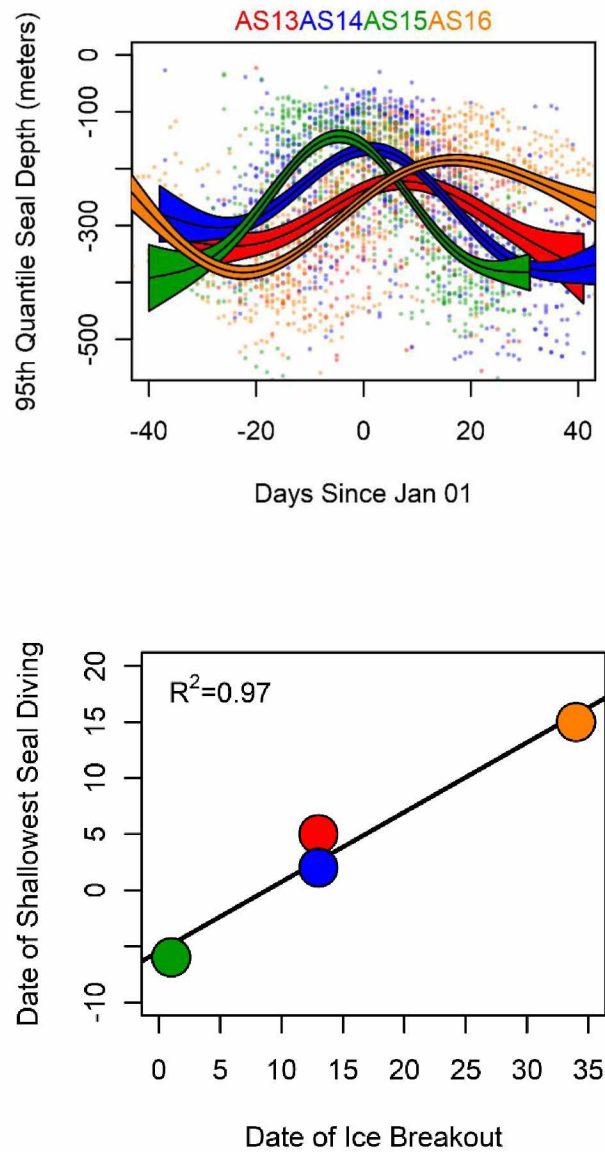


Figure 4.6. Model fits for 95th quantile of dive depth across summer, separated by year (top panel) and the tight relationship between Julian date of shallowest seal diving and Julian date of ice break-out (bottom panel). For each year, the day of shallowest diving occurred within 8-19 days of ice break-out (bottom panel).

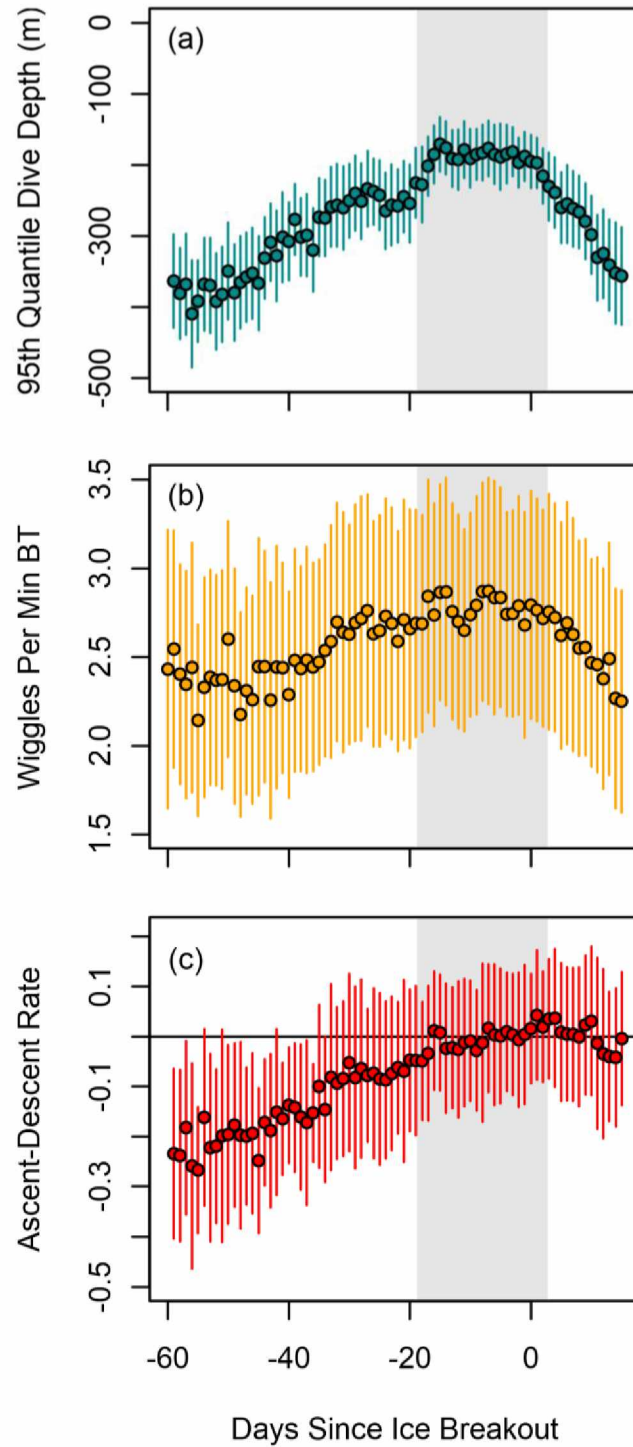


Figure 4.7. Mean \pm standard deviation metrics for non-benthic dives of all seals: 95th quantile of seal dive depth (A), number of bottom wiggles per minute bottom time (proxy for feeding effort,

B) and difference between ascent and descent rate (C) across the summer. For reference, semitransparent boxes encompass the “shallow period” days where the 95th quantile of dive depth does not exceed 231 meters (within 25% of minimum daily dive depth 95th quantile, 23-day duration).

4.6 Literature Cited

1. Hays GC. A review of the adaptive significance and ecosystem consequences of zooplankton diel vertical migrations. *Hydrobiologia*. 2003;503(1-3):163-70.
2. Croxall J, Everson I, Kooyman G, Ricketts C, Davis R. Fur seal diving behaviour in relation to vertical distribution of krill. *The Journal of Animal Ecology*. 1985;54(1):1-8.
3. Dolphin WF. Foraging dive patterns of humpback whales, *Megaptera novaeangliae*, in southeast Alaska: a cost–benefit analysis. *Canadian Journal of Zoology*. 1988;66(11):2432-41.
4. Kooyman G, Cherel Y, Maho YL, Croxall J, Thorson P, Ridoux V, et al. Diving behavior and energetics during foraging cycles in king penguins. *Ecological Monographs*. 1992;62(1):143-63.
5. Bollens SM, Rollwagen-Bollens G, Quenette JA, Bochdansky AB. Cascading migrations and implications for vertical fluxes in pelagic ecosystems. *Journal of Plankton Research*. 2010;33(3):349-55.
6. Jones RM, Smith Jr. WO. The influence of short-term events on the hydrographic and biological structure of the southwestern Ross Sea. *Journal of Marine Systems*. 2017;166:184-95.
7. Smith Jr. WO, Nelson DM. Importance of ice edge phytoplankton production in the Southern Ocean. *BioScience*. 1986;36(4):251-7.
8. Blachowiak-Samolyk K, Kwasniewski S, Richardson K, Dmoch K, Hansen E, Hop H, et al. Arctic zooplankton do not perform diel vertical migration (DVM) during periods of midnight sun. *Marine Ecology Progress Series*. 2006;308:101-16.

9. Cisewski B, Strass VH, Rhein M, Krägefsky S. Seasonal variation of diel vertical migration of zooplankton from ADCP backscatter time series data in the Lazarev Sea, Antarctica. *Deep Sea Research II*. 2010;57(1):78-94.
10. Kaartvedt S, Knutsen T, Holst JC. Schooling of the vertically migrating mesopelagic fish *Maurolicus muelleri* in light summer nights. *Marine Ecology Progress Series*. 1998:287-90.
11. Liu S-H, Sun S, Han B-P. Diel vertical migration of zooplankton following optimal food intake under predation. *Journal of Plankton Research*. 2003;25(9):1069-77.
12. Toole MO, Guinet C, Lea M-A, Hindell MA. Marine predators and phytoplankton: how elephant seals use the recurrent Kerguelen plume. *Marine Ecology Progress Series*. 2017;581:215-27.
13. Hubold G. The early life-history of the high-Antarctic silverfish, *Pleuragramma antarcticum*. *Antarctic Nutrient Cycles and Food Webs*: Springer; 1985. p. 445-51.
14. Daly K, Macaulay M. Influence of physical and biological mesoscale dynamics on the seasonal distribution and behavior of *Euphausia superba* in the Antarctic marginal ice zone. *Marine Ecology Progress Series*. 1991;79(1):37-66.
15. Siegel V. *Biology and ecology of Antarctic krill*. Cham, Switzerland: Springer; 2016. 441 p.
16. Labrousse S, Sallée J-B, Fraser AD, Massom RA, Reid P, Hobbs W, et al. Variability in sea ice cover and climate elicit sex specific responses in an Antarctic predator. *Scientific Reports*. 2017;7:43236.
17. Vacchi M, Pisano E, Ghigliotti L. *The Antarctic silverfish: a keystone species in a changing ecosystem*. Cham, Switzerland: Springer; 2017. 314 p.

18. Pinkerton MH, Bradford-Grieve JM. Characterizing foodweb structure to identify potential ecosystem effects of fishing in the Ross Sea, Antarctica. *ICES Journal of Marine Science*. 2014;71(7):1542-53.
19. Smith Jr WO, Ainley DG, Arrigo KR, Dinniman MS. The oceanography and ecology of the Ross Sea. *Annual Review of Marine Science*. 2014;6:469-87.
20. Arrigo KR, Worthen D, Schnell A, Lizotte MP. Primary production in Southern Ocean waters. *Journal of Geophysical Research: Oceans*. 1998;103(C8):15587-600.
21. Poncet S, Woehler EJ. The distribution and abundance of Antarctic and Subantarctic penguins. United Kingdom: Scientific Committee on Antarctic Research; 1993. 76 p.
22. Mellish JAE, Tuomi PA, Hindle AG, Horning M. Chemical immobilization of Weddell seals (*Leptonychotes weddellii*) by ketamine/midazolam combination. *Veterinary Anaesthesia and Analgesia*. 2010;37(2):123-31.
23. Sadou M. Short Note: A calibration procedure for measuring pinniped vibrissae using photogrammetry. *Aquatic Mammals*. 2014;40(2):213-8. doi: 10.1578/am.40.2.2014.213.
24. Beltran R, Sadou M, Condit R, Peterson S, Reichmuth C, Costa D. Fine-scale whisker growth measurements can reveal temporal foraging patterns from stable isotope signatures. *Marine Ecology Progress Series*. 2015;523:243-53. doi: 10.3354/meps11176.
25. Lübcker N, Condit R, Beltran RS, de Bruyn PN, Bester MN. Vibrissal growth parameters of southern elephant seals *Mirounga leonina*: obtaining fine-scale, time-based stable isotope data. *Marine Ecology Progress Series*. 2016;559:243-55.
26. Beltran RS, Ruscher-Hill B, Kirkham AL, Burns JM. An evaluation of three-dimensional photogrammetric and morphometric techniques for estimating volume and mass in Weddell seals *Leptonychotes weddellii*. *PLOS ONE*. 2018;13(1):e0189865.

27. Kuhn CE, Crocker DE, Tremblay Y, Costa DP. Time to eat: measurements of feeding behaviour in a large marine predator, the northern elephant seal *Mirounga angustirostris*. *Journal of Animal Ecology*. 2009;78(3):513-23. doi: 10.1111/j.1365-2656.2008.01509.x. PubMed PMID: 19040681.
28. Robinson PW, Costa DP, Crocker DE, Gallo-Reynoso JP, Champagne CD, Fowler MA, et al. Foraging behavior and success of a mesopelagic predator in the northeast Pacific Ocean: insights from a data-rich species, the northern elephant seal. *PLOS ONE*. 2012;7(5):e36728.
29. Naito Y, Costa DP, Adachi T, Robinson PW, Fowler M, Takahashi A. Unravelling the mysteries of a mesopelagic diet: a large apex predator specializes on small prey. *Functional Ecology*. 2013;27(3):710-7.
30. Robinson PW, Simmons SE, Crocker DE, Costa DP. Measurements of foraging success in a highly pelagic marine predator, the northern elephant seal. *Journal of Animal Ecology*. 2010;79(6):1146-56. doi: 10.1111/j.1365-2656.2010.01735.x. PubMed PMID: 20673236.
31. Watanabe Y, Mitani Y, Sato K, Cameron MF, Naito Y. Dive depths of Weddell seals in relation to vertical prey distribution as estimated by image data. *Marine Ecology Progress Series*. 2003;252:283-8.
32. Fauchald P, Tarroux A, Tveraa T, Cherel Y, Ropert-Coudert Y, Kato A, et al. Spring phenology shapes the spatial foraging behavior of Antarctic petrels. *Marine Ecology Progress Series*. 2017;568:203-15.

33. Ackley S. McMurdo Sound, Antarctica: An opportunity for long-term investigation of a high-latitude coastal ecosystem. Workshop Report. San Jose, California: 2004 13-15 April 2004. Report No.
34. Huckstadt LA. Dealing with a fast changing environment: the trophic ecology of the southern elephant seal (*Mirounga leonina*) and crabeater seal (*Lobodon carcinophaga*) in the western Antarctica Peninsula: University of California, Santa Cruz; 2012.
35. Lee TN, Buck CL, Barnes BM, O'Brien DM. A test of alternative models for increased tissue nitrogen isotope ratios during fasting in hibernating arctic ground squirrels. *Journal of Experimental Biology*. 2012;215(Pt 19):3354-61. doi: 10.1242/jeb.068528. PubMed PMID: 22735347.
36. Parnell AC, Inger R, Bearhop S, Jackson AL. Source partitioning using stable isotopes: coping with too much variation. *PLOS ONE*. 2010;5(3):e9672.
37. Goetz KT, Burns JM, Hückstädt LA, Shero MR, Costa DP. Temporal variation in isotopic composition and diet of Weddell seals in the western Ross Sea. *Deep Sea Research II*. 2017;140:36-44.
38. Beltran RS, Peterson SH, McHuron EA, Reichmuth C, Hückstädt LA, Costa DP. Seals and sea lions are what they eat, plus what? Determination of trophic discrimination factors for seven pinniped species. *Rapid Communications in Mass Spectrometry*. 2016;30(9):1115-22.
39. Parker SJ, Mormede S, Devries AL, Hanchet SM, Eisert R. Have Antarctic toothfish returned to McMurdo Sound? *Antarctic Science*. 2016;28(1):29-34.

40. Testa JW. Over-winter movements and diving behavior of female Weddell seals (*Leptonychotes weddellii*) in the southwestern Ross Sea, Antarctica. Canadian Journal of Zoology. 1994;72(10):1700-10.
41. DeWitt HH. The character of the midwater fish fauna of the Ross Sea, Antarctica. Antarctic Ecology. 1970;1:305-14.
42. Fuiman L, Davis R, Williams T. Behavior of midwater fishes under the Antarctic ice: observations by a predator. Marine Biology. 2002;140(4):815-22.
43. Burns J, Trumble S, Castellini M, Testa J. The diet of Weddell seals in McMurdo Sound, Antarctica as determined from scat collections and stable isotope analysis. Polar Biology. 1998;19(4):272-82.
44. Smith Jr. WO, Tozzi S, Long MC, Sedwick PN, Peloquin JA, Dunbar RB, et al. Spatial and temporal variations in variable fluorescence in the Ross Sea (Antarctica): Oceanographic correlates and bloom dynamics. Deep Sea Research I. 2013;79:141-55.
45. Haberman KL, Ross RM, Quetin LB. Diet of the Antarctic krill (*Euphausia superba* Dana): II. Selective grazing in mixed phytoplankton assemblages. Journal of Experimental Marine Biology and Ecology. 2003;283(1):97-113.
46. Guglielmo L, Granata A, Greco S. Distribution and abundance of postlarval and juvenile *Pleuragramma antarcticum* (Pisces, Nototheniidae) off Terra Nova bay (Ross sea, antarctica). Polar Biology. 1997;19(1):37-51.
47. Vacchi M, La Mesa M, Dalu M, Macdonald J. Early life stages in the life cycle of Antarctic silverfish, *Pleuragramma antarcticum* in Terra Nova Bay, Ross Sea. Antarctic Science. 2004;16(3):299-305.

48. Granata A, Zagami G, Vacchi M, Guglielmo L. Summer and spring trophic niche of larval and juvenile *Pleuragramma antarcticum* in the Western Ross Sea, Antarctica. *Polar Biology*. 2009;32(3):369-82.
49. O'Driscoll RL, Macaulay GJ, Gauthier S, Pinkerton M, Hanchet S. Distribution, abundance and acoustic properties of Antarctic silverfish (*Pleuragramma antarcticum*) in the Ross Sea. *Deep Sea Research II*. 2011;58(1-2):181-95.
50. Hubold G. Stomach contents of the Antarctic silverfish *Pleuragramma antarcticum* from the southern and eastern Weddell Sea (Antarctica). *Polar Biology*. 1985;5(1):43-8.
51. Kawaguchi S, Yoshida T, Finley L, Cramp P, Nicol S. The krill maturity cycle: a conceptual model of the seasonal cycle in Antarctic krill. *Polar Biology*. 2007;30(6):689-98.
52. Ross R, Quetin L. Reproduction in Euphausiacea. In: Everson I, editor. *Krill: Biology, Ecology and Fisheries*. Oxford, United Kingdom: Blackwell Science Ltd; 2000. p. 150-81.
53. Palmisano A, Sullivan C. Sea ice microbial communities (SIMCO) I. Distribution, abundance and primary production of microalgae in McMurdo Sound, Antarctica. *Polar Biology*. 1983;2(171):489-98.
54. Barry J, Dayton P. Current patterns in McMurdo Sound, Antarctica and their relationship to local biotic communities. *Polar Biology*. 1988;8(5):367-76.
55. Hubold G. Spatial distribution of *Pleuragramma antarcticum* (*Pisces: Nototheniidae*) near the Filchner-and Larsen ice shelves (Weddell sea/Antarctica). *Polar Biology*. 1984;3(4):231-6.

56. Ainley D, Fraser W, Sullivan C, Torres J, Hopkins T, Smith W. Antarctic mesopelagic micronekton: evidence from seabirds that pack ice affects community structure. *Science*. 1986;232:847-50.
57. Kaufmann R, Smith K, Baldwin R, Glatts R, Robison B, Reisenbichler K. Effects of seasonal pack ice on the distribution of macrozooplankton and micronekton in the northwestern Weddell Sea. *Marine Biology*. 1995;124(3):387-97.
58. Sedwick PN, DiTullio GR, Mackey DJ. Iron and manganese in the Ross Sea, Antarctica: seasonal iron limitation in Antarctic shelf waters. *Journal of Geophysical Research: Oceans*. 2000;105(C5):11321-36.
59. Smith Jr WO, Shields AR, Dreyer JC, Peloquin JA, Asper V. Interannual variability in vertical export in the Ross Sea: Magnitude, composition, and environmental correlates. *Deep Sea Research I*. 2011;58(2):147-59.
60. Ainley DG, Ballard G, Jones RM, Jongsomjit D, Pierce SD, Smith WO, et al. Trophic cascades in the western Ross Sea, Antarctica: revisited. *Marine Ecology Progress Series*. 2015;534:1-16.
61. Ainley DG, Ballard G, Dugger KM. Competition among penguins and cetaceans reveals trophic cascades in the western Ross Sea, Antarctica. *Ecology*. 2006;87(8):2080-93.
62. Sato K, Mitani Y, Cameron MF, Siniff DB, Naito Y. Factors affecting stroking patterns and body angle in diving Weddell seals under natural conditions. *Journal of Experimental Biology*. 2003;206(9):1461-70.
63. Beck C, Bowen WD, Iverson SJ. Seasonal changes in buoyancy and diving behaviour of adult grey seals. *Journal of Experimental Biology*. 2000;203(15):2323-30.

64. Miller PJ, Biuw M, Watanabe YY, Thompson D, Fedak MA. Sink fast and swim harder! Round-trip cost-of-transport for buoyant divers. *Journal of Experimental Biology*. 2012;215(20):3622-30.
65. Biuw M, Boehme L, Guinet C, Hindell M, Costa D, Charrassin J-B, et al. Variations in behavior and condition of a Southern Ocean top predator in relation to in situ oceanographic conditions. *Proceedings of the National Academy of Sciences*. 2007;104(34):13705-10.
66. Saenz BT. Predator foraging dynamics in a sea ice edge trophic hotspot. *Marine Ecology Progress Series*. 2018 (Submitted).
67. Breed GA, Don Bowen W, Leonard ML. Behavioral signature of intraspecific competition and density dependence in colony-breeding marine predators. *Ecology and Evolution*. 2013;3(11):3838-54.
68. Perry RI, Smith SJ. Identifying habitat associations of marine fishes using survey data: an application to the Northwest Atlantic. *Canadian Journal of Fisheries and Aquatic Sciences*. 1994;51(3):589-602.
69. Smith WO, Dinniman MS, Hofmann EE, Klinck JM. The effects of changing winds and temperatures on the oceanography of the Ross Sea in the 21st century. *Geophysical Research Letters*. 2014;41(5):1624-31.
70. Quetin LB, Ross RM. Environmental variability and its impact on the reproductive cycle of Antarctic krill. *American Zoologist*. 2001;41(1):74-89.
71. Ropert-Coudert Y, Kato A, Meyer X, Pellé M, MacIntosh AJ, Angelier F, et al. A complete breeding failure in an Adélie penguin colony correlates with unusual and extreme environmental events. *Ecography*. 2015;38(2):111-3.

72. Chapman EW, Hofmann EE, Patterson DL, Fraser WR. The effects of variability in Antarctic krill (*Euphausia superba*) spawning behavior and sex/maturity stage distribution on Adélie penguin (*Pygoscelis adeliae*) chick growth: a modeling study. Deep Sea Research II. 2010;57(7):543-58.
73. Paterson JT, Rotella JJ, Arrigo KR, Garrott RA. Tight coupling of primary production and marine mammal reproduction in the Southern Ocean. Proceedings of the Royal Society of London B: Biological Sciences. 2015;282(1806):20143137.
74. Chambert T, Rotella JJ, Garrott RA. Environmental extremes versus ecological extremes: impact of a massive iceberg on the population dynamics of a high-level Antarctic marine predator. Proceedings of the Royal Society of London B: Biological Sciences. 2012;279(1747):4532-41.

Chapter 5. An evaluation of three-dimensional photogrammetric and morphometric techniques for estimating volume and mass in Weddell seals *Leptonychotes weddellii* ⁴

5.1 Abstract

Body mass dynamics of animals can indicate critical associations between extrinsic factors and population vital rates. Photogrammetry can be used to estimate mass of individuals in species whose life histories make it logistically difficult to obtain direct body mass measurements. Such studies typically use equations to relate volume estimates from photogrammetry to mass; however, most fail to identify the sources of error between the estimated and actual mass. Our objective was to identify the sources of error that prevent photogrammetric mass estimation from directly predicting actual mass, and develop a methodology to correct this issue. To do this, we obtained mass, body measurements, and scaled photos for 56 sedated Weddell seals (*Leptonychotes weddellii*). After creating a three-dimensional silhouette in the image-processing program PhotoModeler Pro, we used horizontal scale bars to define the ground plane, then removed the below-ground portion of the animal's estimated silhouette. We then re-calculated body volume and applied an expected density to estimate animal mass. We compared the body mass estimates derived from this silhouette slice method with estimates derived from two other published methodologies: body mass calculated using photogrammetry coupled with a species-specific correction factor, and estimates using elliptical cones and measured tissue densities. The estimated mass values (mean \pm standard

⁴ RS Beltran, B Ruscher-Hill, AL Kirkham, JM Burns (2018) An evaluation of three-dimensional photogrammetric and morphometric techniques for estimating volume and mass in Weddell seals *Leptonychotes weddellii*. PLOS ONE 13(1): e0189865.
<https://doi.org/10.1371/journal.pone.0189865>.

deviation 345 ± 71 kg for correction equation, 346 ± 75 kg for silhouette slice, 343 ± 76 kg for cones) were not statistically distinguishable from each other or from actual mass (346 ± 73 kg) (ANOVA with Tukey HSD post-hoc, $p > 0.05$ for all pairwise comparisons). We conclude that volume overestimates from photogrammetry are likely due to the inability of photo modeling software to properly render the ventral surface of the animal where it contacts the ground. Due to logistical differences between the “correction equation”, “silhouette slicing”, and “cones” approaches, researchers may find one technique more useful for certain study programs. In combination or exclusively, these three-dimensional mass estimation techniques have great utility in field studies with repeated measures sampling designs or where logistic constraints preclude weighing animals.

5.2 Introduction

Body mass dynamics in animals can elucidate critical associations between environmental factors and prey consumption, as mass changes reflect disparities between energy acquisition and expenditure [1, 2]. Seasonal mass fluctuations also provide a crucial metric against which to judge ecological shifts such as intra- and inter-annual prey availability [3]. In species that are logistically complicated to study, accurate mass or volume measurements can be used to help predict how body condition affects other physiological, behavioral, or life-history traits, including thermal balance [4], social dominance [5], mating success [6], fecundity [7], sexual selection [8], and life history evolution [9]. Obtaining mass measurements of marine mammals has enabled researchers to better understand the spatial and temporal dynamics of ocean ecosystems, which are notoriously difficult to sample. For instance, mass measurements have revealed the effects of El Niño conditions on the quality of maternal care in Northern

elephant seals *Mirounga angustirostris* [10], density-dependence in New Zealand fur seals *Arctocephalus forsteri* [11], and the sensitivity of pregnancies to maternal energy balance in species with different life history strategies (*A. forsteri*, crabeater seals *Lobodon caranophagus*, and grey seals *Halichoerus grypus*) [12]. Links between extrinsic factors and physiologically mediated population dynamics [13] have provided insight into how environmental changes are likely to influence physiological condition [14], maternal attendance [10], and foraging success [15]. For many species, accurate field estimations of mass and volume are key to understanding an animal's condition, physiology, and behavior at the individual and population level.

For many marine mammals, large body sizes [16, 17] and aquatic life histories [18] make it impossible to directly measure body mass or volume using conventional methods. Mass measurements in some species require time-consuming and/or disruptive methods, such as physical and chemical immobilization [1] or luring an animal over a platform scale [19], that are expensive and limit sample sizes. Consequently, marine mammal researchers have been fine-tuning non-invasive mass estimation methods since Usher and Church [20], who initially estimated masses of ringed seals *Pusa hispida* from body lengths and girths. Gales and Burton [21] subsequently developed a method that allowed a seal's weight and condition to be approximated using morphometric measurements (length, girth, and the thickness of the blubber layer as determined by ultrasound). These measurements allow the seal to be modeled as a series of contiguous truncated cones with a lean core and an outer blubber layer. Masses of the lean and blubber compartments may then be estimated based on calculated cone volumes and expected tissue densities. This truncated cones method has been widely used to predict mass and lipid stores in a range of marine mammal species [1, 22, 23]. Recent modifications to this method that account for elliptical shape (body cross-section) and separately estimate skin and blubber volume

have further increased the method's accuracy in predicting both mass and percent blubber (condition) in free-ranging pinnipeds [24, 25]. Truncated cones and related methods that produce estimates of both core tissue and blubber layer volumes can account for differences in the density of specific tissue stores [25, 26]. Yet estimating body mass from morphometrics does require some animal handling, and in some circumstances less invasive methods may be preferable.

Photogrammetry provides a promising alternative to direct morphometric measurements because it does not require any animal handling, thus limiting disturbance, reducing risk, and allowing for larger sample sizes and more frequent mass estimates for individual animals [27]. Many early photogrammetry studies required the use of custom equipment [19, 28] that limited utility; however, advancements in camera and software technologies have allowed photogrammetric mass estimates in many pinnipeds and other mammal, bird and fish species [14, 29-31]. Waite et al. [27] developed a method to produce a 3D wireframe model from which volume could be estimated, but the technique required multiple, time-synchronous photographs of a still animal, and so was not highly workable in a field setting. More recently, de Bruyn et al. [32] used commercial digital image processing software (PhotoModeler) to create scaled 3-dimensional wireframes of animals from sequential photographs based on substrate reference points. In this method, volume was determined from wire-frame models and mass was estimated using species-specific correction factors determined from the difference between actual weight and photogrammetric mass estimates (e.g., Postma et al. [33]). Only after these correction factors are determined can mass be estimated accurately for animals that are not handled [32, 33].

In all cases, for photogrammetric methods to accurately estimate mass from volume, both the volume and density of the animal must be known with sufficient accuracy; however, obtaining true measures of full-body density or volume is almost always impossible. Correction

factors determined from actual mass and photogrammetrically estimated volume can be used to adjust for errors in both of these values, but do not distinguish between the sources of error, nor point to the underlying cause. Unfortunately, to date, studies that use corrective equations typically fail to separate errors due to photogrammetric volume estimates from those associated with estimates of animal density. Therefore, our objective was to evaluate a suite of methods commonly used to estimate mass in marine mammals and to discuss their relative strengths and weaknesses for use under field conditions. To do so, we compared mass, volume, and density estimates from three different methods: 1) Morphometric measurements (“cones”) [24, 25]; 2) 3D photogrammetric analysis corrected for mass overestimation in PhotoModeler via calibration with known mass (“correction equation”) [32]; and 3) a new method we introduce here that modifies the 3D photogrammetric approach by removing a potentially large source of volume overestimation (“silhouette slice”) and then uses a density estimate calculated from actual mass and measured volume.

5.3 Materials and Methods

5.3.1 Ethics statement

Animal handling protocols were approved by the University of Alaska Anchorage and Fairbanks Institutional Animal Care and Use Committee approvals #419971 and #854089. Research and sample import to the United States was authorized under National Marine Fisheries Service Marine Mammal permit #17411. Research activities were approved through Antarctic Conservation Act permit #2014-003.

5.3.2 Field methods

We obtained conventional mass measurements, morphometric measurements, and photographs with scale bars for 56 adult, female Weddell seals (*Leptonychotes weddellii*) in Erebus Bay, Antarctica (77°S, 165°W). We anesthetized free-ranging animals between November and February 2013-2015 as part of a concurrent study using protocols outlined in Shero et al. [24]. We measured the body mass of each seal by enclosing the animal in a sling suspended from a tripod and electronic scale (MSI-7300 Dyna-Link 2, ± 0.25 kg). This measurement was used as the true mass value, against which mass estimates were compared and calibrated.

5.3.3 Cones method

Animals' masses were estimated from direct morphometric measurements using the elliptical truncated cones method developed by Shero et al. [24] and modified by Schwarz et al. [25]. Briefly, cumulative curvilinear length, body width and height were measured to the nearest centimeter at eight body sites (ears, neck, axial, sternum, mid, umbilicus, pelvis, ankles). Total curvilinear length was also measured to the nearest centimeter. Dorsal and lateral blubber depths were measured to the nearest 0.01cm with a Sonosite Edge ultrasound and C60x/5-2 MHz convex transducer (SonoSite Inc., Bothell, Washington, USA) at six of the eight body sites, excluding the ears and ankles. Weddell seal skin thickness, skin density, and blubber density were determined using tissue samples salvaged from two freshly (< 48h) deceased adult female Weddell seals found dead of unknown causes in December 2014 and October 2011. Both animals were in normal body condition. Skin samples were collected from 9 sites across the body of the first seal and fixed in formalin. After placing a scale bar perpendicular to the skin surface,

we took scaled photographs of these skin samples. We measured skin thickness, the distance from the epidermal surface to the dermis-blubber interface, to the nearest 0.01mm in ImageJ (version 1.49v) and averaged skin thickness values to determine the body-wide mean. We measured skin density and blubber density using a previously-frozen (-80° C) sculp (blubber with skin and hair) sample taken from the lateral flank of the second seal. We extracted and weighed five pieces each of skin and blubber to the nearest 0.001 g, and measured the volume of each to the nearest 0.1 mL using displacement methods [34]. We multiplied total volumes of the blubber and skin compartments of each seal by *MeasuredDensity* values from this study, and core volumes by 1.1 g cm^{-3} [35]. Then, we summed blubber, skin, and core masses for each animal to generate whole body mass estimates.

5.3.4 Correction equation method

We also estimated body volume using a photogrammetric technique. Prior to field work, we calibrated a digital camera (Canon EOS Rebel T3i, 18-55mm lens) using a single- or multi-sheet calibration method (details in de Bruyn et al. [32]). We took images at minimum zoom (18 mm) with auto-rotate and image stabilizer functions disabled to ensure repeatability. When animals were sedated and lying on their ventral surface, we placed six one-meter long rebar rods marked with 25-cm color increments on the ice surrounding the animal to provide a reference point for photogrammetric analysis. These rods replaced the substrate markers used in de Bruyn et al. [32]. We placed one rod vertically and the remaining rods horizontally on the ground circling the seal. The photographer slowly circled the animal taking 8 to 12 photographs from all possible perspectives (e.g., kneeling, standing, portrait photographs, and landscape photographs) (Fig 5.1). We then used PhotoModeler Pro (Version 2013.0.3, EOS Systems Inc.), Autodesk

Meshmixer (10.2.32) and Blender (2.70) to process the photographs. For each seal, we imported photographs as a unique PhotoModeler project associated with the calibrated camera. On each photograph, we marked reference points at each colored scale bar increment. We also outlined the seal silhouette in each photograph excluding the fore flippers and including the rear flippers to ensure consistency across animals, as in de Bruyn et al. [32]. We referenced each scale bar point and seal silhouette to itself across all photographs. Then, we processed the project to orient the camera positions, and set the scale bar to 0.25 meters for one color increment. Finally, we processed the project and measured the volume of each three-dimensional seal silhouette.

We developed a species-specific density estimate to convert photogrammetry-estimated volume to mass. For this “correction equation” method, we calculated an apparent density (*ApparentDensityUnsliced*; g cm⁻³) for each individual using Equation 1:

$$ApparentDensityUnsliced = \frac{Mass_{actual}}{VolumeUnsliced} * 0.001 \text{ where } Mass_{actual} \text{ is the actual mass in kg}$$

and *VolumeUnsliced* is the animal volume in m³ from PhotoModeler. The

ApparentDensityUnsliced values for all animals were averaged to produce a species-typical mean density value *MeanDensityUnsliced* (g cm⁻³). This value was then used to derive mass estimates (*MassEstimateUnsliced*) for each animal from their measured volume using Equation 2: *MassEstimateUnsliced* = *VolumeUnsliced* × *MeanDensityUnsliced*. This is an algebraic simplification of the equations used by de Bruyn et al. [32], who calculated an average “correction factor” based on apparent density (true mass/estimated volume) and an ‘assumed density’ of 1.01 that had no effect on their calculation of estimated mass.

5.3.5 Silhouette slice method

For the “silhouette slice” method, we further processed the 3D silhouette produced by the program to account for difficulties that PhotoModeler appeared to have in accurately rendering the ventral surface of the seal. This likely occurs because the program cannot cross-reference a photo taken from directly adjacent to the ground, as the program is unable to see all the substrate markers. To differentiate between portions of the modeled seal that were above and below the ground surface, we created a plane in PhotoModeler by selecting all the scale bar points and creating a best fit plane (Fig 5.2). The new 3D seal shape, including the ground plane, was imported into Autodesk Meshmixer and Blender to split the 3-dimensional seal at the ground plane, slicing off the below-ground volume so that we measured only the above-ground volume. This resulted in a new volume estimate, *VolumeSliced*. Then, we calculated an apparent density (*ApparentDensitySliced*; g cm⁻³) for each individual using Equation 3:

$$ApparentDensitySliced = \frac{Mass_{actual}}{VolumeSliced} * 0.001.$$

The *MeanDensitySliced* (g cm⁻³) was then calculated and used to estimate mass (*MassEstimateSliced*) for each animal using Equation 4:

$$MassEstimateSliced = VolumeSliced \times MeanDensitySliced.$$

5.3.6 Statistical methods

Prior to analysis, we visually assessed data for outliers and used a Shapiro-Wilk test to assess normality. We used an analysis of variance (hereafter, ANOVA) and TukeyHSD post-hoc test to assess whether each mass estimation method was significantly different from actual body mass. Similarly, we used ANOVAs to compare the volume estimates and apparent densities across methods. We then normalized estimation error of each method by calculating percent error: $Error = \frac{M_{estimate} - M_{actual}}{M_{actual}} * 100$ and used an ANOVA to compare the error rates of each method in terms of percent error and kilograms. Additionally, a simple linear regression was

performed to regress actual mass against estimated mass to inspect residuals and ensure the variance was homoscedastic. All analyses were conducted in *R* (version 3.2.0) and significance was assessed at $\alpha=0.05$. Data are presented as mean \pm standard deviation around the mean values ($n=56$) for each photogrammetric estimation method.

5.4 Results

5.4.1 Actual mass

The scale-measured seal masses ranged from 225 to 527 kg (mean \pm standard deviation 346 ± 73 kg) (Table 5.1).

5.4.2 Processing time

For each animal, the elliptical cones process (“cones” method) required an estimated 90 minutes of animal handling time (~30 minutes of direct morphometric measurements within a 90-minute anesthesia procedure) and an additional 15 minutes of data processing time (Table 5.1). The photogrammetric analysis process (“correction equation” method) required approximately 2 minutes in the field and 25-40 minutes on the computer (Table 5.1). The slicing process (“silhouette slice” method) took approximately five minutes per animal beyond that required to generate the first silhouette in PhotoModeler (approximately 30-45 total minutes per project) (Table 5.1).

5.4.3 Volume

Mean overall project residual error for individual projects ($n = 56$) was 2.650 pixels (range: 0.729 to 4.844). Volume estimates for the “cones” method (0.323 ± 0.074 m³, Table 5.1)

ranged from 5 to 9 % ($7 \pm 1\%$) skin, 11 to 36 % ($22 \pm 1\%$) blubber, and 57 to 82 % ($71 \pm 5\%$) core. Skin thickness was 6.94 ± 0.99 mm, skin density was 1.162 ± 0.057 g cm⁻³, and blubber density was 0.920 ± 0.026 g cm⁻³ for the two deceased Weddell seals. The raw photogrammetric volume estimates used for the “correction equation” method (0.254 to 0.600 m³) were significantly larger than volume estimates used for “silhouette slice” (0.223 to 0.547 m³) and “cones” (0.215 to 0.520 m³) methods (ANOVA, df=167, $n=168$, F-value=14.28; Tukey HSD post-hoc, $p=0.001$ and $p<0.0001$, respectively), which were not significantly different from each other (ANOVA, Tukey HSD post-hoc, $p=0.254$). There was a relatively strong positive relationship between percent blubber measured by ultrasound and volume estimates (linear regression, $R^2=0.48$ for “silhouette slice” volume, $R^2=0.43$ for “correction” volume, and $R^2=0.44$ for “cones” volume).

5.4.4 Apparent (estimated) density

Combining actual seal masses with volume estimates for the “cones”, “correction equation”, and “silhouette slice” methods led to estimated (apparent) tissue densities of (minimum to maximum) 0.96 to 1.25 g cm⁻³ for *ApparentDensityCones*, 0.76 to 0.99 g cm⁻³ for *ApparentDensityUnsliced*, and 0.90 to 1.11 g cm⁻³ for *ApparentDensitySliced*, respectively (Fig 5.3). Apparent densities were significantly different across all methods (ANOVA, df=167, $n=168$, F-value=199.4; Tukey HSD post-hoc, $p<0.0001$ for all). The *MeasuredDensity* value from the “cones” method (derived using volume and actual blubber, skin, and lean densities) was 1.04 to 1.08 g cm⁻³. Surprisingly, there was no significant relationship between an individual’s apparent density and percent blubber (linear regression, $R^2<0.05$ for all methods).

5.4.5 Estimated mass

The “cones”, “silhouette slice”, and “correction equation” mass estimates were not significantly different from actual mass (ANOVA, Tukey HSD post-hoc, $p=0.999$; Table 5.1, Fig 5.4). All three estimation methods produced mean mass estimate errors of less than 1.0%; however, there was a relatively wide spread, with standard deviations in calculated error of 5, 6, and 6% for each of the three methods, respectively (Fig 5.5). Root mean square error values for “cones”, “correction equation”, and “silhouette slice” estimations regressed with actual mass were 19.585 kg, 19.062kg, and 19.219 kg, respectively, indicating similar levels of precision.

5.5 Discussion

5.5.1 Summary

Here, we compare several commonly-used morphometric and photogrammetric methods for three-dimensional volume and mass estimation in pinnipeds. Photogrammetry has long been used to minimize invasiveness and maximize accuracy of mass estimation; however, previous studies have reported a consistent, positive bias in photogrammetric mass estimates (see references in de Bruyn et al. [32]). Directly estimating density using the uncorrected, unsliced photogrammetry allowed us to tease apart the contribution of volume and density to the uncertainty surrounding mass estimates. In the current study, the elliptical “cones”, “silhouette slice”, and equation “correction equation” methods each estimate actual mass with relatively high accuracy, although they achieve this in different ways. Methodologies can introduce error during two stages of mass estimation: during the initial volume estimation, and/or in the density

value that is used to calculate mass from volume. Since ‘true’ volume or density values are not available against which to compare estimates, determining the ‘best’ method is not possible; instead, we evaluate the degree to which each method provides reasonable volume and density metrics. Finally, we consider the relative strengths and weaknesses of each approach under different field scenarios (Table 5.1).

The “cones” method estimated the lowest volume and highest apparent density relative to the other two methods, whereas the “correction equation” method produced the highest volume estimate and lowest apparent density. The “silhouette slice” method produced volume estimates and apparent density that were intermediate to the other two methods. The apparent tissue density (0.87 g cm^{-3} ; Table 5.1) required to align estimated volume with directly measured mass in the “correction equation” method was unrealistically low. We can thus conclude that volume was consistently overestimated. We propose that erroneous below-ground volume was the likely reason for the overestimate in photogrammetric volume estimation. A novel “silhouette slice” method for constraining the 3D seal volume to above-ground space improved the ability of the uncorrected photogrammetric method to estimate volume and provided volume estimates comparable to direct morphometric measurements (“cones” method) before the apparent density values were incorporated. Consequently, the silhouette slice approach yielded accurate mass (within $0 \pm 5 \%$; see Fig 5.4) and realistic density estimates. Mass estimates from the other two volume estimates also did not differ significantly from actual mass or from each other, suggesting that they are also viable alternatives to direct mass measurements.

5.5.2 Apparent density values

The accuracy of the “cones” mass estimation method was likely improved by the incorporation of blubber depths into the density value that is used to convert from volume to mass. Whereas the “correction equation” and “silhouette slice” methods used an average seal body density value to convert volume to mass, the “cones” method involved calculating density of individuals by combining directly measured lipid and lean volumes with tissue-specific density estimates. Calculating individual body density values using the “cones” method can help to reduce uncertainty in body mass estimates across individuals with a range of body compositions [24]. Relative to cones, the “silhouette slice” method produced a slightly lower apparent density (1.00 g cm^{-3}).

Although density is nearly impossible to measure in free-ranging animals, realistic density values can be deduced by evaluating physical properties of the marine environment. For instance, researchers have shown that while seal buoyancy fluctuates with body composition, Weddell seals are probably positively buoyant (seal density less than seawater density; 1.027 g cm^{-3} [36, 37]) before lung collapse (in shallower dives), as evidenced by their use of stroke-and-glide swimming during descent and prolonged glide during ascent [38]. Williams et al. [39] found that after a certain depth, Weddell seals may be negatively buoyant as evidenced by gliding locomotion for descent and stoking locomotion for ascent. Based on the assumption that Weddell seals are positively buoyant when lungs are not collapsed (e.g., during haul out periods, as in our study), Weddell seal apparent densities from the “silhouette slice” method are plausible, whereas the “cones” method likely overestimates apparent densities and the “correction equation” likely underestimates apparent densities. Thus, removing the below ground portion (“silhouette slice” method) leads to a more reasonable apparent density value than the “correction equation”

method. Note that the methods in this study do not account for the very low densities of brain (~5% body mass [40]) and lung tissues in seals.

5.5.3 Volume estimates

The uncertainty in body mass estimates contributed by unknown body density can be avoided by using photogrammetric body volume measurements as an independent metric rather than by using them to estimate mass. Indeed, volume is a useful parameter for many research objectives, such as modeling heat flux to the environment (e.g., penguin thermoregulation [41]), understanding the allometry of anatomical features (e.g., volume-specific blood volume [42]), and determining how behavioral processes scale with body size (e.g., whale engulfment capacity [43]). Mass estimates from photogrammetry are derived entirely from volume, with the additional requirement of an apparent tissue density that adds uncertainty. Based on the realistic shape of the 3D silhouettes (Fig 5.2), we believe that the “silhouette slice” method provided the more believable volume estimates ($0.346 \pm 0.075 \text{ m}^3$; Table 5.1) between the photogrammetric estimation methods we compared. Because there are no true measures of density or volume, we assumed that the realistic silhouette volumes were accurate and thus used actual mass measurements to calculate apparent density values. Due to the erroneous below-ground volume assumed by PhotoModeler, the apparent density needed to convert volume to actual mass is unrealistically low, suggesting that the “correction equation” method overestimated total body volume ($0.399 \pm 0.082 \text{ m}^3$; see Table 5.1). We therefore recommend using the “silhouette slice” method to estimate volume in large mammals that have large areas of contact with the ventral surface. Though it provides a tangible metric, mass estimates should be used with caution when an uncertain apparent density is used to convert volume to mass.

The photogrammetric methods appeared to capture seal body shape more precisely because the silhouette method integrates continuous measurements rather than extrapolating the eight discrete measurements in the morphometric “cones” method. Additionally, the higher “cones” *ApparentDensity* values may be due in part to an underestimate of total body volume in this method ($0.323 \pm 0.074 \text{ m}^3$; see Table 5.1) because it did not account for the front or rear flippers [24]. Despite these differences, there was a linear relationship between percent blubber and volume estimates for all methods, suggesting that the three-dimensional silhouette shapes were capturing the “slumping” of fatter seals. If the volume estimate is accurate, then apparent density should reflect actual animal density, and can be informative within an ecological context. Larger blubber volume would cause more pronounced “slumping” [24, 25, 44] and a relatively larger ventral surface where the animal contacts the ground that would be inaccurately modeled to extend below the ground plane. In this study, we did not detect a relationship between an individual’s apparent density and percent blubber. This may be due to measurement error and/or variation in internal lipid reserves, which are substantial in this species [24].

Volume estimate error can result from any deviation in substrate rugosity [28, 32], animal position [19], or angle of the scale bar relative to the camera [28, 45]. In the current study, the relative flatness and stability of the ice compared to other substrates, such as sand [32], provided an opportunity to take unobstructed photographs. Additionally, the study seals were anesthetized, so all individuals were lying flat and extended with limited or no mobility. Thus, this study system was ideal for comparing existing photogrammetric analysis techniques to our new “silhouette slice” technique; however, we recognize that the immobility of sedated seals in this study may have resulted in lower than expected error estimates. We note that this 3D photogrammetry method has been successfully utilized in Weddell seals by opportunistically

taking photographs of sleeping and unresponsive animals (K. Macdonald, J. Rotella, B. Garrott, pers comm). Not all field studies will be as controlled, and natural systems are likely to introduce more error to the photogrammetric results. In situations where unmanned aircraft systems (UAS) can be used and volume estimates are not required, mass estimates may be obtained allometrically rather than using volume and density (D. Krause, pers comm). We note that UAS photogrammetry may be more appropriate for studies of less approachable species (e.g. leopard seals *Hydrurga leptonyx*).

5.5.4 Field applications of morphometric and photogrammetric methods

The differences in data collection and analytical methodologies between the three techniques are likely to render certain methods more useful for certain study programs. For instance, the most notable methodology difference between this study and de Bruyn et al. [32] was the use of six bars rather than many opportunistic substrate markers. This effectively reduced fieldwork setup effort and analytical processing time. However, because the “silhouette slice” process required scale bars to be placed parallel to the ground surface (Fig 5.1), the “correction equation” method may be more appropriate for animals on more rugose substrates. Additionally, the uncertainty surrounding the species-specific *ApparentDensity* depends on the number of individuals used to calculate that value. With our data, an average *ApparentDensity* drawn from five animals would have ranged (difference between maximum and minimum *ApparentDensity* divided by the mean *ApparentDensity*) by ~13% whereas the range would be ~3% if drawn from 25 animals. Thus, researchers should take care to weigh a sufficient sample of animals so that *ApparentDensity* values converge around the presumably true mean. If it is not

possible to weigh enough animals, using the “cones” method with *MeasuredDensity* values is a promising alternative, if study logistics allow blubber depth measurements to be obtained.

Given that no significant difference was found between actual and estimated mass, any of the mass estimation methods described here can be used in field studies where logistic constraints preclude weighing animals, so long as researchers choose a reasonable apparent density to estimate mass from volume. The advantage of the “silhouette slice” method is transparency, where error mechanisms are clearly defined. Further, if a species-specific apparent density value is known, the “silhouette slice” method should be used as it produced the smallest error across all estimates. Alternatively, the “cones” method had the narrowest error distribution and is a plausible substitute to mass measurements if the morphometric measurements can be obtained because animals are sedated. Finally, by incorporating blubber depth measurements, the “cones” method can be used to directly measure body condition, which is of paramount importance in studies of behavior, ecology, life history, and demography. Using these methods, volume estimates can fill in knowledge gaps of year-round energy dynamics in studies that have repeated measures sampling designs or for animals that are too heavy to weigh (e.g., free-ranging elephants [46]), require intensive and potentially stressful weighing methods (e.g., captive manatees [47]), or are in locations with limited accessibility (e.g., stranded whales [48]).

5.6 Acknowledgments

We thank the B-009-M field team led by Robert Garrott and Jay Rotella for their help developing this method and to Nico deBruyn, Martin Postma, and Chris Oosthuizen for help with the analysis. Thank you to Michelle Shero for taking photographs during the first season. This project was made possible by logistical support provided by the National Science Foundation United States Antarctic Program, Lockheed Martin Antarctic Support Contract, and support staff in Christchurch, New Zealand and McMurdo Station. This research was conducted with financial support from ANT-1246463 to J.M.B. and J.W. Testa., an INBRE graduate research fellowship to R.S.B., and a National Science Foundation graduate research fellowship to R.S.B.. Research reported in this publication was supported by an Institutional Development Award (IDeA) from the National Institute of General Medical Sciences of the National Institutes of Health under Award Number P20GM103395. The content is solely the responsibility of the authors and does not necessarily represent the official views of the National Institutes of Health. This material is based upon work supported by the National Science Foundation Graduate Research Fellowship Program under Grant No. DGE-1242789. Any opinion, findings, and conclusions or recommendations expressed in this material are those of the authors and do not necessarily reflect the views of the National Science Foundation.

Table 5.1. Comparison of actual mass, parameter estimations, and percent error across estimation methods given as mean \pm standard deviation for 56 animals. Mass was estimated using three methods: elliptical “cones”, “correction equation”, and “silhouette slice”. Percent error was calculated as $100 \times \frac{\text{difference between the estimated mass and the actual mass}}{\text{actual mass}}$. Superscript letters denote a significant difference in parameters across estimation methods. The sedation, equipment, and time requirements for all methods are noted.

Parameter	Elliptical Cones	Photogrammetry, Correction Equation	Photogrammetry, Silhouette Slice
Actual Mass (kg)	346 \pm 73	346 \pm 73	346 \pm 73
Estimated Volume (m ³)	0.323 \pm 0.074 ^a	0.399 \pm 0.082 ^b	0.346 \pm 0.075 ^a
Estimated Mass (kg)	343 \pm 76 ^a	345 \pm 71 ^a	346 \pm 75 ^a
Apparent Density (g cm ⁻³)	1.08 \pm 0.06 ^{‡a}	0.87 \pm 0.05 ^b	1.00 \pm 0.05 ^c
Error (kg)	-3 \pm 20 ^a	-1 \pm 20 ^a	0 \pm 19 ^a
Error (%)	1 \pm 5 ^a	0 \pm 6 ^a	0 \pm 6 ^a
Sedation Required	Yes	No ^Ω	No ^Ω
Apparent Density Required	No	Yes	Yes
Equipment	Maximum	Moderate	Moderate
Field Data Collection Time (Minutes)	30	2-5 ^θ	2-5 ^θ
Data Processing Time (Minutes)	15	25-40	30-45

^Ω Animals were sedated during this study to measure mass for validations and apparent density calculations.

[‡] To ensure comparability across methods, density for the elliptical cones method was calculated using the estimated volume and actual mass, rather than incorporating the lean and blubber volumes and densities.

^θ The time required for field data collection will be slightly more for non-sedated animals (~5 minutes) than it was in this study (~2 minutes).

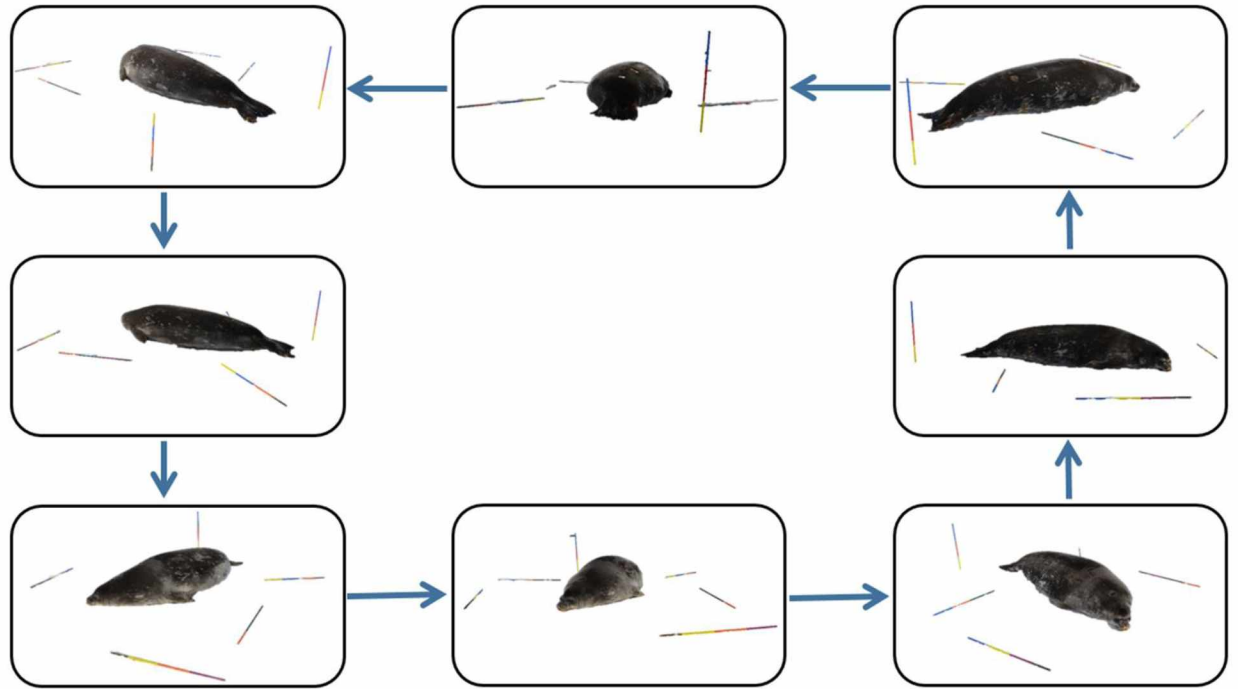


Figure 5.1. The photogrammetry procedure requires the photographer to slowly circle the seal, taking 8-12 photographs from all possible perspectives (i.e. kneeling, standing, portrait photographs, and landscape photographs). Photos are imported into PhotoModeler and a 3D shape is created by referencing scaled photographs to one another.

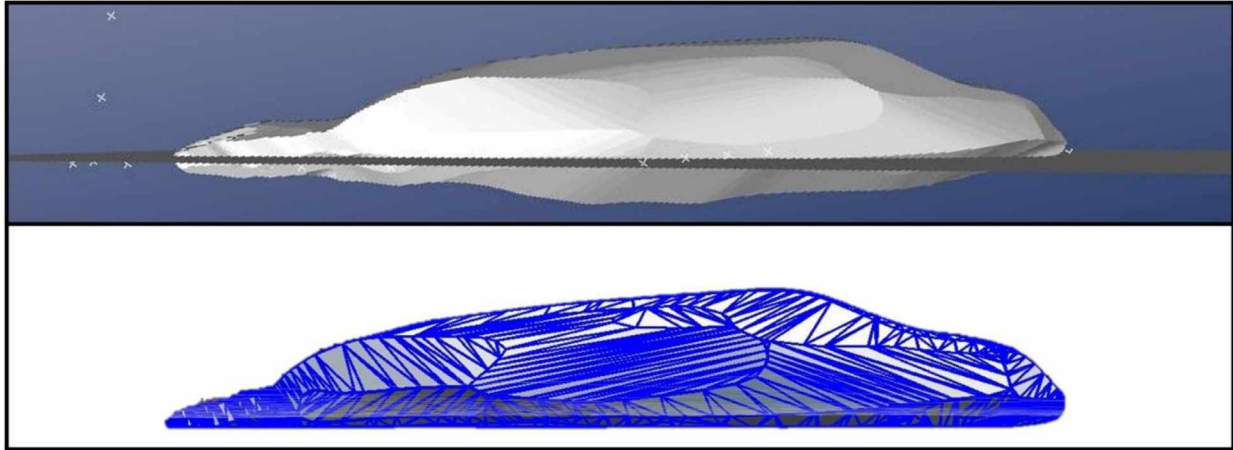


Figure 5.2. For the “silhouette slice” method, the portion of the seal below the ground plane is identified in PhotoModeler (top panel) and is removed to reduce error (bottom panel).

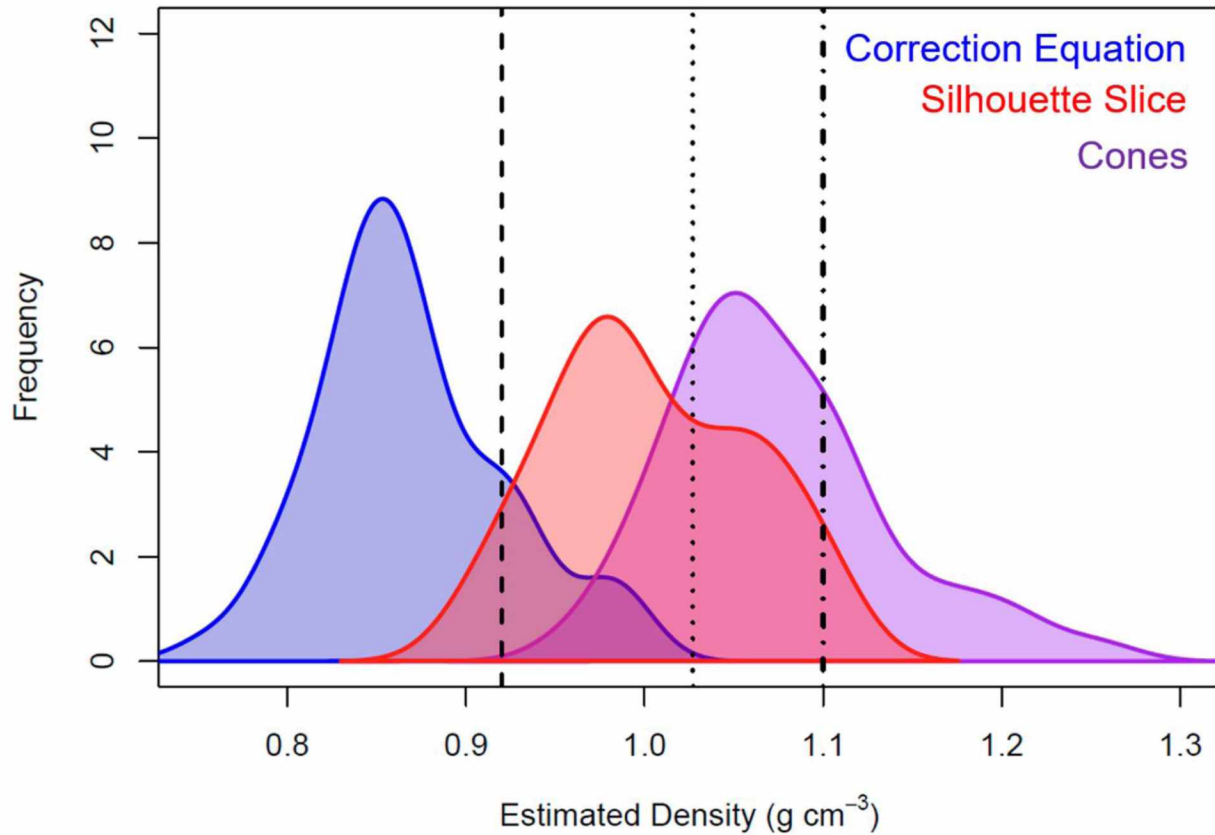


Figure 5.3. Estimated body density for adult, female Weddell seals calculated from actual body mass and estimated volume. The elliptical “cones” method estimated a higher density than both “correction equation” and “silhouette slice” methods. For reference, vertical lines show the density of seawater (black dotted line, 1.027 g cm^{-3} [37]), blubber (black dashed line, 0.920 g cm^{-3} , this paper), and lean tissue (black dashed-dotted line, 1.1 g cm^{-3} [35]).

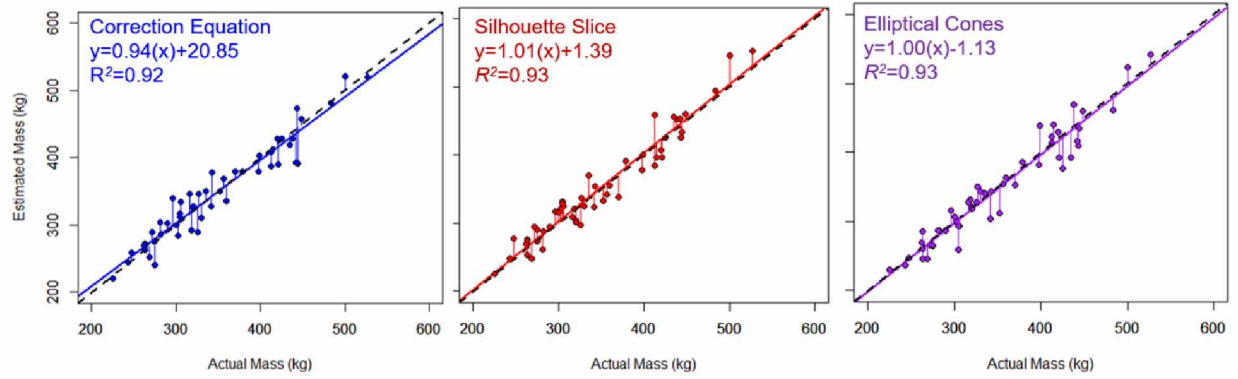


Figure 5.4. Regressions between actual and estimated mass for the three methods discussed: the equations calculated from de Bruyn et al. [32] (“correction equation”, left panel, $p < 0.0001$), the above-ground estimation (“silhouette slice”, middle panel, $p < 0.0001$), and the truncated cones method (“elliptical cones”, right panel, $p < 0.0001$). Black dashed lines show the 1:1 relationship between estimated and actual mass, whereas colored solid lines show the regression for each method. Horizontal lines show the offsets between data points and the 1:1 line.

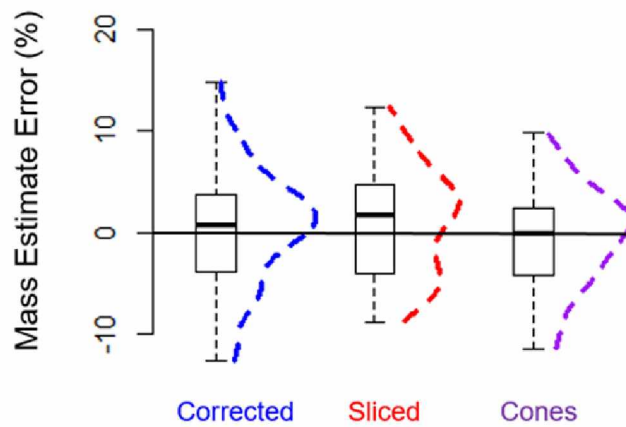


Figure 5.5. Boxplots of the percentage error for each estimation method with frequency distributions overlaid as dashed lines. Mass estimates from each method were not significantly different than actual mass in the Weddell seals.

5.7 Literature Cited

1. McDonald BI, Crocker DE, Burns JM, Costa DP. Body condition as an index of winter foraging success in crabeater seals (*Lobodon carcinophaga*). Deep Sea Research Part II: Topical Studies in Oceanography. 2008;55(3):515-22.
2. Ozgul A, Childs DZ, Oli MK, Armitage KB, Blumstein DT, Olson LE, et al. Coupled dynamics of body mass and population growth in response to environmental change. Nature. 2010;466(7305):482-5.
3. Crocker DE, Costa DP, Le Boeuf BJ, Webb PM, Houser DS. Impact of El Niño on the foraging behavior of female northern elephant seals. Marine Ecology-Progress Series. 2006;309.
4. Mellish J-A, Hindle A, Skinner J, Horning M. Heat loss in air of an Antarctic marine mammal, the Weddell seal. Journal of Comparative Physiology B. 2015;185(1):143-52.
5. Weckerly FW. Sexual-size dimorphism: influence of mass and mating systems in the most dimorphic mammals. Journal of Mammalogy. 1998;79(1):33-52.
6. Haley MP, Deutsch CJ, Le Boeuf BJ. Size, dominance and copulatory success in male northern elephant seals, *Mirounga angustirostris*. Animal Behaviour. 1994;48(6):1249-60.
7. Sand H. Life history patterns in female moose (*Alces alces*): the relationship between age, body size, fecundity and environmental conditions. Oecologia. 1996;106(2):212-20.
8. Carranza J. Sexual selection for male body mass and the evolution of litter size in mammals. The American Naturalist. 1996;148(1):81-100.
9. Damuth J, MacFadden BJ. Introduction: body size and its estimation. Body size in mammalian paleobiology: estimation and biological implications. 1990:1-10.

10. Le Boeuf BJ, Crocker DE. Ocean climate and seal condition. *BMC Biology*. 2005;3(1):9.
11. Bradshaw CJ, Davis LS, Lalas C, Harcourt RG. Geographic and temporal variation in the condition of pups of the New Zealand fur seal (*Arctocephalus forsteri*): evidence for density dependence and differences in the marine environment. *Journal of Zoology*. 2000;252(1):41-51.
12. Boyd I. State-dependent fertility in pinnipeds: contrasting capital and income breeders. *Functional Ecology*. 2000;14(5):623-30.
13. Costa DP. A bioenergetics approach to developing a population consequences of acoustic disturbance model. *The Effects of Noise on Aquatic Life*: Springer; 2012. p. 423-6.
14. Conway CJ, Eddleman WR, Simpson KL. Evaluation of lipid indices of the wood thrush. *Condor*. 1994:783-90.
15. Le Boeuf B, Crocker DE, Costa DP, Blackwell SB, Webb PM, Houser DS. Foraging ecology of northern elephant seals. *Ecological Monographs*. 2000;70(3):353-82.
16. Durban J, Parsons K. Laser metrics of free-ranging killer whales. *Marine Mammal Science*. 2006;22(3):735-43.
17. Shrader AM, Ferreira SM, Van Aarde RJ. Digital photogrammetry and laser rangefinder techniques to measure African elephants. *South African Journal of Wildlife Research*-. 2006;36(1):1-7.
18. Webster T, Dawson S, Slooten E. A simple laser photogrammetry technique for measuring Hector's dolphins (*Cephalorhynchus hectori*) in the field. *Marine Mammal Science*. 2010;26(2):296-308.
19. Ireland D, Garrott RA, Rotella J, Banfield J. Development and application of a mass-estimation method for Weddell seals. *Marine Mammal Science*. 2006;22(2):361-78.

20. Usher PJ, Church M. On the relationship of weight, length and girth of the ringed seal (*Pusa hispida*) of the Canadian Arctic. *Arctic*. 1969;120-9.
21. Gales NJ, Burton H. Ultrasonic measurement of blubber thickness of the southern elephant seal, *Mirounga lonina* (Linn). *Australian Journal of Zoology*. 1987;35(3):207-17.
22. Luque SP, Auriolles-Gamboa D. Sex differences in body size and body condition of California sea lion (*Zalophus californianus*) pups from the Gulf of California. *Marine Mammal Science*. 2001;17(1):147-60.
23. Fowler MA, Champagne CD, Houser DS, Crocker DE. Hormonal regulation of glucose clearance in lactating northern elephant seals (*Mirounga angustirostris*). *Journal of Experimental Biology*. 2008;211(18):2943-9.
24. Shero MR, Pearson LE, Costa DP, Burns JM. Improving the precision of our ecosystem calipers: a modified morphometric technique for estimating marine mammal mass and body composition. *PLOS ONE*. 2014;9(3):e91233.
25. Schwarz LK, Villegas-Amtmann S, Beltran RS, Costa DP, Goetsch C, Hückstädt L, et al. Comparisons and uncertainty in fat and adipose tissue estimation techniques: the northern elephant seal as a case study. *PLOS ONE*. 2015;10(6):e0131877.
26. Villegas-Amtmann S, Schwarz L, Sumich J, Costa D. A bioenergetics model to evaluate demographic consequences of disturbance in marine mammals applied to gray whales. *Ecosphere*. 2015;6(10):1-19.
27. Waite JN, Schrader WJ, Mellish J-AE, Horning M. Three-dimensional photogrammetry as a tool for estimating morphometrics and body mass of Steller sea lions (*Eumetopias jubatus*). *Canadian Journal of Fisheries and Aquatic Sciences*. 2007;64(2):296-303.

28. Haley MP, Deutsch CJ, Boeuf BJL. A method for estimating mass of large pinnipeds. *Marine Mammal Science*. 1991;7(2):157-64.
29. Kastelein R, Van Battum R. The relationship between body weight and morphological measurements in harbour porpoises (*Phocoena phocoena*) from the North Sea. *Aquat Mamm*. 1990;16:48-52.
30. Bundy R, Robel R, Kemp K. Whole body weights estimated from morphological measurements of White-tailed deer. *Transactions of the Kansas Academy of Science*. 1991:95-100.
31. Manimegalai M, Karthikeyeni S, Vasanth S, Ganesh AS, Vijayakumar ST, Subramanian P. Morphometric analysis-a tool to identify the different variants in a fish species *E. maculatus*. *International Journal of Environmental Sciences*. 2010;1(4):481.
32. de Bruyn PJN, Bester MN, Carlini AR, Oosthuizen WC. How to weigh an elephant seal with one finger: a simple three-dimensional photogrammetric application. *Aquatic Biology*. 2009;5:31-9. doi: 10.3354/ab00135.
33. Postma M, Tordiffe A, Hofmeyr M, Reisinger R, Bester L, Buss P, et al. Terrestrial mammal three-dimensional photogrammetry: multispecies mass estimation. *Ecosphere*. 2015;6(12):1-16.
34. Goldman R, Buskirk E. Body volume measurement by underwater weighing: description of a method. *Techniques for Measuring Body Composition*. 1961;3:78-89.
35. Nordoy E, Blix AS. Energy sources in fasting grey seal pups evaluated with computed tomography. *American Journal of Physiology-Regulatory, Integrative and Comparative Physiology*. 1985;249(4):R471-R6.

36. Adachi T, Maresh JL, Robinson PW, Peterson SH, Costa DP, Naito Y, et al. The foraging benefits of being fat in a highly migratory marine mammal. *Proceedings of the Royal Society of London B: Biological Sciences*. 2014;281(1797):2014-120.
37. Quetin L, Ross R. Depth distribution of developing *Euphausia superba* embryos, predicted from sinking rates. *Marine Biology*. 1984;79(1):47-53.
38. Sato K, Mitani Y, Cameron MF, Siniff DB, Naito Y. Factors affecting stroking patterns and body angle in diving Weddell seals under natural conditions. *Journal of Experimental Biology*. 2003;206(9):1461-70.
39. Williams TM, Davis R, Fuiman L, Francis J, Le B, Horning M, et al. Sink or swim: strategies for cost-efficient diving by marine mammals. *Science*. 2000;288(5463):133-6.
40. Worthy GA, Hickie JP. Relative brain size in marine mammals. *The American Naturalist*. 1986;128(4):445-59.
41. Mccafferty DJ, Gilbert C, Thierry A-M, Currie J, Le Maho Y, Ancel A. Emperor penguin body surfaces cool below air temperature. *Biology Letters*. 2013;9(3):20121192.
42. Prosser CL, Weinstein S. Comparison of blood volume in animals with open and with closed circulatory systems. *Physiological Zoology*. 1950;23(2):113-24.
43. Goldbogen JA, Calambokidis J, Croll DA, McKenna MF, Oleson E, Potvin J, et al. Scaling of lunge-feeding performance in rorqual whales: mass-specific energy expenditure increases with body size and progressively limits diving capacity. *Functional Ecology*. 2012;26(1):216-26. doi: 10.1111/j.1365-2435.2011.01905.x.
44. Slip D, Burton H, Gales N. Determining Blubber Mass in the Southern Elephant Seal, *Mirounga-leonina*, by Ultrasonic and Isotopic Techniques. *Australian Journal of Zoology*. 1992;40(2):143-52.

45. Proffitt KM, Garrott RA, Rotella JJ, Lele S. Using form analysis techniques to improve photogrammetric mass-estimation methods. *Marine Mammal Science*. 2008;24(1):147-58.
46. Bester C, Bruyn P. Simplifying photogrammetric analysis for assessment of large mammal mass: automated targeting and 3D model building. *The Photogrammetric Record*. 2015;30(150):227-41.
47. Amaral RS, da Silva VM, Rosas FC. Body weight/length relationship and mass estimation using morphometric measurements in Amazonian manatees *Trichechus inunguis* (*Mammalia: Sirenia*). *Marine Biodiversity Records*. 2010;3:e105.
48. Martin A, Reynolds P, Richardson M. Aspects of the biology of pilot whales (*Globicephala melaena*) in recent mass strandings on the British coast. *Journal of Zoology*. 1987;211(1):11-23.

Chapter 6. General Conclusions

In this dissertation, I synthesized the physiological, behavioral, ecological, and evolutionary drivers of molt frequency and phenology. Across birds and mammals, I found that molt strategies correspond well with seasonal environmental selective pressures (this dissertation, Chapter 2). In birds that inhabit mid-latitudes, sexual selection has led to an incomplete biannual molt that facilitates breeding plumages; in contrast, mammals with poorer vision have stronger selection pressures to camouflage with their habitats. Additional camouflage requirements in snow-covered habitats have led to a complete biannual molt to white feathers/fur in birds (e.g. rock ptarmigan *Lagopus muta*) and mammals (e.g. snowshoe hares *Lepus americanus*). Thus, the molting strategy of each species reflects its social, thermal, and coloration requirements.

Unlike other birds and mammals that exhibit a broad range of molt strategies, all seals and sea lions (e.g. pinnipeds) replace their fur once per year. This likely arises from their limited dependence on fur for thermoregulation; instead, adult pinnipeds utilize blubber, which is a superior insulator in highly conductive water. Pinniped molt durations are related to substrate stability and feeding frequency, ranging from 8 days in Hawaiian monk seals [1] to 105 days in Northern fur seals [2]. Specifically, the shortest molts occur in phocid seals (e.g. spotted seals *Phoca largha*, harp seals *Pagophilus groenlandicus*, and hooded seals *Cystophora cristata*) that haul out on ephemeral substrates (e.g. Arctic and Antarctic pack ice) and do not feed for the entire molt duration. In contrast, longer molts are found in otariids that feed during hair replacement. Weddell seals (this thesis, Chapter 3) and harbor seals *Phoca vitulina* [3, 4] exhibit an intermediate strategy, having molts that last about one month and include intermittent feeding.

Interestingly, both species have reproductive strategies that are intermediate between the true capital breeders that fast while nursing (e.g. northern elephant seals *Mirounga angustirostris*, Hawaiian monk seals *Neomonachus schauinslandi*) and the income breeders that feed while nursing (e.g. Northern fur seals *Callorhinus ursinus*, California sea lions *Zalophus californianus*) [5]. These intermediate strategies may be due to the relatively high resource abundance near pupping and molting colonies, in contrast to species that travel thousands of kilometers to reach their feeding grounds (e.g. elephant seals; [6]). The ecological and evolutionary drivers of interacting life history events have yet to be reviewed; a synthesis would provide valuable insights into the unique strategies developed by pinnipeds.

In relation to molt duration, less is known about the controls of molt phenology. Previous studies on birds and mammals have demonstrated that molt can be delayed in reproductively successful females [7-9], probably due to hormonal inhibition [4] and feedback loops between the endocrine system and body condition [10-12]. The research presented in chapter 3 demonstrates that reproductive Weddell seals molt 16 days later than sexually mature but non-reproductive seals. This molt delay in reproductive seals is similar to that of southern elephant seals *Mirounga leonina* (14 days later; [8]) and notably shorter than Hawaiian monk seals *Monachus schauinslandi* (28 days later; [1]), gray seals *Halichoerus grypus* (60 days later; [7]) and Mediterranean monk seals *Monachus monachus* (6 months later; [9]). After losing up to 40% of their body mass during lactation [13], reproductive Weddell seals spend more time diving and gain more mass than non-reproductive seals [14]. Thus, reproductive success, foraging effort, and body mass likely interact to control molt phenology via endocrine regulation.

With the development of novel methods for body composition measurements at high temporal resolutions [15-17], the links between resources, condition, and phenology can be more

systematically characterized. Photogrammetry provides a particularly promising method for obtaining sequential mass measurements while minimizing animal disturbance. In Chapter 5, I found that several morphometric and photogrammetric techniques produced accurate mass estimates; however, the morphometrics (elliptical cones; [18, 19]) method tended to underestimate volume and overestimate density. Conversely, the photogrammetric methods tended to overestimate volume and underestimate density. In the future, these non-invasive methods could be used to produce longitudinal mass estimates across the summer in Weddell seals.

While reproductive success was the most significant driver of molt start date, ice break-out date was also significantly associated with molt start date. Specifically, later ice break-out in the 2016 austral summer was associated with later molt. Given the tight trophic coupling between primary production and top predators [20], links between ice break-out and molt phenology would not be surprising. Each summer, sea ice break-out triggers a short-lived phytoplankton bloom that provides resources for zooplankton [21] and their predators, including fishes [22], penguins [23], and seals [24]. This physical-biological coupling is important for ecosystem dynamics and has been well documented [20, 23, 25], but until now, the vertical component of that coupling was little studied. In Chapter 4, I demonstrated that summer sea ice break-out strongly influenced the vertical space utilized by seals. It appears that during the phytoplankton bloom, zooplankton and fishes aggregate in shallower waters, and top predators shallow their dives to take advantage of the increased prey availability at these shallower depths. The zooplankton and fish aggregations appear related to spawning, as the reproductive cycles of both trophic levels are triggered by photoperiod (i.e. ice break-out) and occur in shallow waters

[21]. I found that later ice break-out corresponded to later seal dive shallowing, suggesting delayed spawning at lower trophic levels.

Feeding effort and success was significantly higher during the shallow-period (this dissertation, Chapter 4) and this shallow foraging period is likely important for seals to recuperate mass after lactation and before molt. Thus, it is possible that the delayed shallowing period affected molt phenology via altered mass dynamics. These links are not without precedent, as Newton [26] found that delayed abundance of summer resource resulted in late molt onset in bullfinches *Pyrrhula pyrrhula*. Regardless of the mechanism, because ice break-out phenology influences molt phenology (this dissertation, Chapter 3), the consequences of ice break-out delays could have significant energetic repercussions for top predators. These links must be explicitly studied.

In turn, I found that later molt has carry-over effects across seasons, leading to lower reproductive success and lower breeding colony attendance during the following year (this thesis, Chapter 3). Previous studies have found that late-breeding birds have a lower probability of next-year return [26, 27]; in contrast, Flinks et al. [28] found no measurable survival cost in birds with delayed molt. We found that more mass loss occurred in seals that molted for more days during our study (Walcott, pers. comm.), suggesting that the cost of molt is notable; whether the cost of molting is related to fur growth or heat loss remains to be determined (this dissertation, Chapter 3). Interestingly, most information about molt is derived from the visible stages; perhaps the greatest mystery is how the different components of the molt are scheduled, and to what degree they contribute to energetic expenditure. In the mammalian molting process, hair growth (i.e., cellular molt) occurs first and is thought to be associated with skin perfusion and the potential for heat loss [29]. As a result, molt phenology could have energetic

implications, especially for pinnipeds that dive deep and/or inhabit high latitudes [30]. Thermal constraints on time-activity budgets, as have been suggested in other studies, are likely more related to the cellular molt than the visible molt. The energetic costs of these molt processes are also not well understood; there appear to be more questions than answers about the molting process. To fully link molt phenology to vital rates, future studies must address several unknowns, including (1) the energetic losses resulting from sub-optimal molt timing; and (2) the sensitivity of the annual cycle to delays in one life history event.

By providing a holistic review of the physiological, behavioral, ecological, and evolutionary drivers of molt strategies, I provide novel insights into Weddell seal life history strategies during the short but productive austral summer. The research presented in this dissertation was made possible by the 44-year demographic study of Weddell seals in Erebus Bay, Ross Sea, Antarctica [31], during which hundreds of researchers recorded reproductive histories of more than 20,000 unique seals. The value of long-term studies cannot be overlooked, especially given the status of federal research funding. Long-term studies contribute disproportionately to both advancing science and informing policy [32]. Indeed, the establishment of long-term studies has allowed researchers to make progress in characterizing the fundamentals of animal systems, such as highlighting the complexities of their social units [33] and how they survive in extreme conditions [31].

Long-term research programs have also been crucial for quantifying the impacts of environmental perturbations on large marine vertebrates: they have documented complete penguin breeding failure under unusually high precipitation [34], reduced elephant seal weaning weights during El Niño conditions [35], increases in sea lion foraging effort during low productivity [36], decreased sea otter *Enhydra lutris* survival after oil spills [37] and reduced

Weddell seal [25] and penguin [34] reproductive success during the presence of a massive iceberg. Given the difficulty in predicting which research projects will be “transformative” [38] or impactful [39], and when extreme weather and climate events may occur [40], these long-term studies provide the opportunity to retroactively characterize baseline conditions. Moving forward as a scientific community, we must ensure that long-term studies are maintained so that we can continue these interdisciplinary studies of our natural world.

6.1 Literature Cited

1. Johanos TC, Becker BL, Ragen TJ. Annual reproductive cycle of the female Hawaiian monk seal (*Monachus schauinslandi*). Marine Mammal Science. 1994;10(1):13-30.
2. Scheffer VB, Johnson AM. Molt in the northern fur seal: US Department of Interior, Fish and Wildlife Service; 1963.
3. Scheffer VB, Slipp JW. The harbor seal in Washington State. The American Midland Naturalist. 1944;32(2):373-416.
4. Thompson P, Rothery P. Age and sex differences in the timing of moult in the common seal, *Phoca vitulina*. Journal of Zoology. 1987;212(4):597-603.
5. Bowen WD, Oftedal OT, Boness DJ. Mass and energy transfer during lactation in a small phocid, the harbor seal (*Phoca vitulina*). Physiological Zoology. 1992;65(4):844-66.
6. Robinson PW, Costa DP, Crocker DE, Gallo-Reynoso JP, Champagne CD, Fowler MA, et al. Foraging behavior and success of a mesopelagic predator in the northeast Pacific Ocean: insights from a data-rich species, the northern elephant seal. PLOS ONE. 2012;7(5):e36728.
7. Boily P. Metabolic and hormonal changes during the molt of captive gray seals (*Halichoerus grypus*). American Journal of Physiology-Regulatory, Integrative and Comparative Physiology. 1996;270(5):1051-8.
8. Kirkman S, Bester M, Pistorius P, Hofmeyr G, Jonker F, Owen R, et al. Variation in the timing of moult in southern elephant seals at Marion Island. South African Journal of Wildlife Research. 2003;33(2):79-84.
9. Badosa E, Pastor T, Gazo M, Aguilar A. Moulting in the Mediterranean monk seal from Cap Blanc, western Sahara. African Zoology. 2006;41(2):183-92.

10. Daniel RG, Jemison LA, Pendleton GW, Crowley SM. Molting phenology of harbor seals on Tugidak Island, Alaska. *Marine Mammal Science*. 2003;19(1):128-40.
11. Romero LM, Storchlic D, Wingfield JC. Corticosterone inhibits feather growth: potential mechanism explaining seasonal down regulation of corticosterone during molt. *Comparative Biochemistry and Physiology Part A: Molecular & Integrative Physiology*. 2005;142(1):65-73.
12. Danner RM, Greenberg RS, Danner JE, Walters JR. Winter food limits timing of pre-alternate moult in a short-distance migratory bird. *Functional Ecology*. 2015;29(2):259-67.
13. Wheatley KE, Bradshaw CJ, Davis LS, Harcourt RG, Hindell MA. Influence of maternal mass and condition on energy transfer in Weddell seals. *Journal of Animal Ecology*. 2006;75(3):724-33. doi: 10.1111/j.1365-2656.2006.01093.x. PubMed PMID: 16689955.
14. Beltran RS, Kirkham AL, Breed GA, Burns JM. Reproductive effort affects the annual dive behavior of adult, female Weddell seals. *SCAR Biology*; Leuven, Belgium 2017.
15. Andersen JM, Stenson GB, Skern-Maurizen M, Wiersma YF, Rosing-Asvid A, Hammill MO, et al. Drift diving by hooded seals (*Cystophora cristata*) in the Northwest Atlantic Ocean. *PLoS One*. 2014;9(7):e103072. doi: 10.1371/journal.pone.0103072. PubMed PMID: 25051251; PubMed Central PMCID: PMC4106908.
16. Page B, McKenzie J, Hindell MA, Goldsworthy SD. Drift dives by male New Zealand fur seals (*Arctocephalus forsteri*). *Canadian Journal of Zoology*. 2005;83(2):293-300.
17. Robinson PW, Simmons SE, Crocker DE, Costa DP. Measurements of foraging success in a highly pelagic marine predator, the northern elephant seal. *Journal of Animal*

- Ecology. 2010;79(6):1146-56. doi: 10.1111/j.1365-2656.2010.01735.x. PubMed PMID: 20673236.
18. Shero MR, Pearson LE, Costa DP, Burns JM. Improving the precision of our ecosystem calipers: a modified morphometric technique for estimating marine mammal mass and body composition. PLOS ONE. 2014;9(3):e91233.
 19. Schwarz LK, Villegas-Amtmann S, Beltran RS, Costa DP, Goetsch C, Hückstädt L, et al. Comparisons and uncertainty in fat and adipose tissue estimation techniques: the northern elephant seal as a case study. PLOS ONE. 2015;10(6):e0131877.
 20. Paterson JT, Rotella JJ, Arrigo KR, Garrott RA. Tight coupling of primary production and marine mammal reproduction in the Southern Ocean. Proceedings of the Royal Society of London B: Biological Sciences. 2015;282(1806):20143137.
 21. Kawaguchi S, Yoshida T, Finley L, Cramp P, Nicol S. The krill maturity cycle: a conceptual model of the seasonal cycle in Antarctic krill. Polar Biology. 2007;30(6):689-98.
 22. Vacchi M, Pisano E, Ghigliotti L. The Antarctic silverfish: a keystone species in a changing ecosystem. Cham, Switzerland: Springer; 2017. 314 p.
 23. Chapman EW, Hofmann EE, Patterson DL, Fraser WR. The effects of variability in Antarctic krill (*Euphausia superba*) spawning behavior and sex/maturity stage distribution on Adélie penguin (*Pygoscelis adeliae*) chick growth: a modeling study. Deep Sea Research II. 2010;57(7):543-58.
 24. Proffitt KM, Rotella JJ, Garrott RA. Effects of pup age, maternal age, and birth date on pre-weaning survival rates of Weddell seals in Erebus Bay, Antarctica. Oikos. 2010;119(8):1255-64.

25. Chambert T, Rotella JJ, Garrott RA. Environmental extremes versus ecological extremes: impact of a massive iceberg on the population dynamics of a high-level Antarctic marine predator. *Proceedings of the Royal Society of London B: Biological Sciences*. 2012;279(1747):4532-41.
26. Newton I. The moult of the Bullfinch *Pyrrhula pyrrhula*. *Ibis*. 1966;108(1):41-67.
27. Hemborg C. Sexual differences in moult–breeding overlap and female reproductive costs in pied flycatchers, *Ficedula hypoleuca*. *Journal of Animal Ecology*. 1999;68(2):429-36.
28. Flinks H, Helm B, Rothery P. Plasticity of moult and breeding schedules in migratory European Stonechats *Saxicola rubicola*. *Ibis*. 2008;150(4):687-97.
29. Feltz ET, Fay FH. Thermal requirements in vitro of epidermal cells from seals. *Cryobiology*. 1966;3(3):261-4.
30. Boily P. Theoretical heat flux in water and habitat selection of phocid seals and beluga whales during the annual molt. *Journal of Theoretical Biology*. 1995;172(3):235-44.
31. Cameron M, Siniff D. Age-specific survival, abundance, and immigration rates of a Weddell seal (*Leptonychotes weddellii*) population in McMurdo Sound, Antarctica. *Canadian Journal of Zoology*. 2004;82(4):601-15. doi: 10.1139/z04-025.
32. Hughes BB, Beas-Luna R, Barner AK, Brewitt K, Brumbaugh DR, Cerny-Chipman EB, et al. Long-Term Studies Contribute Disproportionately to Ecology and Policy. *BioScience*. 2017;67(3):271-81.
33. Wells RS. Dolphin social complexity: Lessons from long-term study and life history. 2003.

34. Ropert-Coudert Y, Kato A, Meyer X, Pellé M, MacIntosh AJ, Angelier F, et al. A complete breeding failure in an Adélie penguin colony correlates with unusual and extreme environmental events. *Ecography*. 2015;38(2):111-3.
35. Le Boeuf BJ, Crocker DE. Ocean climate and seal condition. *BMC Biology*. 2005;3(1):9.
36. Weise MJ, Costa DP, Kudela RM. Movement and diving behavior of male California sea lion (*Zalophus californianus*) during anomalous oceanographic conditions of 2005 compared to those of 2004. *Geophysical Research Letters*. 2006;33(22).
37. Monson DH, Doak DF, Ballachey BE, Johnson A, Bodkin JL. Long-term impacts of the Exxon Valdez oil spill on sea otters, assessed through age-dependent mortality patterns. *Proceedings of the National Academy of Sciences*. 2000;97(12):6562-7.
38. Gravem SA, Bachhuber SM, Fulton-Bennett HK, Randell ZH, Rickborn AJ, Sullivan JM, et al. Transformative research is not easily predicted. *Trends in ecology & evolution*. 2017.
39. Sinatra R, Wang D, Deville P, Song C, Barabási A-L. Quantifying the evolution of individual scientific impact. *Science*. 2016;354(6312):aaf5239.
40. Solomon S, Qin D, Manning M, Chen Z, Marquis M, Averyt K, et al. Climate change 2007: the physical science basis. Contribution of Working Group I to the Fourth Assessment Report of the Intergovernmental Panel on Climate Change, 2007. 2007.

Appendix. IACUC Approvals and NMFS Marine Mammal Permit



Research &
Graduate Studies
UNIVERSITY of ALASKA ANCHORAGE

3211 Providence Drive
Anchorage, Alaska 99508-4614
T 907.786.1099, F 907.786.1791
www.uaa.alaska.edu/research/ric

DATE: February 18, 2016
TO: Jennifer Burns, PhD
FROM: University of Alaska Anchorage IACUC

PROJECT TITLE: [419971-17] The cost of a new fur coat: Interactions between molt and reproduction in Weddell seals
IRBNET REFERENCE #: 419971-17
SUBMISSION TYPE: Closure/Final Report

ACTION: APPROVED
APPROVAL DATE: February 12, 2016
EXPIRATION DATE: February 8, 2016
REVIEW TYPE: Full Committee Review

The final report to the Institutional Care and Animal Use Committee regarding your study has been approved. Thank you for your support of animal care guidelines and congratulations on the conclusion of your research.

A handwritten signature in black ink, appearing to be 'Cindy Knall', written over a white background.

Cindy Knall, Ph.D.
Associate Professor, WWAMI School of Medical Education
Chair, Institutional Animal Care and Use Committee
University of Alaska Anchorage
3211 Providence Drive
Anchorage, Alaska 99508



Research &
Graduate Studies
UNIVERSITY of ALASKA ANCHORAGE

3211 Providence Drive
Anchorage, Alaska 99508-4614
T 907.786.1099, F 907.786.1791
www.uaa.alaska.edu/research/ric

DATE: January 27, 2016
TO: Jennifer Burns, PhD
FROM: University of Alaska Anchorage IACUC

PROJECT TITLE: [854089-1] The cost of a new fur coat: Interactions between molt and reproduction in Weddell seals, part 2

IRBNET REFERENCE #: 854089-1

SUBMISSION TYPE: New Project

ACTION: APPROVED
APPROVAL DATE: January 27, 2016
EXPIRATION DATE: January 26, 2019
REVIEW TYPE: Designated Member Review

The Institutional Animal Care and Use Committee at the University of Alaska Anchorage reviewed and approved your protocol by a formal Designated Member Review process. Please note that this approval is contingent upon your compliance with all relevant University, city, state, and federal regulations, and requires that you possess all relevant permits before work is initiated. Your approval is good for a period of 3 years. You are required to submit an annual report of your activities prior to January 27 in each of the next two years, and a closure report prior to January 26, 2019. This form is available in the Forms and Reference Library on IRBNet.

We remind you that all changes in personnel and animal handling protocols must be submitted to the committee prior to such changes taking place. In addition, should you experience any unexpected animal mortalities, illnesses, or injury (to animals or personnel involved with the project), you are required to report such to the IACUC immediately.

Thank you for your support of animal care guidelines. We hope that your research goes well.

Cindy Knall, Ph.D.
Associate Professor, WWAMI School of Medical Education
Chair, Institutional Animal Care and Use Committee
University of Alaska Anchorage
3211 Providence Drive
Anchorage, Alaska 99508



UNITED STATES DEPARTMENT OF COMMERCE
National Oceanic and Atmospheric Administration
NATIONAL MARINE FISHERIES SERVICE
Silver Spring, MD 20910

Jennifer M. Burns, Ph.D.
University of Alaska Anchorage
Biology Department
CPISB 202C, 3101 Science Circle
Anchorage, AK 99508

JUN 11 2013

Dear Dr. Burns:

The National Marine Fisheries Service has issued Permit No. 17411-00 to you for research activities on marine mammals. This permit is effective upon your signature and valid through the expiration date indicated in Condition A.1.

Here's what you need to do to use your permit:

1. Read the permit, including attachments. If you have questions, call your permit analyst – Tammy Adams or Amy Sloan – at 301-427-8401 before signing the permit.
2. Sign and date the original signature page and the signature page marked “file copy.”
3. Keep the original signature page with your permit. You need both as proof of your authorization to conduct the research activities.
4. Send the “file copy” signature page to our office as proof of your acceptance of the permit.

Please keep your email contact information current in our online database (<https://apps.nmfs.noaa.gov/>). You will receive automated email reminders of due dates for annual and final reports, and a notice prior to expiration of your permit.

Please return the signature page marked “file copy” to the Permits and Conservation Division (F/PR1), 1315 East-West Highway, Silver Spring, MD 20910. You may also submit the “file copy” of the signature page by facsimile (FAX number: 301-713-0376) and confirm it by mail.

Sincerely,

D. Michael Payne
Chief, Permits and Conservation Division
Office of Protected Resources
(phone: 301-427-8401)

Enclosure



Printed on Recycled Paper

